

REMARKS

Reconsideration of the present application is respectfully requested. Claims 2-8, 12, 14 and 18-38 are pending. Claims 15-17, and 39 have been cancelled. Applicants reserve the right to pursue the content of these claims in a continuing application. Claims 4, 7, 8, 12, 14, 20, 24, 26, 30, 32, and 38 have been amended. Support for the amendments is found in the claims as originally filed, and throughout the specification. No new matter has been added.

Rejections under 35 U.S.C. §112, 1st Paragraph - New Matter:

Claims 24 and 32 are rejected under 35 U.S.C. §112, first paragraph as containing subject matter which was not described in the specification in such a way to reasonably convey to one skilled in the relevant art that the inventor(s) had possession of the claimed invention.

Claims 24 and 32 recite a "non-human host cell". The Examiner asserts that "non-human" has no basis in the specification or in the claims as originally filed, and is considered to be new matter.

Claims 24 and 32 have been amended to delete the term "non-human", therefore the rejection is obviated.

Applicants have properly addressed by argument and amendment the grounds for the rejection of claims 24 and 32 under 35 U.S.C. §112, first paragraph and respectfully request that the rejection be withdrawn.

Rejections under 35 U.S.C. §101 – Utility:

Claims 2-8, 12, and 14-39 are rejected under 35 U.S.C. §101 because the claimed invention is not supported by either a credible or a well-established utility.

The Examiner asserts that the claims to the isolated polynucleotide of SEQ ID NO: 1, a polynucleotide encoding SEQ ID NO: 2, a polynucleotide having at least 80%, 85%, 90%, or 95% sequence identity to SEQ ID NO: 1, and a polynucleotide which hybridizes to SEQ ID NO: 1, wherein all the above polynucleotides encode a

polypeptide having ATP-dependent DNA binding activity do not meet the utility requirements. Further, claims to cells, plants, and seeds comprising the above polynucleotides, a polynucleotide encoding at least 20 contiguous bases of SEQ ID NO: 2, and a polynucleotide comprising at least 30 contiguous nucleotides do not meet the utility requirements. The Examiner asserts that the claims do not meet the utility requirements for the following reasons:

- 1) the predicted function is based solely upon sequence comparison with a Rad50 gene of yeast from the prior art;
- 2) no specific use of a polypeptide having ATP-dependent DNA binding activity or Rad50 activity in a plant has been disclosed;
- 3) the biological functions of a Rad50 gene in plants have not been documented; and
- 4) ATP-dependent DNA binding and Rad50 activity are not specific functions.

Applicants respectfully disagree. Applicants believe that the claims do recite a specific function and that this function is supported in the specification. However, in order to expedite examination, Applicants have cancelled claims 15-17 and 39, and have amended claims 12, 14 and 20 to recite that the polypeptide is involved in double-strand DNA break repair. The specification at pages 1-2, especially page 1, lines 15-16 and page 1, line 27 – page 2, line 2 describes the well-established utility of Rad50 polypeptide involved in DNA double-strand break repair (see also, for example, abstract Ref. A2, in IDS submitted 6/23/00). Rad50 is known to be involved in recombination as well as overall DNA repair. Rad50 has also been shown to interact with a number of other proteins involved in DNA repair and homologous recombination. The present invention proposes to use the well-established utility of Rad50 in order to modulate repair activity, and recombination, in order to improve gene targeting and transformation in plants (see page 2, lines 10-12) therefore establishing specific, substantial and credible utility for the present invention.

Applicants have disclosed a full-length Rad50 polynucleotide (SEQ ID NO: 1) which encodes a full-length Rad50 polypeptide (SEQ ID NO: 2) comprising known conserved and functional motifs (page 1-2 and Example 4). Contrary to the Examiner's conclusion, Applicants' identification of SEQ ID NOS: 1 and 2 as functional Rad50 is not based solely on one sequence comparison to one yeast sequence. As discussed on page 2, Applicants note that Rad50 homologues had been identified and characterized in mammals and in the plant *Arabidopsis*. As discussed on pages 1-2, Example 4 points out the conserved domains found in other Rad50 proteins, and demonstrate that the identification of the SEQ ID NOS: 1 and 2 is not merely from one sequence comparison, or one database search, but also involves multiple sequence comparisons and analyses, including the size of the encoded protein, the presence of conserved domains, the relative localization of the domains (*i.e.* positions similar to known Rad50s), percent sequence identity, and overall homology to known Rad50 sequences. Further, in the amendment filed 2/14/02 Applicants submitted Appendix A containing a multiple sequence alignment (MSA) of SEQ ID NO: 2 with other Rad50 proteins from human, rat, mouse, *Arabidopsis*, yeast and *C. elegans*. The MSA not only showed the overall homology of SEQ ID NO: 2 to other known Rad50 proteins, but also shows conserved amino acids residues and domains shared with other Rad50 proteins, and also shows partially conserved or non-conserved amino acid residues or regions. Given the overall homology to other Rad50 sequences and presence of conserved domains Applicants have disclosed and claimed sequences having credible, specific, and substantial utility.

The Examiner cites a paper from Science (292:1486-87, 2001(X), copy not provided, previous Examiner citations from Action issued 11/19/2001 has ref (X) as GenBank #U668876) and cites Bork et al. (Genome Research 10:398-400 2000 (Y), this is ref (W) in Action issued 11/19/2001) to assert that the state of the art teaches that sequence homology alone is insufficient to determine the functional activity of a gene/protein. The Examiner also asserts that further research not considered to be

routine would be required before one skilled in the art would know how to use the sequences of the claimed invention to achieve a desired trait in a plant, and that, as established in the courts, a utility which requires or constitutes carrying out further research to identify or reasonably confirm a "real world" context of use is not a substantial utility.

Applicants respectfully disagree. The letter to the editor published in Science (Lacombe et al. 292:1486-87 2001) proposed a naming convention for plant glutamate receptors based on their phylogeny. Clearly, the authors do consider the plant sequences to be glutamate receptors. Applicants note that experimental evidence confirms that the plant sequences are glutamate receptor ion channels which conduct cations (page 1487, col. 2, and refs cited col. 3 and submitted herein as Appendix B). The experimental evidence functionally confirms the homology-based identification of the plant sequences as glutamate receptor homologues. As discussed in the response filed 2/14/02, Bork (Genome Res. 10:398-400, 2000) does not assert that homology cannot predict function, he does warn that high-throughput automated annotation of sequences can be inaccurate. Again, the Applicants stress that the identification of SEQ ID NOS: 1 and 2 is not solely based on an automated computer annotation, as warned by Bork. The identification of SEQ ID NOS: 1 and 2 as Rad50 sequences is based on careful and extensive sequence analyses, all of which are consistent with the sequences being Rad50 homologues. For example, SEQ ID NO: 1 encodes a full-length protein (SEQ ID NO: 2) with the expected molecular weight of Rad50, which further contains the expected sequence motifs in the expected order and location as Rad50 (Walker boxes, nuclear localization signals, heptad repeats, and leucine zipper) and further has an overall sequence homology to known Rad50s as evidenced by the specification (e.g. pages 1-2, and Example 4) and the MSA presented in Appendix A submitted 2/14/02. This evidence clearly indicates that SEQ ID NOS: 1 and 2 are Rad50 homologues containing the conserved functional domains, and meet the standards for utility by having credible, specific and substantial utility to use the

claimed Rad50 sequences, having DNA repair activity, in order to modulate DNA repair and recombination in order to increase transformation efficiency in a plant. Applicants further submit that this utility extends to the breadth of the claimed sequences, as the claims explicitly recite the function of the encoded polypeptides *i.e.*, involved in double-strand DNA break repair. Contrary to the Examiner's assertion, one of skill in the art will not have to conduct non-routine research in order to use the claimed sequences. Applicant has disclosed the sequences of SEQ ID NOS: 1 and 2, conserved domains and motifs (*e.g.*, Example 4, and Appendix A), guidance on the construction and isolation of nucleic acids (*e.g.*, page 10, line 29 – page 11, line 4; page 13, line 30 – page 15, line 16; page 24, line 15 – page 26, line 32; and page 31, line 10 – page 37, line 2), codon degeneracy (*e.g.*, page 5, line 23 – page 6, line 3), codon preferences (*e.g.*, page 6, line 30 – page 7, line 11; and page 56, line 10 – page 57, line 2), conservatively modified variants (*e.g.*, page 5, line 20 – page 6, line 25; and page 10, line 29 – page 11, line 23), conservative amino acid substitutions (*e.g.*, page 6, lines 4-25; page 11, lines 6-12; page 12, line 30 – page 13, line 2; and page 19, lines 17-33; see also Appendix A), protein expression (*e.g.*, page 43, line 20 – page 47, line 25; page 49, line 28 – page 50, line 27; and page 53, line 1 – page 54, line 6), sequence analyses, comparisons and sequence identity (*e.g.*, page 16, line 1 – page 21, line 7; page 27, lines 1-24; and page 57, line 28 – page 59, line 18), and vector construction, and cell and plant transformation (*e.g.*, page 11, line 24 – page 12, line 8; page 12, lines 14-29; page 15, lines 30-32; page 37, line 5 – page 43, line 18; page 47, line 28 – page 49, line 26; and page 50, line 29 – page 52, line 31). As shown in an earlier response (filed 12/17/02), assays for Rad50 were well known in the art at the time of filing (page 7-8). For example, assays for protein interactions (*e.g.* Ref. A5, A9, A10, and A11, in IDS submitted 6/23/00) and two-hybrid screens (Ref. A8, IDS submitted 6/23/00), DNA binding assays (Ref. A2, IDS submitted 6/23/00), DNA repair or recombination assays (Ref. A1, A4, A7, and A8, IDS submitted 6/23/00), nuclease assays (Ref. A11, IDS submitted 6/23/00), microscopy studies (Ref. A10, ID submitted 6/23/00),

complementation of mutants (Ref. A8, IDS submitted 6/23/00), and response to DNA damaging agents including chemicals and irradiation (Ref. A1, A8, and A10, IDS submitted 6/23/00). The guidance in the specification and the knowledge in the art clearly enable one of skill in the art to use the claimed sequences, relying only on routine screening methods.

Applicants have properly responded by amendment and argument to the rejection of claims 2-8, 12, and 14-39 under 35 U.S.C. §101, and respectfully request that this rejection be withdrawn and not applied to pending claims 2-8, 12, 14, and 18-38 as amended.

Rejections under 35 U.S.C. §112, 1st Paragraph, Enablement - Utility:

Claims 2-8, 12, and 14-39 are rejected under 35 U.S.C. §112, first paragraph. Specifically, since the claimed invention is not supported by either a credible asserted utility, or a well established utility for the reasons set forth above, one skilled in the art would not know how to use the invention.

Applicants believe they have properly addressed the rejection under 35 U.S.C. §101 by amendment and argument and therefore respectfully request that the corresponding rejection of claims 12-8, 12, and 14-39 under 35 U.S.C. §112, first paragraph for lack of enablement be withdrawn.

Rejections under 35 U.S.C. §112, 1st Paragraph, Enablement:

Claims 2-8, 12, and 14-39 are rejected under 35 U.S.C. §112, first paragraph, because the specification does not enable any person skilled in the art to which it pertains, or with which it is most nearly connected, to make and/or use the invention commensurate in scope with these claims.

The Examiner asserts that it is unclear from the disclosure how Rad50 or a polypeptide having ATP-dependent DNA binding activity is involved in DNA repair and how SEQ ID NO: 1 can be used to achieve "efficiency with which heterologous nucleic acids are incorporated into the genome of a target plant cell". The Examiner

further states that even if the Applicant shows that SEQ ID NO: 1 encoding SEQ ID NO: 2 has specific DNA repair activity and can be used to “modulate the efficiency with which heterologous nucleic acids are incorporated into the genome of a target plant cell” the enablement rejection will further be applied to claims broadly drawn to an isolated polynucleotide having at least 80%, 85%, 90% or 95% sequence identity to SEQ ID NO: 1, a polynucleotide that hybridizes and encodes a polypeptide having ATP-dependent DNA binding activity, transgenic plants, cells, seeds comprising the polynucleotide, a polynucleotide encoding a polypeptide comprising at least 20 contiguous amino acids of SEQ ID NO: 2, and a polynucleotide comprising at least 30 contiguous nucleotides of SEQ ID NO: 1 because Applicant has not provided guidance for how to obtain and use the polynucleotides. The Examiner asserts that the Applicant has not provided sufficient guidance as how to obtain any and all polynucleotides having the claimed structural property and still encoding a polypeptide having the desired functional activity. The Examiner asserts that no guidance has been provided for any modification to SEQ ID NO: 1 that resulted in the polynucleotides of claims 12, 14, 16-17, 20-21, and 39. The Examiner asserts that specific guidance is required for modifications to SEQ ID NO: 1 so that polynucleotides having both the desired structural and function characteristics can be obtained.

Applicants respectfully disagree. It is clear from the specification and the art that Rad50 is involved in DNA repair (e.g. see pages 1-2 of the specification, and the IDS submitted 6/23/00, e.g. Abstract of Ref. A2). Rad50 is known to be involved in DNA repair and recombination, e.g. non-homologous end joining. Applicants propose (see page 2, lines 10-14) that by modulating the level of Rad50 protein, a protein involved in non-homologous end joining, one can modulate the integration of heterologous polynucleotides into the genome of a plant cell. Applicants have provided sufficient guidance for how to obtain and use the claimed Rad50 polynucleotides and polypeptides as discussed above, including nucleic acid and protein isolation, determination of nucleic acid or protein sequence identity,

hybridizations and conserved structural features. Further, Applicants have disclosed the full-length polynucleotide (SEQ ID NO: 1) encoding the full-length polypeptide (SEQ ID NO: 2), and have deposited a plasmid comprising SEQ ID NO: 1 with the ATCC under Accession No. 207194. Contrary to the Examiner's assertion, one of skill in the art would not be required to make any and all of the claimed polynucleotides having the claimed structural properties and encoding a functional polypeptide in order to use the invention. One of skill in the art would use the guidance above and knowledge in the art to readily produce polynucleotides having at least 90% sequence identity to SEQ ID NO: 1 and encode SEQ ID NO: 2, a polypeptide involved in DNA repair, or readily produce polynucleotides which encode polypeptides having at least 90% sequence identity to SEQ ID NO: 2 and are involved in DNA repair. Using the disclosed sequences, the conserved domains, guidance in the specification, and the knowledge in the art, for example a multiple sequence alignment as earlier presented in Appendix A, one of skill in the art could identify conserved, partially conserved and non-conserved amino acid residues and regions, and could reasonably predict whether a conservative or non-conservative amino acid substitution would likely significantly impact the function of the modified protein compared to the unmodified protein. Only routine screening is required to confirm functional variants, routine screening is not undue experimentation. It is respectfully submitted that 35 U.S.C. §112 does not require a working example. Further, case law does not require that an application provide a working example. Nor does 35 U.S.C. §112 require that the Applicant make every embodiment. It is only required that the application teach the person skilled in the art how to make and use the invention. The present application meets that requirement.

The Examiner asserts that the state of the prior art teaches that structural identity between two DNA/protein sequences does not necessarily mean that the sequences have the same function. The Examiner cites Lazar et al. (MCB 1988 8(3):1247-1257 (U), (ref (V) in action issued 11/19/01)) and Broun et al. (Science 1998 282:131-133 (U)) which each provide examples of very specific limited amino

acid changes which resulted in elimination or alteration of the experimental protein's catalytic activity. The Examiner also states "the nucleic acid sequences encoding the proteins disclosed by either Lazar or Broun would share at least 90% or 95% sequence identity and would hybridize to each other under the defined stringency conditions". Therefore, it is unpredictable whether modifications to DNA/protein will retain the desired functional activity and that sequence identity alone cannot be used to predictably determine the function of a protein/DNA. The Examiner also states that no transgenic plant with a desired phenotype has been disclosed. Therefore, given the lack of guidance, the unpredictability, lack of working examples, and the state of the art, one skilled would not be able to practice the invention as broadly as claimed.

Applicants respectfully disagree. One of skill in the art does believe that structural identity, as well as the presence of functional domains and conserved motifs are predictive of polypeptide function, as is clearly demonstrated by the pervasive use of sequence searching algorithms such as BLAST, FASTA, and the like. As claimed, the structural identity, *i.e.* percent sequence identity is not the only criteria used, the disclosure also points out conserved functional motifs known in the art and the claims further recite a functional limitation that the encoded polypeptide is involved in DNA double-strand break repair. If the sequences of Lazar or Broun were similarly claimed, while the modified sequences may hybridize to the original sequence, they would not meet the functional limitation, and therefore would be explicitly excluded by the claim. Lazar discloses modifications to a human transforming growth factor α (TGF α) sequence, Broun discloses modifications to a oleate 12-desaturase sequence. Applicants wish to point out that both references use the known homology to related proteins to identify and target particular amino acids. The references used homology to predict important conserved amino acids where substitution with another amino acid would likely have an impact on the activity of the protein. For example, Lazar's study shows that even conservative substitution of L48 with similar amino acids (M or I) dramatically impacted activity, as

predicted by the absolute conservation of leucine (L) at this position. Broun et al. actually note the high sequence similarity between the oleate 12-desaturase and oleate hydroxylase and use this to identify seven residues conserved in desaturases and to target them for modification of activity (see page 131, column 2 – column 3). Broun et al. actually use the sequence similarity of the desaturase and the hydroxylase to predict which residues to change to alter the activity of the desaturase. In all cases, the modified protein had to be screened for the effect(s) of the modification. Similarly, the disclosure of SEQ ID NOS: 1-2, the conserved domains and motifs shown in Example 4 and known in the art, the sequence identity and similarity to other known Rad50 sequences (for example, pages 1-2, and Appendix A submitted 2/14/02), the guidance on sequence analyses, comparison, and identity, the guidance on codon degeneracy, silent variants, and preferences, the guidance on conservative amino acid substitutions, the guidance on nucleic acid isolation and evaluation, and the ready availability in the art for assays for Rad50 (see above) show the specification coupled with the knowledge in the art enables a person in the art to make and use sequences having at least 90% or 95% sequence identity to SEQ ID NO: 1, or that hybridize to the full-length complement of SEQ ID NO: 1 and encode Rad50 polypeptides involved in DNA double-strand break repair.

The Examiner cites Amgen Inc. Chugai Pharmaceutical Co. Ltd., 18 USPQ 2d 1016 at 1021 and 1027 (Fed. Cir. 1991). At page 1021 it is taught that a gene is not reduced to practice until the inventor can define it by its “physical or chemical properties” and at page 1027 it is taught that the disclosure of a few sequences did not enable claims broadly drawn to any analog thereof.

In *Amgen v. Chugai*, the Federal Circuit concluded that the patent specification was insufficient to enable one of ordinary skill in the art to make and use the invention claimed in claim 7 of the '008 patent without undue experimentation. As stated on page 1027, however, “it is not necessary that a patent applicant test all the embodiments of his invention, In re Angstadt, 537 F.2d 498, 502, 190 USPQ 214, 218 (CCPA 1976); what is necessary is that he provide a

disclosure sufficient to enable one skilled in the art to carry out the invention commensurate with the scope of his claims. For DNA sequences, that means disclosing how to make and use enough sequences to justify grant of the claims sought.” Applicants respectfully submit, that has been done in the instant specification. The present invention discloses how to make and use the sequences of the invention, *i.e.* sequences having at least 90% identity to SEQ ID NO: 1, as discussed in the paragraph above.

The question of experimentation is a matter of degree. The fact that some experimentation is necessary does not preclude enablement; what is required is the amount of experimentation must not be unduly extensive. *PPG Inc. v. Guardian Industries Corp.* (37 USPQ 1218, 1623, (Fed. Cir. 1996). The test is not merely quantitative, since a considerable amount of experimentation is permissible, if it is merely routine, or if the specification in question provides a reasonable amount of guidance with respect to the direction in which the experimentation should proceed to enable the determination of how to practice a desired embodiment of the invention claimed. *Ex parte Jackson*, 217 USPQ 804, 807 (1982 PTOBA).

With the guidance provided in the present specification, one skilled in the art can readily practice the claimed invention. Therefore, it is respectfully requested that the rejection of claims 2-8, 12, 14-39 under 35 U.S.C. §112, first paragraph be withdrawn.

Response to Arguments

The Examiner maintains that the rejection of the claims was proper given that the claimed nucleic acid sequence of SEQ ID NO: 1 or nucleic acid sequences encoding SEQ ID NO: 2 do not have a specific utility because “ATP-dependent DNA binding” activity is not a specific function. Therefore, one skilled in the art cannot readily use SEQ ID NO: 1 or nucleic acid sequences encoding SEQ ID NO: 2 to achieve a desired agronomic trait in a plant without further research, therefore the rejection is maintained.

Applicants respectfully disagree with the Examiner's conclusion that "ATP-dependent DNA binding" is not a specific function when considered in light of the specification and claims directed to the Rad50 sequences SEQ ID NO: 1 and 2. It is a specific function associated with Rad50 polypeptides and is associated with the DNA repair activity. However, in order to expedite prosecution, Applicants have amended claims 12, 14 and 20 to recite that the polypeptide is involved in double-strand DNA break repair, a known function of Rad50. Further, Applicants believe they have properly addressed the rejection of the claims under 35 U.S.C 101 and 112, 1st paragraph, and respectfully request that these rejections be withdrawn.

Rejections under 35 U.S.C. §112, 1st Paragraph, Written Description:

Claims 2-8, 12, and 14-39 are rejected under 35 U.S.C. §112, first paragraph, as containing subject matter not sufficiently described in the specification to indicate the inventor(s) had possession of the invention.

The Examiner asserts that the claimed invention does not meet the current written description requirements because ATP-dependent DNA binding activity is not a specific function, the specification only described SEQ ID NO: 1 the isolated encoding SEQ ID NO: 2, and that substantial variation is expected among polynucleotides comprising 30 contiguous bases of SEQ ID NO: 1 or encoding 25 contiguous amino acids of SEQ ID NO: 2. The Examiner also states that since the Applicant has not described a single species of the polynucleotides of claims 12, 14, 16-17, 20-21, and 39, the specification fails to sufficiently describe the claimed invention in such full, clear, concise, and exact terms that one skilled in the art would recognize that Applicants are in possession of the invention as broadly claimed. The dependent claims comprising the polynucleotides are therefore similarly not described.

Applicants respectfully disagree, the specification does clearly indicate that the Applicants had possession of the invention as claimed. As stated above, ATP-dependent DNA binding activity is a specific function, however to expedite

examination, Applicants have amended claims 12, 14, and 20 to recite that the encoded polypeptides are involved in double-strand DNA break repair. Further, as stated above, the specification discloses full-length Rad50 sequences (SEQ ID NO: 1 & 2) comprising known functional and conserved regions, the ATCC deposited polynucleotide comprising SEQ ID NO:1, and further describes methods to isolate and analyze polynucleotides and polypeptides having a given percent sequence identity, and polynucleotides which hybridize to the full-length complement of SEQ ID NO: 1. The Examiner is reminded that every species encompassed by the claimed invention need not be disclosed in the specification to satisfy the written description requirement of 35 U.S.C. § 112, first paragraph. *Utter v. Hiraga*, 845 F.2d 993, 6 USPQ2d 1709 (Fed. Cir. 1988). In fact, the description of a claimed genus can be by structure, formula, chemical name, or physical properties. See *Ex parte Maizel*, 27 USPQ2d 1662, 1669 (B.P.A.I.1992), (citing *Amgen v. Chugai*, 927 F.2d 1200, 1206 (Fed. Cir. 1991)).

Claims 12 and 17 recite that the sequence shares at least 90% sequence identity to the sequence of SEQ ID NO: 1 or SEQ ID NO: 2, respectively. The recitation of at least 90% sequence identity is a very predictable structure of the sequences encompassed by the claimed invention. Further, as noted above, Applicants have provided guidance on conserved domains, and a multiple sequence alignment (Appendix A, 2/14/02) of SEQ ID NO: 2 with known Rad50 proteins. The description of a representative number of species does not require the description to be of such specificity that it would provide individual support for each species that the genus embraces. 66 Fed. Reg. 1099, 1106 (2000). Satisfactory disclosure of a "representative number" depends on whether one of skill in the art would recognize that the Applicants were in possession of the necessary common attributes or features of the elements possessed by the members of the genus in view of the species disclosed. 66 Fed. Reg. 1099, 1106 (2000). Applicants submit that the knowledge and level of skill in the art would allow a person of ordinary skill to

envision the claimed invention, *i.e.*, a sequence having at least 90% sequence identity to the sequence set forth in SEQ ID NO: 1 or 2.

A genus of DNAs may be described by means of a recitation of a representative number of DNAs, defined by nucleotide sequence, falling within the scope of the genus, or by means of a recitation of structural features common to the genus, which features constitute a substantial portion of the genus. Regents of the University of California v. Eli Lilly & Co., 119 F.3d 1559, 1569 (Fed. Cir. 1997); see also Guidelines for Examination of Patent Applications Under the 35 U.S.C. 112, first paragraph, "Written Description" Requirement, 66 Fed. Reg. 1099, 1106 (2000). The recitation of a predictable structure of at least 90% sequence identity to SEQ ID NO: 1 or 2 is sufficient to satisfy the written description requirement.

In addition, an Applicant may rely upon functional characteristics in the description, provided there is a correlation between the function and structure of the claimed invention. *Id.*, citing Lilly at 1568. Claims 12 and 17 recite that the claimed sequences are, or encode, a polypeptide involved in double-strand DNA break repair (Rad50) thereby providing a functional characterization of the sequences claimed in the genus.

Example 14 of the Revised Interim Written Description Guidelines is directed to a generic claim: a protein having at least 95% sequence identity to the sequence of SEQ ID NO:3, wherein the sequence catalyzes the reaction $A \rightarrow B$. The Training Materials concludes that the generic claim of Example 14 is sufficiently described under § 112, first paragraph, because 1) "the single sequence disclosed in SEQ ID NO:3 is representative of the genus" and 2) the claim recites a limitation requiring the compound to catalyze the reaction from $A \rightarrow B$.

Following the analysis of Example 14, Applicants submit that claims 12 and 17 satisfy the written description requirements of § 112, first paragraph, one of skill in art would recognize that the Applicants were in possession of the necessary common attributes possessed by the members of the genus. The claims recite a defined structural parameter, *i.e.* percent sequence identity, and further recite a

functional requirement, *i.e.* encoding a polypeptide involved in DNA double strand break repair. This functional requirement is the specific description of the function of Rad50. Specifically, the claims of the present invention encompass sequences having at least 90% sequence identity to the sequence of SEQ ID NO: 1 or 2 (structural parameter), wherein the claimed sequences encode a polypeptide involved double-strand DNA break repair (Rad50) activity (functional parameter). Claim 14 also follows the format of Example 14. The recitation of a polynucleotide which selectively hybridizes to the full length complement of SEQ ID NO: 1 under explicit high stringency hybridization and wash conditions and which encodes a polypeptide involved in double-strand DNA break repair also follows the guideline for claiming a genus of sequences by coupling a structural parameter, *i.e.* hybridization, and a functional parameter, *i.e.* encoding a polypeptide involved in DNA double strand break repair.

Consequently, contrary to the Examiner's conclusion, the sequences encompassed by the genus of claims 12, 14 and 17 are defined by relevant identifying physical and chemical properties. In fact, the common attributes or features of the elements possessed by the members of the genus is that they are Rad50 sequences and share at least 90% sequence identity to the disclosed sequences of SEQ ID NOS: 1 or 2, or which selectively hybridize to the full-length complement of SEQ ID NO: 1 under high stringency conditions. The necessary common features of the claimed genus are clear.

Applicants have disclosed a full-length isolated polynucleotide and the encoded Rad50 polypeptide in SEQ ID NOS: 1 and 2, and have provided further guidance on sequence isolation, analysis, and identification, codon degeneracy, conserved protein domains and motifs, as well as conservative amino acid substitutions. Applicants clearly had possession of sequences having at least 90% or 95% sequence identity to SEQ ID NO: 1 or 2, therefore the rejection of claims 2-8, 12, and 14-39 are rejected under 35 U.S.C. §112, first paragraph written description should be withdrawn.

Rejections under 35 U.S.C. §102:

Claim 39 is rejected under 35 U.S.C. §102(b) as being anticipated by Dolganov (in Sequence Search Result). Dolganov teaches an isolated nucleic acid sequence encoding a polypeptide having at least 31 contiguous amino acids of SEQ ID NO: 2.

In order to expedite prosecution, claim 39 has been cancelled, thereby obviated the rejection under 35 U.S.C. §102. Therefore, Applicants respectfully request that the rejection be withdrawn.

CONCLUSION

In light of the foregoing remarks and amendments, it is believed that claims 2-8, 12, 14 and 18-38 are in condition for allowance. Withdrawal of the outstanding rejections and allowance of all of the remaining claims is respectfully requested.

Respectfully submitted,



Virginia Dress
Agent for Applicant(s)
Registration No. 48,243

PIONEER HI-BRED INTERNATIONAL, INC.
Corporate Intellectual Property
7100 N.W. 62nd Avenue
P.O. Box 1000
Johnston, Iowa 50131-1000
Phone: (515) 270-4192
Facsimile: (515) 334-6883

Molecular Evolution of Glutamate Receptors: A Primitive Signaling Mechanism that Existed Before Plants and Animals Diverged

Joanna Chiu,* Rob DeSalle,† Hon-Ming Lam,‡ Lee Meisel,* and Gloria Coruzzi*

*Department of Biology, New York University; †Department of Entomology, American Museum of Natural History, New York, New York; and ‡Department of Biology, The Chinese University of Hong Kong, Shatin, Hong Kong

We performed a genealogical analysis of the ionotropic glutamate receptor (iGluR) gene family, which includes the animal iGluRs and the newly isolated glutamate receptor-like genes (*GLR*) of plants discovered in *Arabidopsis*. Distance measures firmly placed the plant *GLR* genes within the iGluR clade as opposed to other ion channel clades and indicated that iGluRs may be a primitive signaling mechanism that predated the divergence of animals and plants. Moreover, phylogenetic analyses using both parsimony and neighbor joining indicated that the divergence of animal iGluRs and plant *GLR* genes predated the divergence of iGluR subtypes (NMDA vs. AMPA/KA) in animals. By estimating the congruence of the various glutamate receptor gene regions, we showed that the different functional domains, including the two ligand-binding domains and the transmembrane regions, have coevolved, suggesting that they assembled together before plants and animals diverged. Based on residue conservation and divergence as well as positions of residues with respect to functional domains of iGluR proteins, we attempted to examine structure-function relationships. This analysis defined M3 as the most highly conserved transmembrane domain and identified potential functionally important conserved residues whose function can be examined in future studies.

Introduction

Ionotropic glutamate receptors (iGluRs) were first discovered in vertebrates, in which they have been shown to be involved in mediating fast neuronal responses in excitatory synapses via the amino acid neurotransmitter L-glutamate (Sprengel and Seeburg 1995). Two classes of animal glutamate receptors exist: iGluRs, which are ligand-gated ion channels, and metabotropic glutamate receptors (mGluRs), which are G-protein-linked receptors. Vertebrate iGluRs are pharmacologically classified into three major groups based on their ligand selectivity: (1) AMPA (α -amino-3-hydroxy-5-methyl-4-isoxazole propionate), (2) KA (kainate), and (3) NMDA (*N*-methyl-D-aspartate). Very often, the AMPA and KA receptors are further grouped together as non-NMDA types due to their sequence similarity and cross-reactivity. That is, AMPA receptors can respond to kainate as well as AMPA and vice versa. Besides these three major classes of iGluRs, there are two other classes of iGluRs that are related to the AMPA/KA class with respect to sequence similarity: the delta class (Yamazaki et al. 1992; Lomeli et al. 1993) and the kainate-binding proteins (Gregor et al. 1989; Wada et al. 1989). The delta class includes $\delta 1$ and $\delta 2$ subunits that were isolated in rat and mouse brain cDNA libraries. Although researchers have yet to demonstrate that the wild-type delta genes encode proteins with ion channel activity, a mutation in $\delta 2$ shown to cause a neurodegenerative disorder in Lurcher mice results in a constitutively open ion channel as tested in *Xenopus laevis* oocytes (Zuo et al. 1997). Using electrophysiological techniques, Rosenmund, Stern-Bach, and Stevens (1998) presented data that indicate iGluR channels exist as tet-

rameric structures, much like the voltage-gated potassium channels (Doyle et al. 1998). In contrast, other groups previously presented data to support a pentameric structure for iGluRs (Premkumar and Auerbach 1997) similar to the acetylcholine receptor, another ligand-gated ion channel. Ionotropic glutamate receptors can either be homomeric or heteromeric. In both cases, each subunit is encoded by a single gene, and depending on the subunit composition of the channel, the functional properties of the channel differ. All identified animal iGluRs contain six conserved domains that are believed to be functionally important. These include the two ligand-binding domains (GlnH1 and GlnH2, also known as S1 and S2) that have similarity to a glutamine-binding protein (GlnH) in *Escherichia coli* (Nakanishi, Shneider, and Axel 1990; Stern-Bach et al. 1994), and the four transmembrane domains (M1–M4) (fig. 1A). M2 is believed to be a major part of the pore and is important in the selective filtering of ions (Wo and Oswald 1995). Unlike the other three transmembrane domains, M2 was proposed not to span the membrane, thus exposing the two ligand-binding domains to the extracellular side of the membrane (fig. 1B) (Hollmann, Maron, and Heinemann 1994; Bennett and Dingledine 1995). It was suggested that the two ligand-binding domains act in concert on the extracellular side of the membrane to provide a ligand-binding site (Stern-Bach et al. 1994).

While iGluRs were originally discovered in vertebrates, more recently they have been identified in invertebrates, including *Caenorhabditis elegans* (Maricq et al. 1995), and *Drosophila melanogaster* (Schuster et al. 1991; Ultsch et al. 1992, 1993). A deletion mutation in *C. elegans* *glr-1* suggests a role for these receptors in mechanosensation and signal transduction (Maricq et al. 1995). Surprisingly, putative iGluRs have also recently been identified in an organism lacking a nervous system, the model plant *Arabidopsis thaliana* (Lam et al. 1998). The similarity between the plant *GLR* genes and the an-

Key words: glutamate receptor, evolution, plant, *Arabidopsis thaliana*, ion channel, structure-function relationship.

Address for correspondence and reprints: Gloria Coruzzi, Department of Biology, New York University, 100 Washington Square East, New York, New York 10003.

Mol. Biol. Evol. 16(6):826–838, 1999

© 1999 by the Society for Molecular Biology and Evolution. ISSN: 0737-4038

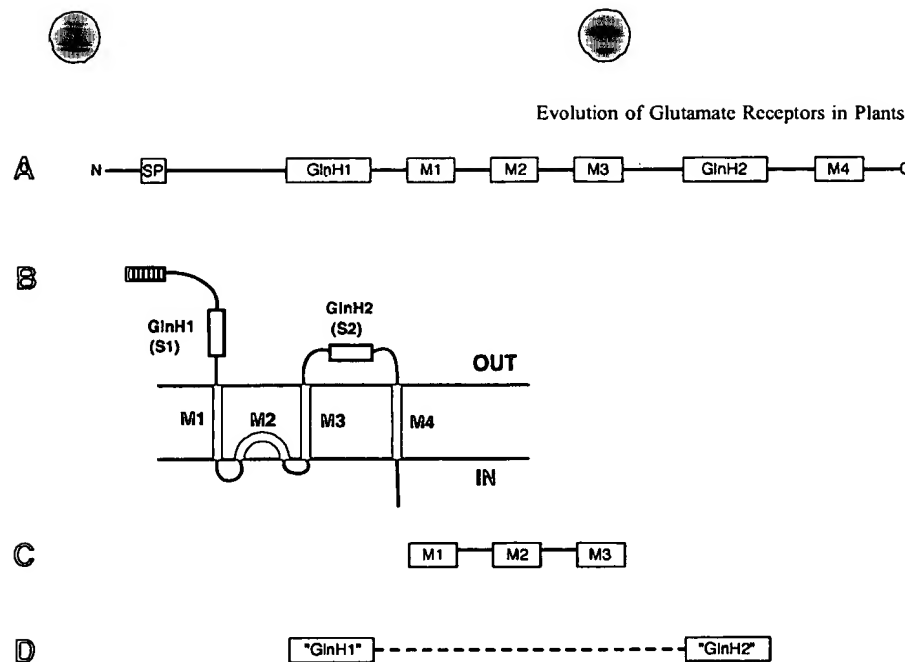


FIG. 1.—A, Diagrammatic representation of the iGluR protein showing the important functional domains, the two ligand-binding domains (GlnH1 and GlnH2), and the four transmembrane domains (M1–M4). SP at the N-terminal end represents the signal peptide. N and C represent the amino- and carboxy-terminal ends, respectively. B, Diagram showing the current model of the membrane topology of animal iGluRs. C, Diagram of the three transmembrane domains used in the ION analysis. D, Diagram showing the bacterial periplasmic amino-acid-binding protein and its putative region of homology with the animal iGluR proteins.

imal iGluRs spans all the important domains that are conserved among the animal iGluRs, including the two ligand-binding domains and the four transmembrane segments (M1–M4). The highest similarity between plant *GLR* genes and animal iGluRs is observed in M3, in which the percentage of identity is above 60% (data not shown). Currently, there are at least four plant *GLRs*. Based on sequence similarity, the plant genes seem to be more closely related to the non-NMDA class of animal iGluRs, but the exact classification has yet to be determined functionally in a heterologous expression system. In planta studies using iGluR antagonists suggest plant *GLRs* may be involved in light signal transduction (Lam et al. 1998). The discovery of iGluRs in plants suggests that signaling by excitatory amino acids in human brains has evolved from a primitive signaling mechanism that existed prior to the divergence of plants and animals.

In this study, we performed a phylogenetic analysis of the iGluR gene family of plants and animals. By including the plant *GLR* genes in the analysis, we examined how the plant genes fit into the evolutionary history of these receptors. By examining the genealogy of the iGluR gene family, we also attempted to make predictions concerning the functional properties of the plant receptors based on residue conservation. Moreover, by looking at amino acid character state changes, we identified residues that are invariant or are diagnostic of the various classes of iGluRs. Absolutely conserved residues are likely to be functionally important, while class-specific variations may control subtype specificity for ligand. By correlating this information to the location of the residue within the gene as well as the functional properties of the various receptor classes, we identified possible structure–function relationships.

Materials and Methods

Sequences

The animal glutamate receptor channel genes used in this study were obtained from GenBank. Table 1 lists all of these genes and their GenBank accession numbers. The four putative plant glutamate receptors were isolated by a combination of cDNA screening and genomic and EST sequence analysis as described in Lam et al. (1998) and are included in this study. We used a two-step approach in examining the plant *GLR* genes. First, we aligned and compared them with amino acid sequences of various kinds of ion channels (animal glutamate receptors, potassium channels, acetylcholine receptors, and GABA_A receptors) in the database to determine if reasonable similarity to any ion channel genes could be established at least in the transmembrane domains (ION analysis). These genes are listed in tables 1 and 2 with their GenBank accession numbers. The second step was to limit the study to glutamate receptors only (GLU analysis). Bacterial periplasmic amino-acid-binding protein gene sequences from *Escherichia*, *Salmonella*, and an archaebacteria (also listed in table 1) were obtained and used as outgroups.

Alignment

CLUSTAL was used to align all amino acid sequences. All alignments using the default parameters in CLUSTAL for both the GLU and ION analyses showed large regions of difficult-to-align amino acids. We therefore implemented a “culling” procedure (Gatesy, DeSalle, and Wheeler 1993) to remove alignment-ambiguous regions.

In the ION analysis, in which we used several kinds of ion channel genes, only three transmembrane domains were used in our alignments in the following way.

Table 1
GenBank Accession Numbers and Abbreviations for All Glutamate Receptors and Bacterial Periplasmic Amino-Acid-Binding Proteins Examined in this Study

Gene	Species	Accession Number	Abbreviation Used (if different from gene name)
Animal glutamate receptors			
hNMDAR1	<i>Homo sapiens</i>	D13515	
rNMDAR1	<i>Rattus norvegicus</i>	X63255	
$\sigma 1$	<i>Mus musculus</i>	D10028	
rNR2A	<i>R. norvegicus</i>	M91561	
rNR2B	<i>R. norvegicus</i>	M91562	
rNR2C	<i>R. norvegicus</i>	M91563	
rNR2D	<i>R. norvegicus</i>	L31612	
dNMDAR1	<i>Drosophila melanogaster</i>	X71790	
NMDAR	<i>Xenopus laevis</i>	X94156	frogglur
r $\delta 1$	<i>R. norvegicus</i>	Z17238	
r $\delta 2$	<i>R. norvegicus</i>	Z17239	
GluH1	<i>H. sapiens</i>	M64752	
$\alpha 1$	<i>M. musculus</i>	X57497	
rGluRK2	<i>R. norvegicus</i>	X54655	ratk2
rGluRC	<i>R. norvegicus</i>	M36420	
rGluR6	<i>R. norvegicus</i>	Z11715	
$\beta 2$	<i>M. musculus</i>	D10054	
rKA1	<i>Rattus rattus</i>	X59996	
h-EAA2	<i>H. sapiens</i>	S40369	humeaa2
$\gamma 2$	<i>M. musculus</i>	D10011	
dGluR1	<i>D. melanogaster</i>	M97192	
dGluR2	<i>D. melanogaster</i>	M73271	
GLR1	<i>Caenorhabditis elegans</i>	U34661	celegansglr1
Putative GluR	<i>C. elegans</i>	Z75545	celegansglur
GluR3/C	<i>Gallus gallus</i>	X89509	gallusglur3
GluR-II	<i>Columba livia</i>	S47031	pigeonglur
GluR4	<i>Carassius auratus</i>	U12018	goldfishglur
fGluR2Ac	<i>Oreochromis nilotica</i>	L46366	cichlidglur
fGluR2A	<i>Tilapia nilotica</i>	L34036	fishglur
GluR	<i>Lymnaea stagnalis</i>	ACGAE	snailglur
GluR-K1	<i>L. stagnalis</i>	X87404	lymgglur
Plant GLRs			
GLR1	<i>Arabidopsis thaliana</i>	AF079998	
GLR2	<i>A. thaliana</i>	AF079999	
GLR3	<i>A. thaliana</i>	AF007271	
GLR4	<i>A. thaliana</i>	AC000098	
Bacterial periplasmic amino-acid-binding proteins			
glnH	<i>Escherichia coli</i>	X14180	ecolignh
glnP	<i>Archaeoglobus fulgidus</i>	AE001090	afggln
glnP	<i>Salmonella typhimurium</i>	U73111	salglnp

The entire amino acid sequences were trimmed to include only M1–M3 in glutamate receptors and the corresponding transmembrane regions in other ion channel genes (fig. 1C). Since no experimental data are available for assigning transmembrane identity to sequences of the plant GLRs at the present moment, the transmembrane regions of plant GLRs used in this study are predicted based on hydropathy plots and their alignment with animal glutamate receptors (data not shown). These sequences of only approximately 100 amino acids were then aligned using CLUSTAL and a gap-to-change cost of 10. These alignments were of inferior quality in the regions of proposed transmembrane identity as determined by CLUSTAL and showed extremely limited levels of similarity. In the GLU analysis, the entire amino acid sequences of all animal glutamate receptor genes and plant GLRs were aligned using three separate sets of alignment parameters (gap to change = 10, 20, 30).

These alignments were examined for regions of alignment stability (columns of amino acids that did not change from alignment cost to alignment cost) and ambiguity (as defined in Gatesy, DeSalle, and Wheeler 1993). The alignment-ambiguous amino acid columns were "culled" from the data matrix. All of these preliminary alignments are available on request from the authors.

Data Coding

Two data-coding issues involved in the analysis of these sequences were the coding of outgroups and the coding of long gaps. A major problem we encountered with incorporating outgroup sequences into our data matrices was the lack of amino acid similarity in several regions of the genes examined. For the GLU analysis, we chose two bacterial and one archaeobacterial periplasmic amino-acid-binding protein genes as outgroups.

Table 2
GenBank Accession Numbers and Abbreviations for Non-Glutamate-Receptor Ion Channel Genes Examined in this Study

Gene	Species	Accession Number	Abbreviation Used (if different from gene name)
Potassium channels			
MBK1 (Kv1.1)	<i>Mus musculus</i>	Y00305	
AKT1	<i>Arabidopsis thaliana</i>	X62907	
ECOKCH	<i>Escherichia coli</i>	L12044	
dShaker	<i>Drosophila melanogaster</i>	M17211	
KAT1	<i>A. thaliana</i>	M86990	
HuK4 (Kv1.2)	<i>Homo sapiens</i>	L02752	
dShab	<i>D. melanogaster</i>	M32659	
Raw3 (rKv3.4)	<i>Rattus rattus</i>	X62841	
mShal (Kv4.1)	<i>M. musculus</i>	M64226	
MIRK1	<i>M. musculus</i>	X73052	
GIRK1	<i>Rattus norvegicus</i>	L25264	
nIRK1	<i>Caenorhabditis elegans</i>	U40947	
PaK1	<i>Paramecium tetraurelia</i>	U19907	
Acetylcholine receptors			
$\alpha 1$	<i>Heliothis virescens</i>	AJ000399	worm $\alpha 1$
unc-38	<i>C. elegans</i>	X98600	
ACR-3	<i>C. elegans</i>	Y08637	
$\alpha 3$	<i>D. melanogaster</i>	Y15593	d $\alpha 3$
$\alpha 4-2$	<i>R. norvegicus</i>	AF007212	r $\alpha 4-2$
$\alpha 2$	<i>R. norvegicus</i>	L10077	r $\alpha 2$
γ	<i>M. musculus</i>	M30514	myachr
$\alpha 6$	<i>Gallus gallus</i>	X83889	g $\alpha 6$
$\alpha 8$	<i>G. gallus</i>	X52296	g $\alpha 8$
δ	<i>G. gallus</i>	K02903	g δ
$\alpha 6$	<i>H. sapiens</i>	Y16282	h $\alpha 6$
$\alpha 7$	<i>H. sapiens</i>	Y08420	h $\alpha 7$
GABA_A receptors			
GABA- ϵ	<i>H. sapiens</i>	Y09765	
GABA-p1	<i>M. musculus</i>	AF024620	
GABA-p3	<i>R. norvegicus</i>	D50671	
GABA- $\gamma 3$	<i>R. norvegicus</i>	X63324	
GABA- β	<i>D. melanogaster</i>	L17436	
GABA-rd1	<i>Aedes aegypti</i>	U28803	

Paas (1998) demonstrated that there are two major regions of supportable similarity between these bacterial genes and eukaryotic ionotropic glutamate receptor genes, and we chose to use these two regions as out-group sequences for rooting the eukaryotic ionotropic glutamate receptor analysis (fig. 1D). All other regions of the glutamate receptor genes that were deemed alignment-unambiguous (see above) that are not in these two regions were coded as missing in the outgroups (indicated by question marks in the matrix; fig. 2).

In many cases, long stretches of positions in our alignment showed gaps. We chose to gap code these positions so as not to heavily weigh these regions in phylogenetic analysis. Our gap coding was implemented as unordered, and indel events were coded as distinct on the basis of their lengths (DeSalle and Brower 1997). Figure 2 shows some examples of how we implemented the gap coding.

Phylogenetic Analysis

Phylogenetic analysis using parsimony (PAUP*; Swofford 1998) was used to infer phylogeny. All characters were equally weighted in all analyses. This weighting scheme allowed us to most efficiently and severely test hypotheses of relationships (Kluge 1997)

among the genes in this multiple gene family. For the ION analysis, uncorrected absolute distances between amino acid sequences of plant *GLRs* and various types of ion channel genes were calculated in PAUP* based on the data matrix which includes transmembrane regions only (fig. 3). Two different distance measures were generated in this analysis, one for M1–M3, and another one for M3 only. Characters 46–71 in this alignment were excluded in the distance calculation from M1 to M3. Dglur1 has an insertion in this region which created gaps in all other sequences. By excluding this region, we avoid the introduction of similarity due to the gaps present in all of the sequences. The range and mean values for each comparison were then computed using the distances between different plant *GLRs* and the members of each ion channel class.

For the GLU parsimony analysis, we implemented heuristic searches with 10 random-addition searches with TBR branch swapping to explore the tree space and narrowed the possibility that we obtained suboptimal trees. It was not necessary to place a limit on the number of trees saved in each search. When multiple equally parsimonious trees were obtained, we constructed strict-consensus trees to represent our phylogenetic hypothe-

A			B		
Alignment Region Position 1-34 (N terminal end of GlnH1)			Alignment Region Position 344-368 (Start of GlnH2)		
gallusglut3	EGTC-VGLAAEIA-KHGGKTKLIVG0	000TGA	COTNRV0771	GLHLSKGTGVAATPG	
rgluc0	EGTC-VGLAAEIA-KHGGKTKLIVG0	000TGA	COTNRV0771	GLHLSKGTGVAATPG	
goldfishglut3	EGTC-VGLAAEIA-KHGGKTKLIVG0	000TGA	COTNRV0771	GLHLSKGTGVAATPG	
ol	EGTC-VGLAAEIA-KHGGKTKLIVG0	000TGA	COTNRV0771	GLHLSKGTGVAATPG	
glut3	EGTC-VGLAAEIA-KHGGKTKLIVG0	000TGA	COTNRV0771	GLHLSKGTGVAATPG	
ciclidglut3	EGTC-VGLAAEIA-KHGGKTKLIVG0	000TGA	COTNRV0771	GLHLSKGTGVAATPG	
flabglut3	EGTC-VGLAAEIA-KHGGKTKLIVG0	000TGA	COTNRV0771	GLHLSKGTGVAATPG	
plagocglut3	EGTC-VGLAAEIA-KHGGKTKLIVG0	000TGA	COTNRV0771	GLHLSKGTGVAATPG	
ratgl3	EGTC-VGLAAEIA-KHGGKTKLIVG0	000TGA	COTNRV0771	GLHLSKGTGVAATPG	
eneigglut3	EGTC-VGLAAEIA-KHGGKTKLIVG0	000TGA	COTNRV0771	GLHLSKGTGVAATPG	
dgglut3	EGTC-VGLAAEIA-KHGGKTKLIVG0	000TGA	COTNRV0771	GLHLSKGTGVAATPG	
oeleaganglir1	EGTC-VGLAAEIA-KHGGKTKLIVG0	000TGA	COTNRV0771	GLHLSKGTGVAATPG	
β2	EGTC-VGLAAEIA-KHGGKTKLIVG0	000TGA	COTNRV0771	GLHLSKGTGVAATPG	
rgluc6	EGTC-VGLAAEIA-KHGGKTKLIVG0	000TGA	COTNRV0771	GLHLSKGTGVAATPG	
rt	EGTC-VGLAAEIA-KHGGKTKLIVG0	000TGA	COTNRV0771	GLHLSKGTGVAATPG	
hamaa3	EGTC-VGLAAEIA-KHGGKTKLIVG0	000TGA	COTNRV0771	GLHLSKGTGVAATPG	
rka1	EGTC-VGLAAEIA-KHGGKTKLIVG0	000TGA	COTNRV0771	GLHLSKGTGVAATPG	
lynglglut3	EGTC-VGLAAEIA-KHGGKTKLIVG0	000TGA	COTNRV0771	GLHLSKGTGVAATPG	
oeleaganglir2	EGTC-VGLAAEIA-KHGGKTKLIVG0	000TGA	COTNRV0771	GLHLSKGTGVAATPG	
dgglut2	EGTC-VGLAAEIA-KHGGKTKLIVG0	000TGA	COTNRV0771	GLHLSKGTGVAATPG	
r61	EGTC-VGLAAEIA-KHGGKTKLIVG0	000TGA	COTNRV0771	GLHLSKGTGVAATPG	
r62	EGTC-VGLAAEIA-KHGGKTKLIVG0	000TGA	COTNRV0771	GLHLSKGTGVAATPG	
hamaa1	EGTC-VGLAAEIA-KHGGKTKLIVG0	000TGA	COTNRV0771	GLHLSKGTGVAATPG	
reuda1	EGTC-VGLAAEIA-KHGGKTKLIVG0	000TGA	COTNRV0771	GLHLSKGTGVAATPG	
ol	EGTC-VGLAAEIA-KHGGKTKLIVG0	000TGA	COTNRV0771	GLHLSKGTGVAATPG	
ecrogglut3	EGTC-VGLAAEIA-KHGGKTKLIVG0	000TGA	COTNRV0771	GLHLSKGTGVAATPG	
gmda1	EGTC-VGLAAEIA-KHGGKTKLIVG0	000TGA	COTNRV0771	GLHLSKGTGVAATPG	
rwa2	EGTC-VGLAAEIA-KHGGKTKLIVG0	000TGA	COTNRV0771	GLHLSKGTGVAATPG	
rwa2b	EGTC-VGLAAEIA-KHGGKTKLIVG0	000TGA	COTNRV0771	GLHLSKGTGVAATPG	
rwa2c	EGTC-VGLAAEIA-KHGGKTKLIVG0	000TGA	COTNRV0771	GLHLSKGTGVAATPG	
GLR2	EGTC-VGLAAEIA-KHGGKTKLIVG0	000TGA	COTNRV0771	GLHLSKGTGVAATPG	
GLR4	EGTC-VGLAAEIA-KHGGKTKLIVG0	000TGA	COTNRV0771	GLHLSKGTGVAATPG	
GLR1	EGTC-VGLAAEIA-KHGGKTKLIVG0	000TGA	COTNRV0771	GLHLSKGTGVAATPG	
ecoliglnh	EGTC-VGLAAEIA-KHGGKTKLIVG0	000TGA	COTNRV0771	GLHLSKGTGVAATPG	
salglip	EGTC-VGLAAEIA-KHGGKTKLIVG0	000TGA	COTNRV0771	GLHLSKGTGVAATPG	
afgln	EGTC-VGLAAEIA-KHGGKTKLIVG0	000TGA	COTNRV0771	GLHLSKGTGVAATPG	

FIG. 2.—Examples of gap coding. Two regions from the glutamate receptor alignments are shown. In both examples, alignment using CLUSTAL resulted in the insertion of gaps longer than a single peptide. Such areas were recoded so as not to outweigh these regions in phylogenetic analysis. *A*, Alignment from position 1 to position 34 (our alignment positions) using CLUSTAL. Question marks denote gaps introduced by CLUSTAL. The three gaps in the plant *GLR* genes right after the space are the gaps in question. The column with 0 and 1 shows the recoded character states for these gaps. 0 indicates that no gaps are present, and 1 indicates the presence of two gaps. All question marks are treated as missing data in the phylogenetic analysis. *B*, Alignment from position 344 to position 368 (our alignment positions). Question marks denote gaps introduced by CLUSTAL. The two gaps in most sequences three positions to the left of the space are the gaps in question, and the column to the right of these two gaps represents the scoring system. (Accession numbers for these genes may be found in table 1.)

sis. The amino acid sequence character matrix used in the maximum-parsimony analysis was also analyzed using neighbor joining (Saitou and Nei 1987). Uncorrected absolute distances were calculated and analyzed by neighbor joining in PAUP*.

Node Robustness

We generated three measures of node robustness for all nodes in our parsimony analysis: bootstrap values (Felsenstein 1985), Bremer (1994) indices, and jackknife estimates (Farris et al. 1996). Bootstrap and jackknife analyses were performed using PAUP*, and Bremer indices were calculated using AUTODECAY (Eriksson 1996). Ten random-addition searches with TBR branch swapping were used for each replicate in bootstrap analysis and for the searches at each node for AUTODECAY analysis. For our neighbor-joining analysis, robustness of nodes was inferred using 1,000 bootstrap replicates performed by PAUP*.

Inhomogeneity Estimates

Estimates of the congruence of different gene regions were obtained through the ILD test developed by Farris et al. (1994, 1995) as implemented in PAUP*. We partitioned our data matrix between transmembrane domains (M), GlnH domains (GlnH), and domains outside

of these two areas (INTER) and tested for incongruence of these gene regions to see if there were significantly different phylogenetic signals emanating from the three different regions.

Character Mapping

The final data matrices were transported to MacClade (Maddison and Maddison 1992) and manipulated in that program. By using the "chart and trace" option in the program, we were able to examine the number of possible character states at each residue. We targeted regions from the transmembrane domains and the GlnH domains that had previously been determined as functional regions for analysis. In our analysis, we simply looked for regions of conservation as well as significant correlation of character changes with respect to changes in amino acids and functionality in the proteins.

Results and Discussion

Placement of Putative Plant Glutamate Receptors in the Context of Ion Channel Classes

Previous distance measures demonstrated a high degree of identity between plant *GLRs* and animal *iGluRs*, but did not accomplish a phylogenetic analysis (Lam et al. 1998). To determine where these plant *GLR* genes fit within the context of ion channel evolution, we constructed a matrix with amino acid sequences for the transmembrane domains from all *GLRs* in table 1 and all ion channel genes, including both ligand and voltage-gated ion channels, in table 2 (ION analysis). In addition to animal *iGluRs* which are shown to have extensive identity with the plant *GLRs* (Lam et al. 1998), we chose to examine the relationship of plant *GLRs* and other ion channel classes such as acetylcholine receptors, GABA_A receptors, and potassium channels due to structural similarities suggested in other reports (Hollmann, Maron, and Heinemann 1994; Bennett and Dingledine 1995; Wo and Oswald 1995). Glutamate receptors, nicotinic acetylcholine receptors, glycine receptors, serotonin receptors, γ -aminobutyric acid (GABA) receptors, etc. are all members of the ligand-gated ion channel superfamily (Barnard 1992). Although in the same superfamily, *iGluRs* are distinct in terms of primary structure (fig. 3) as well as membrane topology (fig. 4). The initial hypothesis based on generating hydropathy plots indicated that the animal glutamate receptor protein, like the nicotinic acetylcholine receptors, has four transmembrane segments (Hollmann et al. 1989). However, more in-depth investigation has now led to the current model, in which the second transmembrane segment of *iGluRs* does not actually span the membrane (Hollmann, Maron, and Heinemann 1994; Bennett and Dingledine 1995). This major structural difference distinguishes the *iGluRs* from other ligand-gated ion channels, but, on the other hand, it suggests a closer structural and functional relationship between *iGluRs* and other ion channels. For example, membrane-spanning M1 and M3 together with non-membrane-spanning M2 in glutamate receptors fit the description of a structure known as a pore loop,

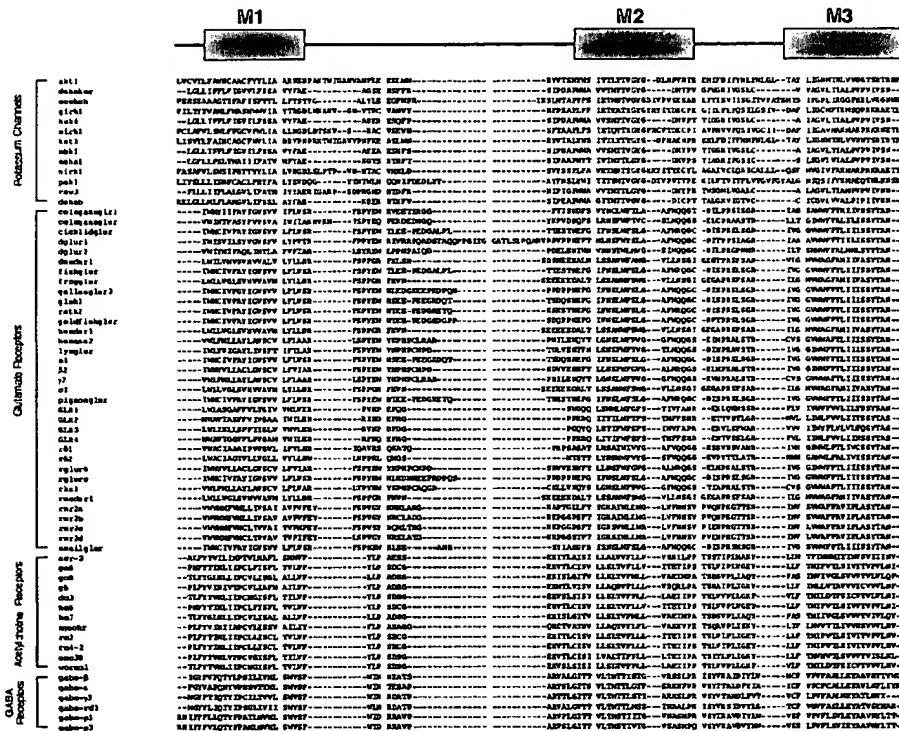


FIG. 3.—Alignment of animal and putative plant glutamate receptor transmembrane regions with several ion channel transmembrane regions that have putative similarity. Transmembrane regions 1–3 of glutamate, acetylcholine, and GABA_A receptors are used in this analysis. For potassium channels, regions S5, P, and S6 are used due to their suggested homology with M1–M3 of animal iGluRs (Wo and Oswald 1995). The three transmembrane regions were aligned by determining the limits of the three regions in all genes in the figure. The three transmembrane regions are labeled using the transmembrane region numbering for animal glutamate receptors. (Accession numbers for these genes may be found in tables 1 and 2.)

which is common in other ion channels, such as voltage-gated potassium, sodium, and calcium channels, as well as inward rectifier potassium channels and nucleotide-gated cation channels (MacKinnon 1995). Wo and Oswald (1995) reported conservation of amino acid residues between glutamate receptors and potassium channels within this functionally important region.

The main purpose of this first analysis was to attempt to discover elements of the plant *GLR* transmembrane sequences that might diagnose the plant *GLR* genes as glutamate receptors compared with other ion channels. We limited our analysis to relevant parts of the proteins which are possibly homologous across all the ion channels, i.e., the characters which make up the pore loop region in the potassium channels and the iGluRs and the corresponding transmembrane segments (M1–M3) in acetylcholine and GABA_A receptors (fig. 4). The resulting alignment (fig. 3) is unstable, as evidenced by drastic changes in alignment columns with slight changes in gap-to-change cost parameters (data not shown). The phylogenetic tree resulting from parsimony analysis is not strongly supported except for the node which groups the plant *GLRs* with the animal iGluRs and the nodes which group the members of the distinct ion channel classes (data not shown). This may indicate different evolutionary origins for the various ion channel classes, or it may simply indicate that it is not possible to homologize amino acid sequences in

transmembrane domains of iGluRs and other ion channels. In this respect, it is important to note that although Wo and Oswald (1995) suggested possible homology between transmembrane regions of potassium channels and animal iGluRs, our alignment leads us to suggest that this homology is doubtful. Instead, the similarity in the pore loop structure present in both classes of ion channels may be due to convergent evolution.

Distance calculations of the data matrix aligned in figure 3 are shown in figure 4. The smaller the distance value, the more closely related are the sequences compared. Although the ranges for absolute distances of the different categories overlap slightly when considering M1–M3 in glutamate receptors and the corresponding regions in other ion channels, the mean values indicate that the plant *GLRs* are most closely related (smaller distance values) to animal glutamate receptors. This result is strongly supported by previous analyses, such as hydropathy plots and BLAST searches (data not shown). This suggests that the plant *GLRs* have amino acid residues in their transmembrane domains that are diagnostic of animal glutamate receptor genes rather than other ion channel classes. In addition, when considering only M3 in glutamate receptors and the corresponding transmembrane domain in other ion channels, the absolute distances between plant *GLRs* and animal iGluRs decrease, while those between plant *GLRs* and non-glutamate-receptors increase dramatically.

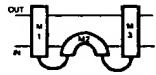
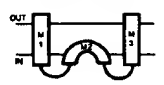
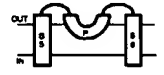
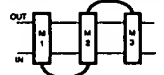
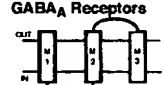
	<p style="text-align: center;">Plant GLRs</p> 
<p style="text-align: center;">Animal iGluRs</p> 	<p>M1-M3: Mean = 0.658 Range = 0.594-0.745</p> <p>M3 only: Mean = 0.537 Range = 0.368-0.737</p>
<p style="text-align: center;">Potassium Channels</p> 	<p>M1-M3: Mean = 0.833 Range = 0.708-0.934</p> <p>M3 only: Mean = 0.916 Range = 0.737-1.0</p>
<p style="text-align: center;">Acetylcholine Receptors</p> 	<p>M1-M3: Mean = 0.747 Range = 0.689-0.783</p> <p>M3 only: Mean = 0.926 Range = 0.789-1.0</p>
<p style="text-align: center;">GABA_A Receptors</p> 	<p>M1-M3: Mean = 0.769 Range = 0.736-0.792</p> <p>M3 only: Mean = 0.943 Range = 0.895-1.0</p>

FIG. 4.—Uncorrected absolute distances between plant *GLRs* and four classes of ion channels (animal iGluRs, potassium channels, acetylcholine receptors, and GABA_A receptors) based on the transmembrane region alignment shown in figure 3. The membrane topology for each of the different ion channels in the three transmembrane segments considered in this analysis is also shown here. For distance calculations using M1-M3 of glutamate receptors and the corresponding transmembrane regions in the other ion channels, characters 46-71 from the alignment shown in figure 3 are excluded. In this region, gaps are introduced in the alignment in all sequences due to an insertion in *dglur1* (see fig. 3). For distance calculations using only M3 of glutamate receptors and the corresponding regions of other ion channels, characters 1-117 were excluded. In each of the comparisons, uncorrected absolute distances for all different combinations of plant *GLRs* and members of each ion channel class were calculated using PAUP*. The mean value and the range were then computed and are presented. Note: The smaller the distance values, the more related the sequences.

The alignment of the transmembrane regions of the various ion channels brings renewed significance to the similarity observed in the transmembrane regions of the animal iGluRs and plant *GLRs*. Unlike the comparison between the transmembrane segments of glutamate receptor genes and other ion channel genes, which shows very limited similarity, the transmembrane regions of animal iGluRs and plant *GLRs* are similar not only in terms of hydrophobicity, but also in terms of primary sequence. This evidence supports common ancestry of animal iGluRs and plant *GLR* genes rather than convergence.

Based on the information from this analysis, we predict that the membrane topology of the *Arabidopsis*

GLRs will be similar to that of animal iGluRs where the second hydrophobic segment of the protein does not span the membrane, thus leaving the two ligand-binding domains on the extracellular side of the cell membrane (fig. 1B). This coincides with the prediction of TMPred analysis done on two of the plant *GLR* genes (Lam et al. 1998). Functional assays and membrane topology experiments will be required to confirm this prediction experimentally.

Plant Glutamate Receptor Genes in the Context of Glutamate Receptor Gene Evolution

The ION analysis described above suggests that the plant *GLR* genes belong to the iGluR family. The next step of our analysis was to examine where they fit into the evolutionary history within the iGluR receptor gene family. We therefore constructed a matrix composed of amino acid sequences from the glutamate receptor genes of plants and animals listed in table 1. One of the challenges of this analysis was to choose an appropriate outgroup. This is not straightforward, since no putative iGluRs have been uncovered in the genomes of eubacteria, archaeobacteria, or yeast whose entire genomes have been completely sequenced. However, a group of genes known as the bacterial periplasmic amino-acid-binding proteins has been known to share identity with one of the functionally important modules of the animal iGluRs, the ligand-binding domain GlnHs (Nakanishi, Shneider, and Axel 1990). It was suggested that perhaps with the rise of multicellularity, there was increased selection pressure toward the development of membrane proteins necessary for cell-cell signaling (Wo and Oswald 1995). We therefore used three noneukaryotic periplasmic amino-acid-binding protein sequences (two eubacteria and one archaeobacteria) that share similarity with the putative ligand-binding domains of iGluRs as outgroups (fig. 1D). Visual inspection of the alignments we obtained using the bacterial sequences as outgroups reveals a much greater degree of similarity when compared with the alignment in the ION analysis (fig. 2). However, the regions prior to the conserved GlnH1 and after GlnH2 showed no similarity and were easily "culled" (Gatesy, DeSalle, and Wheeler 1993) from the matrix.

Parsimony analysis of this glutamate receptor data matrix using the bacterial sequences as outgroups gave two equally parsimonious trees of 2,686 steps with a consistency index of 0.705 and a retention index of 0.782. Figure 5 shows the consensus parsimony tree with Bremer support and jackknife and bootstrap values. The plant *GLR* genes are consistently placed as the most basal group of glutamate receptors in the gene family, and the support for this arrangement is relatively robust (Bremer support at the node = 7; bootstrap at the node = 98%; jackknife at the node = 97%). Our neighbor-joining analysis generated a tree with a very similar topology and led to identical conclusion in terms of the placement of the plant *GLRs* (fig. 6). This placement indicates that the putative plant receptors diverged from the other animal iGluRs well before the various iGluRs that reside in animals (e.g., AMPA vs. NMDA) began

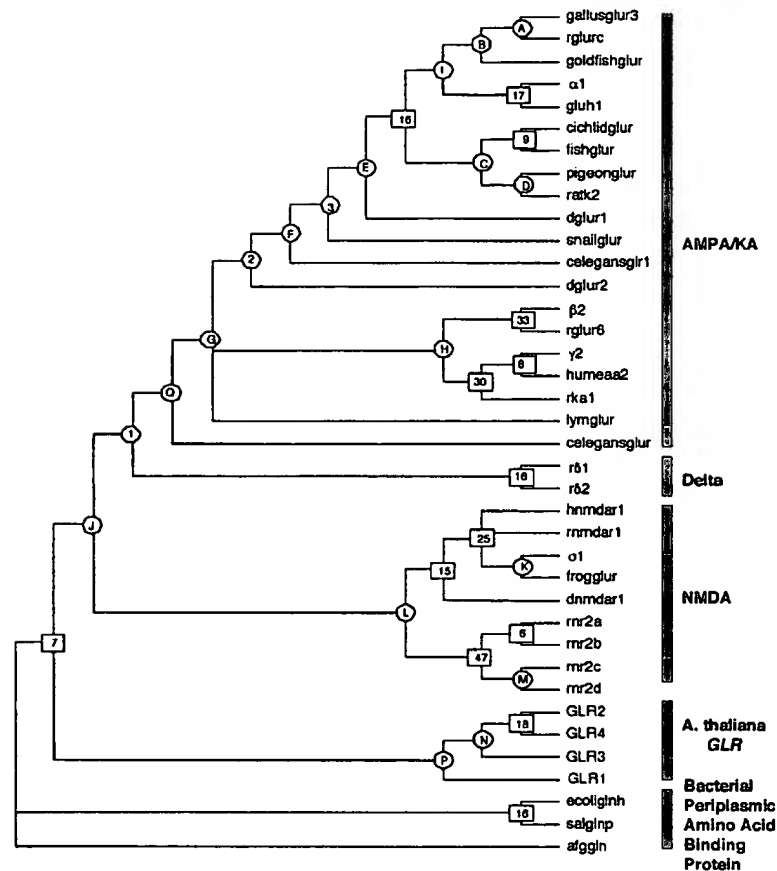


FIG. 5.—Phylogenetic tree generated from parsimony analysis of 35 glutamate receptor genes and 3 bacterial periplasmic amino-acid-binding protein sequences. This is the consensus of two most-parsimonious trees obtained from our search. Nodes are labeled in the following way: Nodes with squares on them are strongly supported. The number in the square is the Bremer support value, and all nodes with squares had bootstrap and jackknife values of 95%–100%. The nodes with circles on them are less strongly supported. Nodes with letters on them had Bremer support values, bootstrap values, and jack-knife values, respectively, as follows: A = 3/96/92, B = 2/72/77, C = 3/82/79, D = 3/85/83, E = 3/67/58, F = 10/84/88, G = 1/59/58, H = 8/80/83, J = 7/86/85, K = 1/60/52, L = 9/92/96, M = 1/74/66, N = 0/50/61, P = 6/97/92, and Q = 20/93/93. All other nodes with circles show the Bremer support value in the circle and at least one of the measures for robustness (bootstrap and jackknife) is less than 50%.

to diverge. In addition to the placement of the plant GLRs, the branch lengths in the neighbor-joining tree (fig. 6) also indicate that whereas most of the animal iGluRs, with the exception of snail, *C. elegans*, and *Drosophila* iGluRs, are very closely related, the plant GLRs show more significant differences. Moreover, our analysis establishes the relationship among members of the plant GLR gene family, in which GLR2 and GLR4 are related more closely to each other than to either GLR1 or GLR3. Members of each of the three subdivisions within the plant GLR gene family may represent proteins that have different functions, e.g., ligand selectivity, as in the case of animal iGluR subtypes. This hypothesis needs to be tested experimentally in future functional assays. According to this analysis, the members of the various classes of animal iGluRs, AMPA/KA, NMDA, and delta, each reside within their appropriate groups with strong node support. Previously, the cloned glutamate receptor gene (*glr-1*) from *C. elegans* was classified into the AMPA/KA family due to sequence similarity (Maricq et al. 1995). This analysis

supports the hypothesis, although no functional data are available at present.

Due to the early divergence of the plant genes, it is difficult to predict the function of putative glutamate receptors in plants. However, based on our phylogenetic trees (figs. 5 and 6), it is likely that the plant GLRs will have ligand-binding capability, since most of the animal GluRs retained the ligand-binding property of the bacterial periplasmic binding proteins. It is interesting to note that no ligand-binding or channel activity has been recorded with a class of animal iGluR genes known as the delta class. Wild-type delta genes showed no channel activity in heterologous systems such as *X. laevis* oocytes, even when glutamate, the natural ligand for glutamate receptors, was added to the bath solutions (Araki et al. 1993; Lomeli et al. 1993; Zuo et al. 1997). However, when a mutated form of the rat $\delta 2$ gene that causes the phenotype of the neurodegenerative Lurcher mice was used in similar experiments, the channels seemed to be constitutively open in the presence or absence of ligand (Zuo et al. 1997). This raises two major ques-

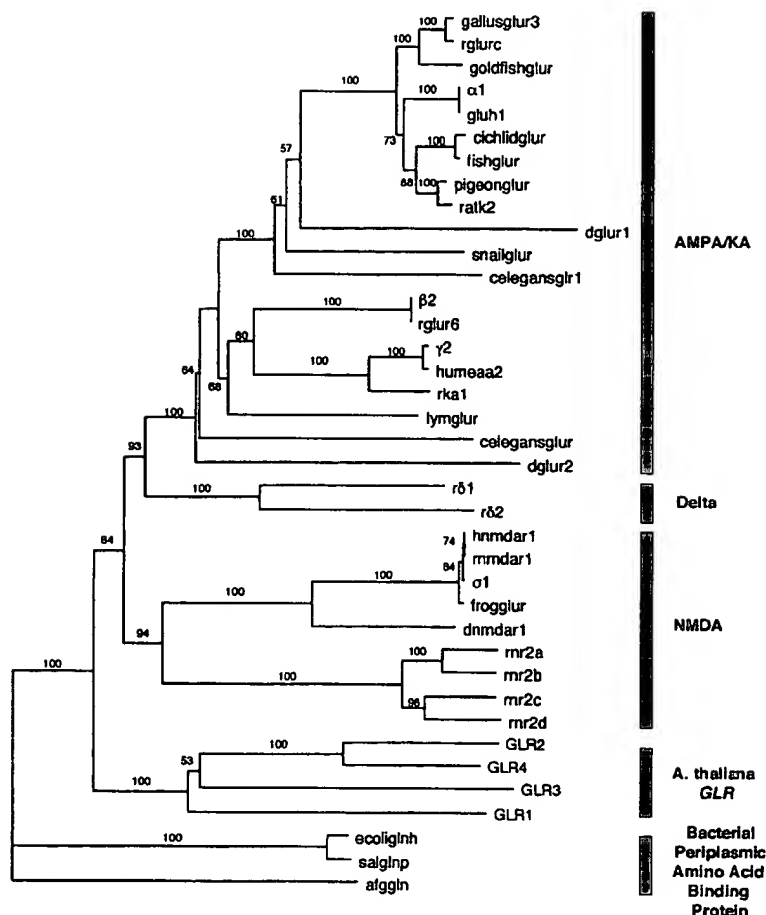


FIG. 6.—Phylogenetic tree generated from neighbor-joining analysis of 35 glutamate receptor genes and 3 bacterial periplasmic amino-acid-binding protein sequences showing branch lengths and bootstrap values. Uncorrected absolute distances were calculated from the same amino acid data matrix used in the maximum-parsimony analysis and analyzed by neighbor-joining in PAUP*. Bootstrap values are also generated in PAUP* and are shown for each of the nodes except one. The node which holds all the AMPA/KA genes except for *celegansglur* and *dglur2* collapses in the tree from the bootstrap analysis and is not shown here.

tions: (1) Do the plant *GLRs* retain ligand-binding ability? (2) Will they respond to the same ligand as the animal receptors, or can they be constitutively open? In the rat $\delta 2$ mutants, a single nucleotide alteration causes an alanine in M3 of the wild-type protein to change to a threonine in the mutant (Zuo et al. 1997). While most functional studies of animal iGluRs have concentrated on M2 due to the presence of RNA editing in this region, it is significant that the greatest sequence similarity between animal iGluRs actually resides in M3. The same thing is true when the plant *GLR* genes are aligned with the animal iGluRs (fig. 4). Due to the high sequence conservation of M3 among animal iGluRs and between plant *GLRs* and animal iGluRs, this region is suggested to have functional importance. The location of the mutation in the Lurcher mice (Zuo et al. 1997) in the M3 domain supports this hypothesis. A close examination of the residues in the plant *GLR* genes corresponding to the Lurcher mutation residue raises an interesting speculation. Instead of having a sequence of "LAA," as in wild-type delta proteins, the putative plant receptors have a sequence of "LTS" or "LAS" at the

corresponding location. Like in the case of the rat $\delta 2$ mutation, which results in "LAT" at that location, the crucial second alanine is altered. However, instead of changing alanine to a threonine, as in the rat $\delta 2$ mutant, it is substituted with serine in the plant proteins. The amino acid serine is very closely related to threonine in terms of charge and size and may confer similar functional properties. Although it is not likely that the putative plant channels are constitutively open, as in the case with the rat $\delta 2$ mutant, it is possible that they are constitutively open in certain cellular conditions, such as at certain extracellular ion concentrations. This and other possibilities are yet to be tested experimentally. On the other hand, perhaps these plant proteins do not function primarily via channel activity, but via protein-protein interactions. In this case, that would mean that channel activity actually evolved after the divergence of plants and animals.

Homogeneity of the Transmembrane Domains and the GlnH Domains

We tested the homogeneity of the phylogenetic signal in the transmembrane domains versus that in the

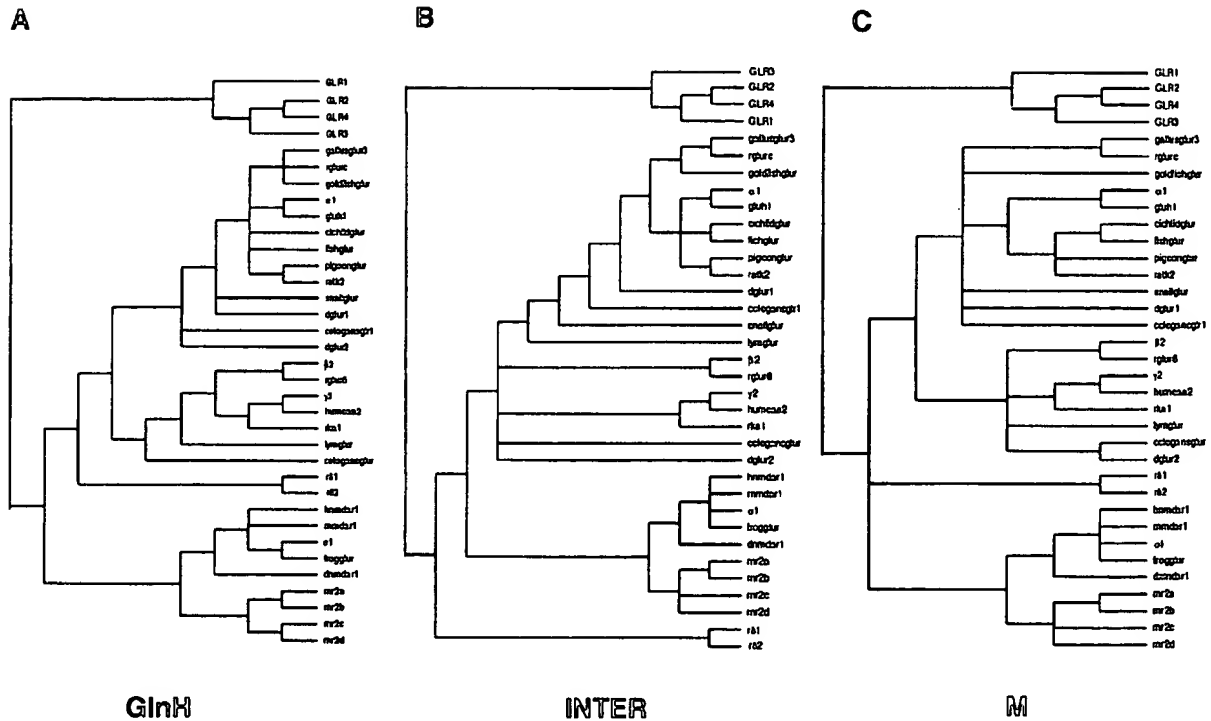


FIG. 7.—*A*, Consensus tree generated using parsimony for the GlnH regions of 35 glutamate receptor genes. There were 16 most-parsimonious trees of length 811; consistency index (CI) = 0.667 and retention index (RI) = 0.755. *B*, Consensus tree generated using parsimony for the regions of 35 glutamate receptor genes that lie between the GlnH and transmembrane domains. There were eight most-parsimonious trees of length 1,036; CI = 0.749 and RI = 0.810. *C*, Consensus tree generated using parsimony for the transmembrane regions of 35 glutamate receptor genes. There were 26 most-parsimonious trees of length 699; CI = 0.735 and RI = 0.818.

GlnH domains using the ILD test devised by Farris et al. (1994, 1995). This test was implemented to determine if the phylogenetic signals emanating from two (or more) data partitions are homogeneous. We reasoned that an inference of homogeneity of the two kinds of regions would be indicative of a common evolutionary history or linkage. In this case, the hypothesis that these regions were united in an exon-shuffling scenario late in evolution would be rejected. In contrast, inhomogeneity would be indicative of incongruent evolutionary history, and the hypothesis that these two regions of the gene coevolved before plants and animals diverged would be rejected. Figure 7 shows the individual phylogenetic analyses of the three partitions (transmembrane domains [M], ligand-binding domains [GlnH], and the regions [INTER] between the transmembrane domains and GlnH domains) we erected. Visual inspection of these trees indicates some evident topological differences. However, statistical analysis of the incongruence length difference reveals no statistically significant incongruence among the three partitions (M vs. GlnH: $P = 0.87$; INTER vs. M: $P = 0.44$; INTER vs. GlnH: $P = 0.84$). These results indicate that the transmembrane domains and GlnH domains have most likely coevolved since their assembly before the divergence of plants and animals.

Predicting Function from Sequence

By including the plant *GLRs* in our analysis, we have the opportunity to identify residues of the iGluR

proteins that were conserved before the divergence of plant *GLRs* and animal iGluRs. Since these residues have not mutated throughout the evolution of iGluRs, they are most likely functionally important residues that are crucial to the basic operations of these receptors. The invariant residues in plant *GLRs* and animal iGluRs are presented in figure 8A. Conservation is apparent in a stretch of characters at the end of M3. Several invariant residues are also present in the ligand-binding domains, GlnH1 and GlnH2. In addition, two tryptophan residues (W) are universally conserved in M1 and M2, respectively. Whereas at least one of these residues has been studied in mutagenesis experiments—mutations of R499 result in nonfunctional channels (Uchino et al. 1992)—published data from mutagenesis studies are not available on other invariant residues identified in this study. By conducting mutagenesis studies on these universally invariant residues, one should be able to gain insight into possible structure–function relationships.

On the other hand, by recognizing the difference in the locations of conserved regions in the different classes of iGluRs, we hope to identify regions of the proteins that may cause them to function differently, e.g., ligand and ion selectivity. In addition, by comparing the plant genes with the different classes of animal iGluRs separately (NMDA, AMPA/KA, and delta), we hope to gain insight into the functional properties of the putative plant receptors. Residues that are conserved only between plant *GLRs* and each animal iGluR subclass are

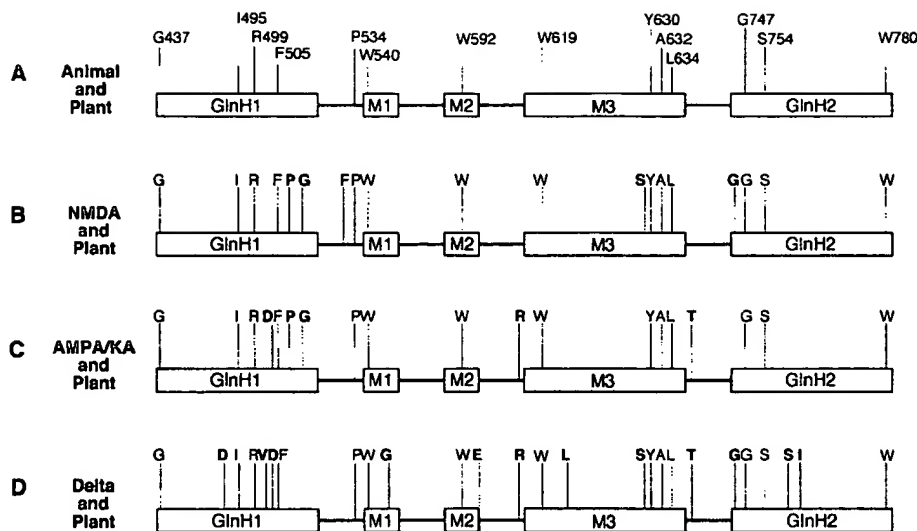


FIG. 8.—Diagrams showing the invariant residues between plant *GLRs* and different animal *iGluR* classes: all animal *iGluRs* (A), NMDA (B), AMPA/KA (C), and delta (D) *iGluRs*. In panel A, the positions of the invariant residues between plant *GLRs* and all animal *iGluRs* are given, and the numbers correspond to amino acid positions in the human *GluH1* gene (GenBank accession number M64752). The approximate positions of the conserved residues are shown in relation to the functional domains, GlnH1, M1–M3, and GlnH2. In panels B–D, residues that are invariant between all plant and animal genes are shown as in panel A. In addition, invariant residues between plant *GLRs* and each *iGluR* subclass (NMDA, AMPA/KA, and delta) are shown in bold. The residues shown in bold can be uniquely invariant between plant *GLRs* and one *iGluR* subclass or invariant between plant *GLRs* and two of the three *iGluR* subclasses. By definition, these residues have to be conserved among members of each *iGluR* subclass as well. In fact, the number of residues that are conserved in each *iGluR* gene class is underestimated by adding the plant genes to each of the three analyses. The boxes representing the domains do not reflect actual sequence length.

shown in bold in figure 8B–D. The phylogenetic analyses shown in figures 5 and 6 failed to classify the plant *GLRs* into one of the gene classes of *iGluRs*—NMDA, AMPA/KA, or delta—based on a comparison using all of the important functional domains. However, it is still possible that the plant *GLRs* may be more closely related to a certain class of *iGluR* when looking at individual functional domains. According to figure 8, this is not the case. There appears to be more conservation between the plant *GLRs* and the delta *iGluRs* in all functional domains. As mentioned earlier, the wild-type delta *iGluRs* have no channel activity (Araki et al. 1993; Lomeli et al. 1993; Zuo et al. 1997); therefore, it is possible that this is the case for the plant genes. However, it is interesting to note that two residues, proline (P) and glycine (G), present at the end of GlnH1 in NMDA and AMPA/KA are conserved in the plant *GLRs* but altered in the delta *iGluRs*. GlnH1 is believed to function as part of the ligand-binding site in *iGluRs*. Since NMDA and AMPA/KA *iGluRs* are both functional in terms of ligand-binding, the plant *GLRs* may have the capacity for ligand binding as well, but the presence of channel activity that is totally identical to NMDA and AMPA/KA *iGluRs* is another matter. It would be informative to conduct mutagenesis studies in which proline and glycine are altered in NMDA or AMPA/KA *iGluRs* to resemble the delta residues, or vice versa. Such studies will give us answers as to whether the delta *iGluRs* have lost proper ligand-binding ability due to the loss of these two conserved residues, or whether residues other than the two mentioned are also crucial.

Besides looking at residues in the *iGluR* proteins that are invariant between plants and animals, it is also

interesting to look at the differences between the two. To examine more detailed structure–function relationships in this respect, we isolated M3 and examined it more closely. M3 was chosen because it is the most conserved region of the protein, as observed in figures 4, 8 and 9, as well as in previous sequence alignment analyses (data not shown). Whereas it is believed that M2 serves as a major part of the channel pore (Sommer et al. 1991; Köhler et al. 1993), the function of M3 is not exactly clear yet. While most researchers have concentrated their studies on M2 due to its structural importance and RNA-editing property, the analysis presented here could identify residues that may be functionally important in M3. We identified residues that are conserved in all of the animal *iGluRs* (fig. 9A), as well as those that are conserved in both animal *iGluRs* and plant *GLRs* (fig. 9B) in M3. As observed in fig. 9, the longest stretch of conserved residues in animal *iGluRs* is at the end of M3 (YTANLA), although the sixth residue in M3, tryptophan (W), is strikingly conserved in both plant *GLRs* and animal *iGluRs*. When the plant *GLRs* are added to the analysis, the conservation generally decreases, but the level of conservation and the properties of the amino acids in the M3 C-terminal region barely change. In other cases, possible amino acid character states added to the animal character states (shown in bold) by the addition of the plant genes are sometimes quite different in terms of amino acid charge and size. This is apparent in characters 1, 9, 14, 15, and 20. For character 1 in M3, two of the four plant *GLRs* (*GLR1* and *GLR4*) have an aromatic phenylalanine (F) instead of a nonaromatic amino acid such as isoleucine (I) or valine (V). Although this character is not extreme-

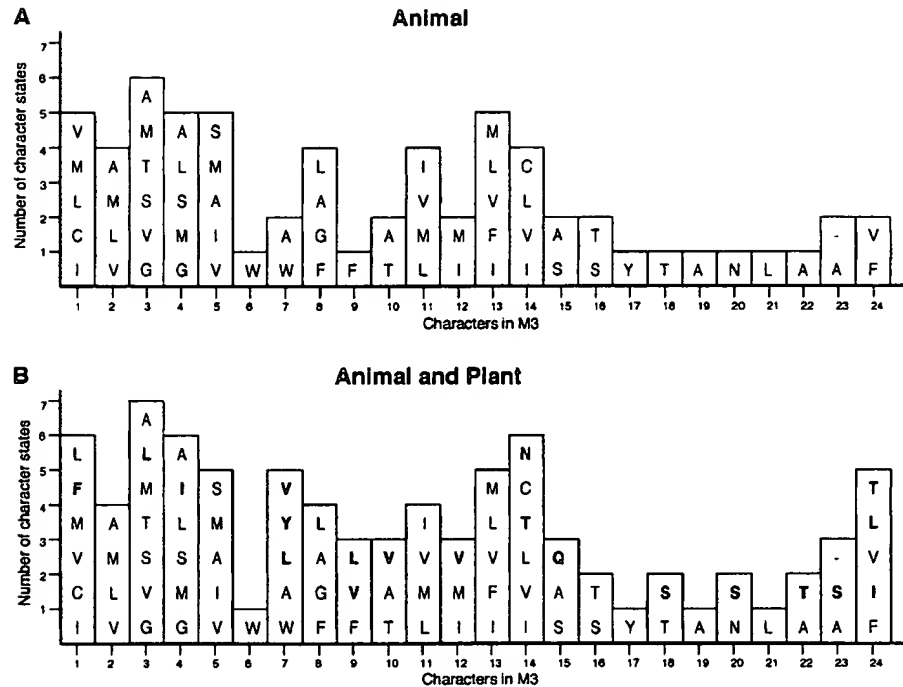


FIG. 9.—Graphs showing the number of possible character states at each amino acid position in M3 in the GLU analysis. The number of possible amino acids is shown on the Y-axis, and the amino acid positions in M3 from the N-terminal to the C-terminal end are shown from left to right on the X-axis. Character 1 in M3 corresponds to amino acid position 614 in the human GluH1 gene (GenBank accession number M64752). The possible amino acids at each character are shown inside the bar. The most common amino acid at each character is located at the bottom of each bar, while the least common is located at the top. *A*, The animal graph was generated by excluding the plant and bacterial genes. By using the trace character function in MacClade (Maddison and Maddison 1992), each character of M3 was examined, and the number of possible amino acids at each position was recorded. *B*, The animal-and-plant graph was generated by excluding only the bacterial genes. In the animal-and-plant graph, the amino acids in bold are added onto the possible character state list with the incorporation of the plant genes in the second graph.

ly conserved even in animal iGluRs with five possible character states, this drastic change in amino acid size and properties may have functional consequences. The case of character 9 in M3 seems to be the opposite of that of character 1 (fig. 9). Instead of having an aromatic phenylalanine (F) that is conserved in all of the animal iGluRs, the plant *GLRs* have nonaromatic leucine (L) or valine (V). Although these amino acids are similar in terms of hydrophobicity, their sizes are different. Therefore, if M3 is a structural part of the channel pore or vestibule, this character change may affect the selectivity and permeability of ions passing through the channels. In general, this part of the analysis points to possible sites for mutagenesis at which residues in animal iGluRs are altered to resemble the corresponding plant residues. Results of these studies can help to uncover the function of residues in M3 as well as the functional properties of the plant *GLRs*.

In conclusion, using the plant *GLR* genes as a tool to identify invariant residues may provide "fossil" evidence with which to explore how cell-cell signaling by excitatory amino acids in animal brains evolved from a primitive signaling mechanism that existed before plants and animals diverged. The fact that iGluRs appear to exist in plants and animals and not in the genomes of unicellular organisms whose genomes are completely sequenced suggests that cell-cell signaling in multicel-

lular organisms may predate the divergence of animals and plants.

Acknowledgments

We thank D. Swofford for advance access to PAUP version 4d64 and appreciate his permission to report results obtained from this program. This work was supported by NIH grant GM32877 to G.C.

LITERATURE CITED

- ARAKI, K., H. MEGURO, E. KUSHIYA, C. TAKAYAMA, Y. INOUE, and M. MISHINA. 1993. Selective expression of the glutamate receptor channel delta 2 subunit in cerebellar Purkinje cells. *Biochem. Biophys. Res. Commun.* 197:1267–1276.
- BARNARD, E. A. 1992. Receptor classes and the transmitter-gated ion channels. *Trends Biochem. Sci.* 17:368–374.
- BENNETT, J. A., and R. DINGLELINE. 1995. Topology profile for a glutamate receptor: three transmembrane domains and a channel-lining reentrant membrane loop. *Neuron* 14:373–384.
- BREMER, K. 1994. Branch support and tree stability. *Cladistics* 10:295–304.
- DESALLE, R., and A. BROWER. 1997. Process partitions, congruence and the independence of characters: inferring relationships among closely related Hawaiian *Drosophila* from multiple gene regions. *Syst. Biol.* 46:752–765.
- DOYLE, D. A., J. M. CABRAL, R. A. PFUETZNER, A. KUO, J. M. GULBIS, S. L. COHEN, B. T. CHAIT, and R. MACKINNON.

1998. The structure of the potassium channel: molecular basis of K⁺ conduction and selectivity. *Science* **280**:69–77.
- ERIKSSON, T. 1996. Autodecay. Version 2.9.2. Stockholm, Sweden.
- FARRIS, J. S., V. A. ALBERT, M. KALLERSJO, D. LIPSCOMB, and A. G. KLUGE. 1996. Parsimony jackknifing outperforms neighbor joining. *Cladistics* **12**:99–124.
- FARRIS, J. S., M. KALLERSJO, A. G. KLUGE, and C. BULT. 1994. Testing the significance of congruence. *Cladistics* **10**:315–320.
- FARRIS, J. S., M. KALLERSJO, A. G. KLUGE, and C. BULT. 1995. Constructing a significance test for incongruence. *Syst. Biol.* **44**:570–572.
- FELSENSTEIN, J. 1985. Confidence limits on phylogenies: an approach using the bootstrap. *Evolution* **39**:783–791.
- GATESY, J., R. DESALLE, and W. WHEELER. 1993. Alignment-ambiguous nucleotide sites and the exclusion of systematic data. *Mol. Phylogenet. Evol.* **2**:152–157.
- GREGOR, P., I. MANO, I. MAOZ, M. MCKEOWN, and V. I. TEICHBURG. 1989. Molecular structure of the chick cerebellar kainate-binding subunit of a putative glutamate receptor. *Nature* **342**:689–692.
- HOLLMANN, M., C. MARON, and S. HEINEMANN. 1994. N-glycosylation site tagging suggests a three transmembrane domain topology for the glutamate receptor GluR1. *Neuron* **13**:1331–1343.
- HOLLMANN, M., A. O'SHEA-GREENFIELD, S. W. ROGERS, and S. HEINEMANN. 1989. Cloning by functional expression of a member of the glutamate receptor family. *Nature* **342**:643–648.
- KLUGE, A. 1997. Testability and the refutation and corroboration of cladistics hypotheses. *Cladistics* **13**:81–96.
- KÖHLER, M., N. BURNASHEV, B. SAKMANN, and P. H. SEEBURG. 1993. Determinants of Ca²⁺ permeability in both TM1 and TM2 of high affinity kainate receptor channels: diversity by RNA editing. *Neuron* **10**:491–500.
- LAM, H. M., J. CHIU, M. H. HSIEH, L. MEISEL, I. C. OLIVEIRA, M. SHIN, and G. CORUZZI. 1998. Glutamate receptor genes in plants. *Nature* **396**:125–126.
- LOMELI, H., R. SPRENGEL, D. J. LAURIE, G. KÖHR, A. HERB, P. H. SEEBURG, and W. WISDEN. 1993. The rat delta-1 and delta-2 subunits extend the excitatory amino acid receptor family. *FEBS Lett.* **315**:318–322.
- MACKINNON, R. 1995. Pore loops: an emerging theme in ion channel structure. *Neuron* **14**:889–892.
- MADDISON, W. P., and D. R. MADDISON. 1992. *MacClade: analysis of phylogeny and character evolution*. Sinauer, Sunderland, Mass.
- MARICQ, A. V., E. PECKOL, M. DRISCOLL, and C. I. BARGMANN. 1995. Mechanosensory signaling in *C. elegans* mediated by the GLR-1 glutamate receptor. *Nature* **378**:78–81.
- NAKANISHI, N., N. A. SHNEIDER, and R. AXEL. 1990. A family of glutamate receptor genes: evidence for the formation of heteromultimeric receptors with distinct channel properties. *Neuron* **5**:569–581.
- PAAS, Y. 1998. The macro- and microarchitectures of the ligand-binding domain of glutamate receptors. *Trends Neurosci.* **21**:117–125.
- PREMKUMAR, L. S., and A. AUERBACH. 1997. Stoichiometry of recombinant N-methyl-D-aspartate receptor channels inferred from single-channel current patterns. *J. Gen. Physiol.* **110**:485–502.
- ROSENMUND, C., Y. STERN-BACH, and C. F. STEVENS. 1998. The tetrameric structure of a glutamate receptor channel. *Science* **280**:1596–1599.
- SAITOU, N. and M. NEI. 1987. The neighbor-joining method: a new method for reconstructing phylogenetic trees. *Mol. Biol. Evol.* **4**:406–425.
- SCHUSTER, C. M., A. ULTSCH, P. SCHLOSS, J. A. COX, B. SCHMITT, and H. BETZ. 1991. Molecular cloning of an invertebrate glutamate receptor subunit expressed in *Drosophila* muscle. *Science* **254**:112–114.
- SOMMER, B., M. KÖHLER, R. SPRENGEL, and P. H. SEEBURG. 1991. RNA editing in brain controls a determinant of ion flow in glutamate-gated channels. *Cell* **67**:11–19.
- SPRENGEL, R., and P. H. SEEBURG. 1995. Ionotropic glutamate receptors. Pp. 213–263 in R. A. NORTH, eds. *Handbook of receptors and channels: ligand- and voltage-gated ion channels*. CRC Press, Boca Raton, Fla.
- STERN-BACH, Y., B. BETTLER, M. HARTLEY, P. O. SHEPPARD, P. J. O'HARA, and S. F. HEINEMANN. 1994. Agonist selectivity of glutamate receptors is specified by two domains structurally related to bacterial amino acid-binding proteins. *Neuron* **13**:1345–1357.
- SWOFFORD, D. L. 1998. PAUP*. Test version 4d64. Laboratory of Molecular Systematics, Smithsonian Institution, Washington, D.C., Sinauer, Sunderland, Mass.
- UCHINO, S., K. SAKIMURA, K. NAGAHARI, and M. MISHINA. 1992. Mutations in a putative agonist binding region of the AMPA-selective glutamate receptor channel. *FEBS Lett.* **308**:253–257.
- ULTSCH, A., C. M. SCHUSTER, B. LAUBE, H. BETZ, and B. SCHMITT. 1993. Glutamate receptors of *Drosophila melanogaster*: primary structure of a putative NMDA receptor protein expressed in the head of the adult fly. *FEBS Lett.* **324**:171–177.
- ULTSCH, A., C. M. SCHUSTER, B. LAUBE, P. SCHLOSS, B. SCHMITT, and H. BETZ. 1992. Glutamate receptors of *Drosophila melanogaster*: cloning of a kainate-selective subunit expressed in the central nervous system. *Proc. Natl. Acad. Sci. USA* **89**:10484–10488.
- WADA, K., C. J. DECHESNE, S. SHIMASAKI, R. G. KING, K. KUSANO, A. BUONANNO, D. R. HAMPSON, C. BANNER, R. J. WENTHOLD, and Y. NAKATANI. 1989. Sequence and expression of a frog brain complementary DNA encoding a kainate-binding protein. *Nature* **342**:684–689.
- WO, Z. G., and R. E. OSWALD. 1995. Unraveling the modular design of glutamate-gated ion channels. *Trends Neurosci.* **18**:161–168.
- YAMAZAKI, M., K. ARAKI, A. SHIBATA, and M. MISHINA. 1992. Molecular cloning of a novel member of the mouse glutamate receptor channel family. *Biochem. Biophys. Res. Commun.* **183**:886–892.
- ZUO, J., P. L. DE JAGER, K. A. TAKAHASHI, W. JIANG, D. J. LINDEN, and N. HEINTZ. 1997. Neurodegeneration in Lurcher mice caused by mutation in $\delta 2$ glutamate receptor gene. *Nature* **388**:769–773.

NARUYA SAITOU, reviewing editor

Accepted February 25, 1999

Glutamate-receptor genes in plants

In animal brains, ionotropic glutamate receptors (GluRs) function as glutamate-activated ion channels in rapid synaptic transmission. We have now discovered that genes encoding putative ionotropic GluRs exist in plants, and we present preliminary evidence for their involvement in light-signal transduction. It may be that signalling between cells by excitatory amino acids in animal brains evolved from a primitive signalling mechanism that existed before the divergence of plants and animals. Our findings also help to explain why neuroactive compounds made by plants work on receptors in human brains.

We isolated from *Arabidopsis* two full-length complementary DNAs, *GLR1* and *GLR2*. Each of these cDNAs encodes all of the signature domains of animal ionotropic GluRs, including the 'three-plus-one'

transmembrane domains (M1 to M4) and the putative ligand-binding domains (GlnH1 and GlnH2), previously shown to be conserved between *Escherichia coli* glutamine permease (GlnH) and animal ionotropic GluRs¹ (Fig. 1). Hydrophathy plots, transmembrane prediction² and protein-sorting³ programs predict that the *Arabidopsis* *GLR* cDNAs encode a plasma-membrane signal peptide and four transmembrane domains (M1 to M4), of which M2 is predicted not to span the membrane (Fig. 1b). This membrane topology is analogous to animal ionotropic GluRs in which the putative ligand-binding GlnH domains are exposed to the external side of the membrane⁴.

In addition to their similar secondary structures, the *Arabidopsis* GLRs also share extensive sequence identity with animal ionotropic GluRs in the signature domains

GlnH1 (including the ligand-binding residue R), GlnH2, and M1 to M4, especially within M3 (Fig. 1a). The degree of identity between *Arabidopsis* GLRs and animal ionotropic GluRs within these domains (63% to 16%) is similar to that between animal ionotropic GluR subtypes that have kainate/AMPA rather than NMDA as agonists (60% to 32%). *Arabidopsis*, like animals, seems to have a family of expressed genes encoding ionotropic GluRs, as judged by the existence of other *GLR* genes (Fig. 1a) and northern blot analysis (data not shown). *GLR*-related genes also seem to exist in a variety of higher plants, including both dicotyledons (tobacco and pea) and monocotyledons (rice and maize), as judged by heterologous Southern blot analysis (not shown).

To investigate the possible *in vivo*

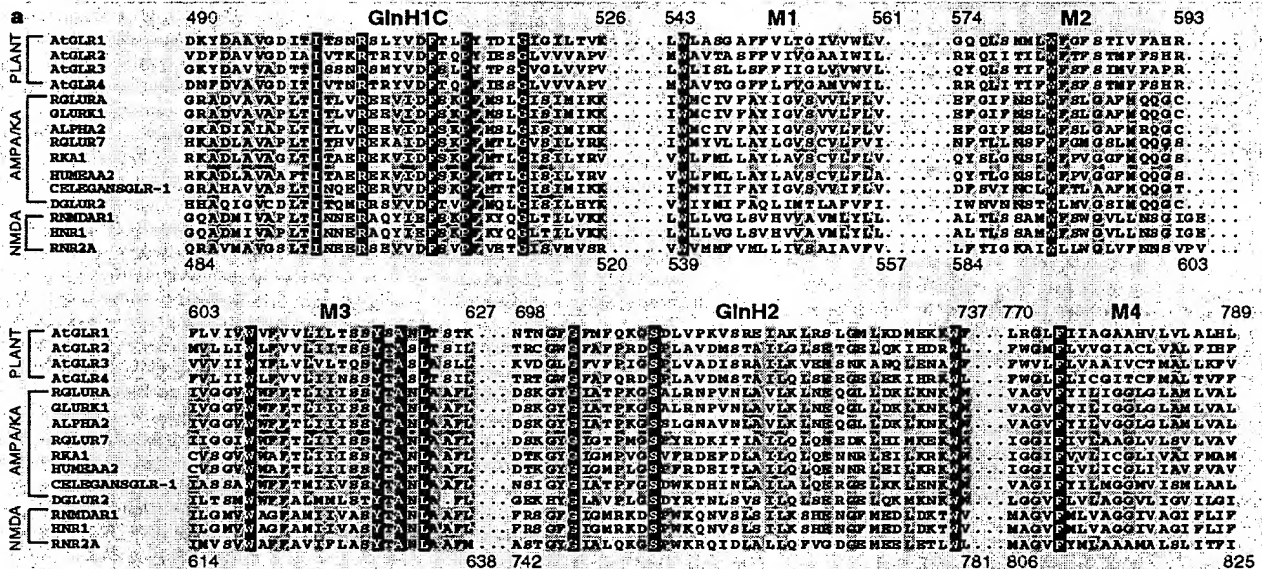


Figure 1 *Arabidopsis* *GLR* cDNAs encode proteins with sequence identity to animal ionotropic glutamate receptors. **a**, Sequence alignment of signature ionotropic GluR domains conserved between *Arabidopsis* *GLR* genes (*AtGLR1-4*) and animal ionotropic GluR subtypes using kainate/AMPA or NMDA as agonists. Numbers above the sequences correspond to residues of *Arabidopsis* *GLR1*; numbers underneath correspond to residues in rat *GluR1*. Residues between the conserved domains are shown as dots. *Arabidopsis* *GLR1* (Genbank accession no. AF079998) and *GLR2* (AF079999) sequences are from full-length cDNAs obtained by screening cDNA libraries with expressed sequence tag clones (accession nos T22862 and R29880, respectively). The *GLR2* cDNA corresponds to *Arabidopsis* genomic sequence (accession no. AC002329). *GLR3* and *GLR4* sequences were derived from *Arabidopsis* genomic sequences of a bacterial and yeast artificial chromosome clones (AF007271 and AC000088, respectively). Animal ionotropic GluR genes used in the alignment are: AMPA/kainate subtypes, accession numbers M36418, X17184, X57498, M83552, X59996, S40369, U34661, M73271; or NMDA subtypes, accession numbers X63255, L05666, M91561. Sequences were aligned using Clustal X⁶.

b, Transmembrane organization of *Arabidopsis* *GLR1* based on hydrophathy plot, TMpred² and PSORT³ analysis. Hydrophobic domains include a putative plasma-membrane signal sequence (hatched box) and four transmembrane domains M1-M4 (filled boxes), of which M2 is predicted not to span the membrane. Open boxes denote the two putative extracellular glutamate-binding domains GlnH1 and GlnH2 (also called S1 and S2), identified in animal ionotropic GluR genes as sharing sequence identity with *Escherichia coli* glutamine permease¹. GlnH1C denotes identity within the carboxy-terminal half of the GlnH1 domain.

function(s) of putative ionotropic GluRs in plants, *Arabidopsis* seedlings were grown in the presence of DNQX, an antagonist of animal kainate/AMPA ionotropic GluRs. Plants grown on media containing DNQX phenocopy *Arabidopsis* long-hypocotyl (*hy*) mutants impaired in light-signal transduction⁵, as judged by two independent criteria: DNQX at least partly blocks the ability of light to inhibit hypocotyl elongation (Fig. 2a–c) and to induce chlorophyll synthesis (Fig. 2d–f). Plants grown in the light in the presence of DNQX display a significant light- and dose-dependent increase in hypocotyl elongation compared with control untreated plants (Fig. 2b,c). This effect is specific for light, as the same DNQX concentration has no such effect in the dark (Fig. 2a). The increase in hypocotyl length in DNQX-treated plants (1.5- to 2-fold) is similar to that of *Arabidopsis hy* mutants

deficient in the synthesis of the phytochrome photoreceptor chromophore (*hy1* and *hy2*; 1.5- to 2.5-fold)^{5,6}.

Because light and hormones interact to control hypocotyl elongation, one or both may be responsible for the DNQX effect. We therefore measured the effects of DNQX on a second light-dependent process, chlorophyll synthesis. DNQX treatment impairs the ability of light to induce the synthesis of chlorophyll in plants grown in the dark and exposed to light for 5 hours (Fig. 2d–f). DNQX-treated plants exhibited a 60% reduction in light-induced chlorophyll accumulation (Fig. 2e) compared with controls (Fig. 2d). This effect is light specific as growth and chlorophyll levels are unaffected in DNQX-treated plants grown in the dark (Fig. 2a,f).

Taken together, these findings indicate that ionotropic GluRs may be involved in

light-signal transduction in plants. Because *Arabidopsis*, like animals, seems to possess a family of *GLR* genes, the *in planta* effects of DNQX-treated plants may be due to inhibition of one or more ionotropic GluR receptors *in vivo*.

The existence of putative ionotropic GluRs in plants is surprising, and provides an insight into why plants make chemicals that act on human brains. Several classical ionotropic GluR agonists that activate and define specific ionotropic GluR subtypes in brains are natural plant products. Examples include kainate, synthesized in the seaweed *Digenia simplex*, and quisqualic acid, found in *Quisqualis indica* seeds⁷. Other less well known plant-derived ionotropic GluR agonists include β -N-methyl-amino-L-alanine, produced in cycads, and β -N-oxalylamino-L-alanine, from chick-peas, both of which are associated with neurodegenerative diseases in animals⁷.

It is traditionally believed that plants produce such neurotoxins for defence against herbivory. However, the discovery of putative ionotropic GluRs in plants and their possible role in light-signal transduction suggest an alternative theory: that plants may synthesize ionotropic GluR agonists in order to regulate their endogenous ionotropic GluR receptors, and that selective pressure in certain species then led to high-level production for defence against herbivores.

The existence of putative glutamate receptors in plants raises the possibility that other neurologically active compounds made by plants (such as nicotine, cocaine and caffeine), which act on receptors in animal brains, may also act as ligands for endogenous receptors in plants to regulate a variety of as yet unknown cell-to-cell signalling systems in higher plants.

Hon-Ming Lam*, Joanna Chiu†, Ming-Hsiun Hsieh†, Lee Meisel†, Igor C. Oliveira†, Michael Shint†, Gloria Coruzzi†

* The Chinese University of Hong Kong, Shatin, New Territories, Hong Kong

† Department of Biology,

New York University, 1009 Main Building, 100 Washington Square East, New York, New York 10003, USA

e-mail: coruzzi01@mcrcr.med.nyu.edu

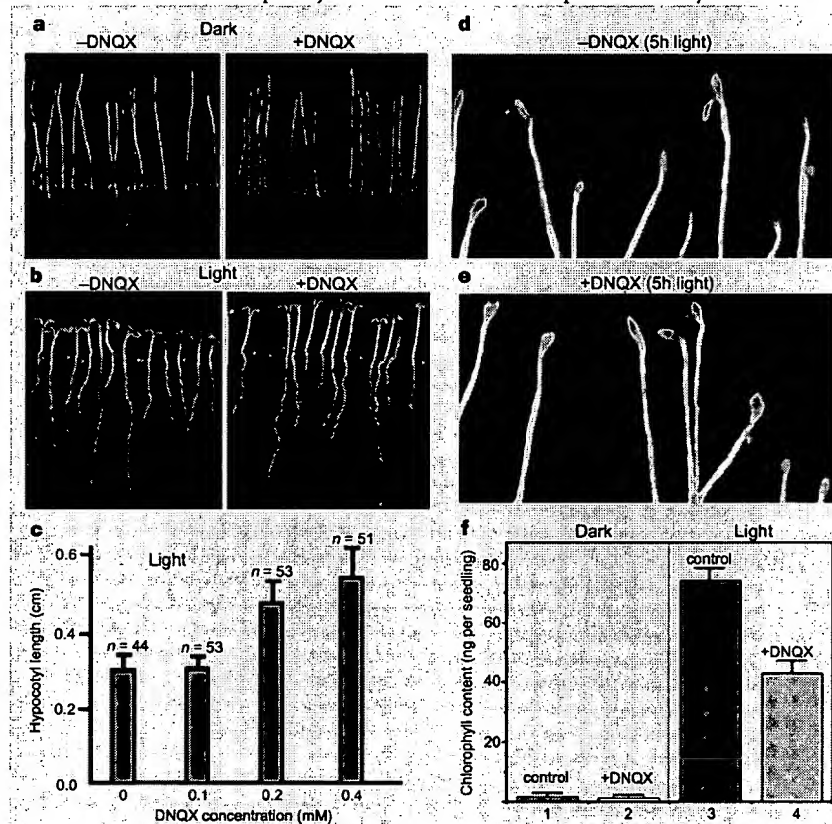


Figure 2 Effects of ionotropic GluR antagonist DNQX on *Arabidopsis* seedlings. Seedlings were sown on MS medium (Gibco BRL, Murashige and Skoog basal medium containing 3% sucrose and 0.9% Difco bactoagar) in the absence or presence of the ionotropic GluR antagonist DNQX. All plates contained the solvent dimethyl sulphoxide at 1.6 μ l per ml medium. **a–c**, Effect of DNQX on hypocotyl length. Seedlings were germinated for 7 days either in the dark (**a**) or in a normal day–night cycle (16 h light/8 h dark) at 22 °C in the presence (400 μ M) or absence of DNQX. Hypocotyl length was determined for light-grown seedlings (n , 44–51) germinated on 0, 100, 200 and 400 μ M DNQX (**c**). An unpaired *t*-test comparing values from control and DNQX treatments: 100 μ M DNQX (no significant difference); 200 μ M DNQX ($P < 0.0001$); 400 μ M DNQX ($P < 0.0001$). **d–f**, Effect of DNQX on light-induced chlorophyll levels. Seedlings were germinated in total darkness in the absence (**d**) or presence (**e**) of 400 μ M DNQX for 7 days. Plants were transferred to light for 5 h and chlorophyll levels quantified, in three separate pools of 30–40 seedlings grown in the dark (columns 1, 2) and subsequently exposed to light for 5 h (columns 3, 4) (**f**). An unpaired *t*-test indicates a significant difference ($P = 0.0031$) in chlorophyll levels between DNQX-treated and untreated controls in light-treated plants, and no difference in dark-grown plants.

1. Nakanishi, N., Schneider, N. A. & Axel, R. *Neuron* 5, 569–581 (1990).
2. Hofmann, K. & Stoffel, W. *Biol. Chem. Hoppe-Seyler* 374, 166 (1993).
3. Nakai, K. & Kanehisa, M. *Genomics* 14, 897–911 (1992).
4. Barinaga, M. *Science* 267, 177–178 (1995).
5. Koornneef, M., Rolff, E. & Spruit, C. J. P. Z. *Pflanzenphysiol.* 100, 147–160 (1980).
6. Goto, N., Yamamoto, K. T. & Watanabe, M. *Photochem. Photobiol.* 57, 867–871 (1993).
7. *Neurotoxins* (eds Adams, M. & Swanson, G.) *Trends Neurosci.* (suppl.) 20–22 (1996).
8. Thompson, J., Higgins, D. G. & Gibson, T. J. *Nucleic Acids Res.* 22, 4673–4680 (1994).

Arabidopsis Mutants Resistant to S(+)- β -Methyl- α , β -Diaminopropionic Acid, a Cycad-Derived Glutamate Receptor Agonist¹

Eric D. Brenner, Nora Martinez-Barboza, Alexandra P. Clark, Quail S. Liang, Dennis W. Stevenson, and Gloria M. Coruzzi*

Department of Biology, New York University, New York, New York 10003 (E.D.B., A.P.C., Q.S.L., G.M.C.); Department of Biology, City University of New York, New York, New York 10016 (N.M.-B.); and New York Botanical Garden, Bronx, New York 10458 (D.W.S.)

Ionotropic glutamate receptors (iGluRs) are ligand-gated ion channels that are the predominant neuroreceptors in the mammalian brain. Genes with high sequence similarity to animal iGluRs have been identified in Arabidopsis. To understand the role of Arabidopsis glutamate receptor-like (AtGLR) genes in plants, we have taken a pharmacological approach by examining the effects of BMAA [S(+)- β -methyl- α , β -diaminopropionic acid], a cycad-derived iGluR agonist, on Arabidopsis morphogenesis. When applied to Arabidopsis seedlings, BMAA caused a 2- to 3-fold increase in hypocotyl elongation and inhibited cotyledon opening during early seedling development. The effect of BMAA on hypocotyl elongation is light specific. Furthermore, BMAA effects on early morphogenesis of Arabidopsis can be reversed by the simultaneous application of glutamate, the native iGluR agonist in animals. To determine the targets of BMAA action in Arabidopsis, a genetic screen was devised to isolate Arabidopsis mutants with a BMAA insensitive morphology (*bim*). When grown in the light on BMAA, *bim* mutants exhibited short hypocotyls compared with wild type. *bim* mutants were grouped into three classes based on their morphology when grown in the dark in the absence of BMAA. Class-I *bim* mutants have a normal, etiolated morphology, similar to wild-type plants. Class-II *bim* mutants have shorter hypocotyls and closed cotyledons when grown in the dark. Class-III *bim* mutants have short hypocotyls and open cotyledons when grown in the dark, resembling the previously characterized constitutively photomorphogenic mutants (*cop*, *det*, *fus*, and *shy*). Further analysis of the *bim* mutants should help define whether plant-derived iGluR agonists target glutamate receptor signaling pathways in plants.

Glu is the predominant neurotransmitter in the brain. As a neurotransmitter, it activates Glu receptors at the post-synaptic membrane, which are involved in sensing environmental cues and in memory function (Nowak et al., 1984; Isquierdo and Medina, 1995; Tsien et al., 1996). Improper ionotropic Glu receptor (iGluR) function has been implicated in a variety of human diseases including Alzheimers and Parkinsons dementia (Ikonomidou and Turski, 1996; Forsythe and Barnes-Davies, 1997). One subgroup of Glu receptors is comprised of the iGluRs, which function as Glu-gated ion channels that convey rapid synaptic transmission. iGluRs are pharmacologically classified into subgroups based on agonist response. The two main iGluR subfamilies in animals are N-methyl-D-Asp (NMDA) and α -amino-3-hydroxy-5-methylisoxazole-4-propionic acid (AMPA)/kainate (KA) (non-NMDA) activated iGluRs (Ikonomidou and Turski, 1996; Forsythe and Barnes-Davies, 1997).

In plants, it appears that Glu may also act as a signaling molecule. Glu supplied to plant growth

media has been shown to alter the expression of genes encoding enzymes involved in amino acid metabolism (Lam et al., 1994, 1998b; Oliveira and Coruzzi, 1999). Despite the evidence that amino acids may act as signals in higher plants, the mechanism of amino acid sensing and signaling is poorly understood. Genes for putative amino acid sensors have been uncovered in Arabidopsis that have high sequence similarity to ionotropic Glu receptors of animals (Lam et al., 1998a; Chiu et al., 1999). Arabidopsis GLRs have all the signature features of animal iGLRs, including a plasma membrane signaling peptide, two putative ligand-binding domains, and a "three-plus-one" transmembrane region (Lam et al., 1998a; Chiu et al., 1999).

To assess the function of putative Glu receptor genes in plants, Arabidopsis seedlings were treated with the iGluR antagonist 6,7 dinotroquinoxaline 2,3(1H, 4H) dione (DNQX), known to block AMPA/KA iGLRs in animals (Muller et al., 1989). It was shown that DNQX inhibits two key aspects of seedling photomorphogenesis in Arabidopsis: light-induced hypocotyl shortening and light-induced greening (Lam et al., 1998a). To further explore the targets of AtGLR function in plants, we tested whether other compounds known to block iGluR function in animals could also block aspects of Ara-

¹ This work was supported by the National Institutes of Health (grant no. GM32877 to G.C.), the National Institutes of Health postdoctoral fellowship (to E.B.), and a Humana fellowship from the City University of New York (to N.M.).

* Corresponding author; e-mail gloria.coruzzi@nyu.edu; fax 212-995-4204.

bidopsis growth and development. Several of these iGluR agonists are plant-derived products: kainate (KA; Monaghan et al., 1989; Bettler and Mulle, 1995) made by seaweed (*Digenea simplex*); β -N-oxalylamino-L-alanine (Ross et al., 1989) made by chickpeas (*Lathyrus* sp.), and BMAA (Copani et al., 1991) made by cycads. BMAA [S(+)- β -methyl- α , β -diaminopropionic acid] has been detected in members of the family Cycadaceae or "cycads" (Pan et al., 1997). Cycads are believed to be the most primitive of gymnosperms, whose remnant surviving members descended from the Mesozoic and the Paleozoic when cycads predominated the vegetation (Chamberlain, 1919). BMAA was first isolated as the suspected cause of Parkinsonians dementia complex and amyotrophic lateral sclerosis in Guam's Chamorro human population, where consumption of *Cycas circinalis* L., a local food source, was prevalent (Whiting, 1963; Spencer et al., 1987). Subsequent to its detection and purification, BMAA has been shown to cause neural degeneration in primates when supplemented in their food (Spencer et al., 1987). Because BMAA is a natural plant product that blocks iGluR function in animals, we decided to test whether it would have any effect on plant GLRs using Arabidopsis as a model. In this study, we show that BMAA promotes hypocotyl elongation and inhibits cotyledon opening when applied to light-grown Arabidopsis seedlings. To identify the targets of BMAA action in plants, we used BMAA as a pharmacological tool to screen for Arabidopsis mutants resistant to BMAA-induced changes in photomorphogenesis. The isolation and preliminary characterization of these mutants is described below.

RESULTS

BMAA, a Cycad-Derived Glu Receptor Agonist, Causes a Long Hypocotyl Phenotype in Arabidopsis

To probe the putative function of AtGLR genes in plants, we sought to determine whether the iGluR agonist, BMAA, caused any observable phenotypic effects on plant growth when supplied to Arabidopsis seedlings. Arabidopsis seedlings were germinated and cultivated on Murashige and Skoog media in the presence or absence of BMAA. BMAA-treated seedlings were evaluated for phenotypic alterations in treated plants compared with untreated control plants. At 8 d post-germination, the hypocotyls of seedlings grown in the light on Murashige and Skoog media containing 50 μ M BMAA, displayed elongated hypocotyls (Fig. 1A), compared with control untreated plants (Fig. 1B). The effect of BMAA on hypocotyl elongation was quantified. A dose-dependent response was observed at increasing concentrations of BMAA (Fig. 2A). In light-grown plants, a concentration of 20 μ M BMAA caused an increase in length of approximately 30%, and 50 μ M BMAA caused approx-

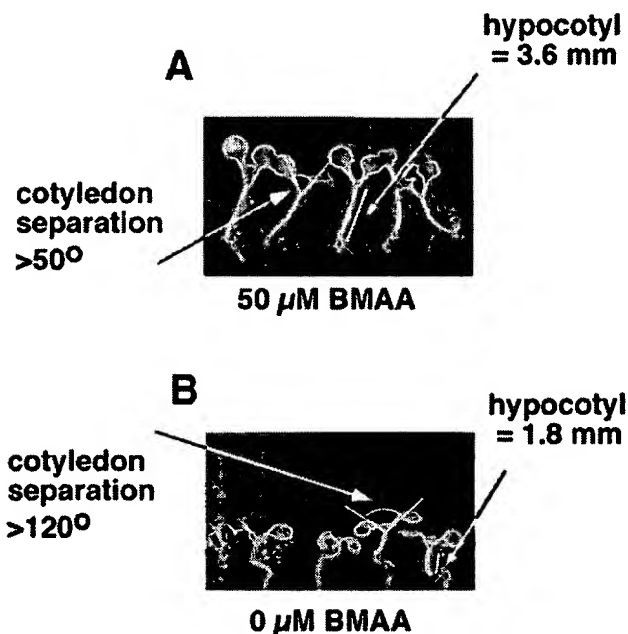


Figure 1. BMAA causes hypocotyl elongation and inhibits cotyledon unfolding in light-grown Arabidopsis. Arabidopsis plants were germinated and cultivated on Murashige and Skoog media and 0.7% (w/v) agar containing 50 μ M BMAA (A) or no BMAA (B) for 8 d in the light. The average hypocotyl length for each treatment, as well as the arc-angle of opening for the cotyledons, is shown ($n = 30$).

imately a 100% increase in hypocotyl length when compared with untreated plants (Fig. 2A). The effect on hypocotyl elongation is weaker at 100 μ M BMAA, and at greater concentrations (200 μ M) BMAA becomes inhibitory to growth (data not shown). In contrast, BMAA does not induce hypocotyl elongation in dark-grown plants (Fig. 2B). Instead, BMAA has an increasingly negative effect on hypocotyl length in dark-grown plants at concentrations of 50 μ M or greater (Fig. 2B). BMAA was also inhibitory to root growth (Fig. 1A). BMAA also inhibits cotyledon opening in the light (Fig. 1A). The arc of cotyledon opening is reduced to 50° in BMAA-treated plants (Fig. 1A) when compared with 120° in control plants (Fig. 1B).

To determine whether the effects of BMAA (a Glu analog) could be reversed by Glu (the native agonist of iGluRs in animals), plants treated with 25 μ M BMAA were grown on media containing increasing amounts of L-Glu (Fig. 3). The BMAA-induced effects on hypocotyl elongation and inhibition of cotyledon opening can be partially reversed by the simultaneous addition of L-Glu to the growth media (Fig. 3, A and B). The L-Glu reversal of the BMAA effects occurs in a dose-dependent manner. BMAA-induced hypocotyl elongation is reversed by approximately 50% with 1 mM L-Glu and by approximately 100% with 10 mM L-Glu (Fig. 3A). BMAA-induced inhibition of cotyledon opening is reversed by 20% with 1

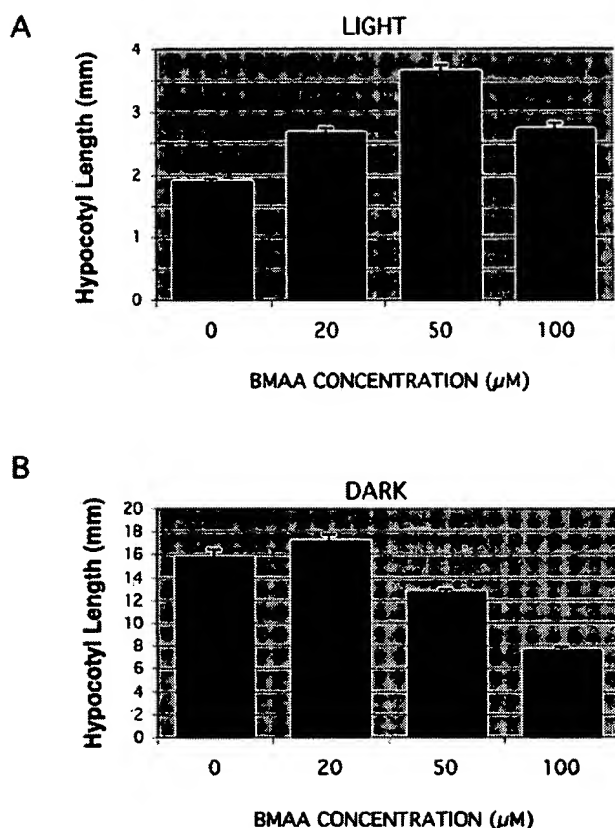


Figure 2. Quantification of BMAA-induced hypocotyl elongation in light-grown and etiolated plants. Arabidopsis plants were grown on increasing concentrations of BMAA (0–100 μM), in the light (A) or in continuous dark (B) for 5 d. The average hypocotyl length for each treatment is shown. Error bars show the SE of the mean ($n = 30$).

mm L-Glu, and by nearly 50% with 10 mm L-Glu (Fig. 3B). To determine whether the reversal of BMAA effects on morphogenesis was specific to the amino acid L-Glu, we tested whether two other amino acids could similarly counteract the effects of BMAA. L-Asp could not reverse the effects of BMAA, however L-Gln could also reverse the effects of BMAA (data not shown).

Selection of Arabidopsis Mutants Resistant to the Effects of BMAA on Morphogenesis

To determine the targets and mode of action of BMAA in Arabidopsis, a screen was devised to isolate mutants insensitive to the BMAA-induced effects on seedling morphology. For this screen, mutagenized (M2) Arabidopsis seeds were plated and grown in the light on Murashige and Skoog media containing 50 μM BMAA (Fig. 4). On this BMAA-containing media, wild-type plants exhibit elongated hypocotyls and partially closed cotyledons. M2 plants that exhibited short hypocotyls and open cotyledons when grown on BMAA were identified as "BMAA insensitive morphology" (*bim*) mutants (Fig. 4A). A total of

18,000 ethyl methanesulfonate (EMS) M2 seedlings were screened in the light on 50 μM BMAA, and 10 *bim* mutants were isolated (*bim* 18, 26, 40, 50, 59, 77, 131, 136, 167, and 175). A representative *bim* mutant seedling, *bim* 26, identified in the M2 screen is shown in Figure 4B.

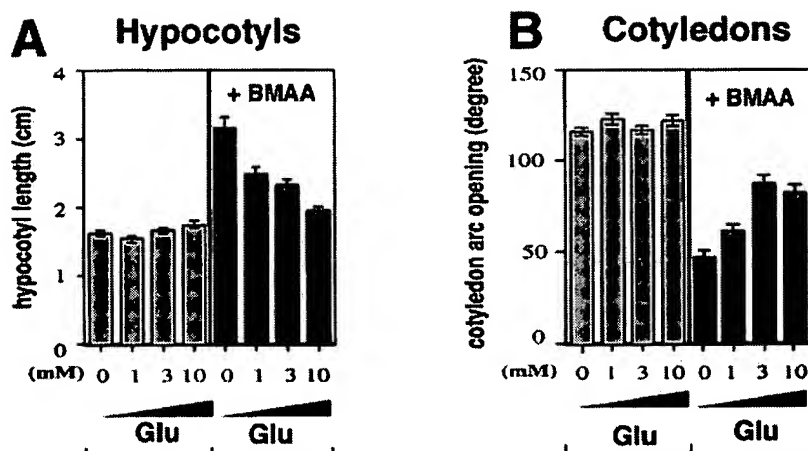
M3 progeny from M2 *bim* plants were tested for genetic inheritance of resistance to the effects of BMAA. M3 progeny of two *bim* mutants are shown in Figure 5. When treated with 50 μM BMAA and grown in the light, wild-type plants have elongated hypocotyls (Fig. 5A). In contrast, two representative mutants, *bim* 131 and *bim* 26, each have visibly shorter hypocotyls when grown in the light on 50 μM BMAA (Fig. 5A). When grown in the light minus BMAA, *bim* 131 and *bim* 26 are indistinguishable from wild type as young seedlings (Fig. 5B). BMAA treatment impairs root growth in wild-type plants, and in the majority of *bim* mutants. However, one mutant, *bim* 50, showed partial resistance to BMAA-mediated inhibition of root growth when compared with wild type (data not shown).

The effect of BMAA on hypocotyl length of light-grown plants was quantified for all *bim* mutants and wild-type plants (Fig. 6A) and was compared with untreated plants (Fig. 6B). When grown in the light plus 50 μM BMAA, wild type has a 2- to 3-fold increase in hypocotyl length, compared with *bim* mutants (Fig. 6A). In contrast, when grown in the light minus BMAA, the majority of *bim* mutants are indistinguishable from wild type with regard to hypocotyl length (Fig. 6B). Only *bim* 131 and *bim* 167 have obviously shorter hypocotyls than wild type, when grown in the absence of BMAA (Fig. 6B).

A Subset of *bim* Mutants Exhibit Constitutive Photomorphogenesis in the Dark

The *bim* mutants have been grouped into three classes based on their dark morphology when grown in the absence of BMAA (Fig. 7). Hypocotyl length of the etiolated plants is quantified in Figure 8. Class I *bim* mutants have a normal etiolated morphology (elongated hypocotyls and closed cotyledons) when cultivated in the dark in the absence of BMAA (Fig. 7A). This is shown for a representative *bim* mutant (*bim* 131) (Figs. 7A and 8A). Class-II and class-III *bim* mutants each have short hypocotyls when grown in the dark minus BMAA (Figs. 7, B and C, and 8A). Class-II *bim* mutants (*bim* 18, 40, 77, 136, 59, 167) have short hypocotyls in the dark, but their cotyledons remain closed (Fig. 7B). Class-III *bim* mutants (*bim* 26 and 50) have short hypocotyls but also display open cotyledons in the dark (Figs. 7C and 8A), similar to the *cop/det/fus* mutants. The effects of BMAA on a representative *cop* mutant (*cop1-6*), is shown in Figure 6 and 8. BMAA has no effect on hypocotyl elongation of the *cop 6-1* mutation in the light (Fig. 6B versus 6A) or in the dark (Fig. 8B versus 8A). By contrast, BMAA

Figure 3. BMAA-induced hypocotyl elongation, as well as inhibition of cotyledon opening is reversed in a dose-dependent manner by Glu. Arabidopsis seedlings were cultivated in the light on Murashige and Skoog media containing 1, 3, or 10 mM Glu in the absence (left, A and B) or presence (right, A and B) of 25 μ M BMAA. A, The average hypocotyl length for each treatment. B, The arc of cotyledon opening. Error bars show the SE of the mean ($n = 30$)



causes slight elongation of *bim* mutants grown in the light (Fig. 6A). Thus, it appears that the mutation conferring BMAA-resistance in the *bim* mutants affects aspects of skotomorphogenesis.

DISCUSSION

We have shown that BMAA, a plant-derived agonist that blocks Glu receptor function in animals, appears to alter early morphogenesis of light-grown Arabidopsis seedlings. BMAA promotes hypocotyl elongation and inhibits cotyledon opening in the light. As such, BMAA-induced effects on Arabidopsis seedlings phenocopy the long hypocotyl or “*hy*” mutants, defective in perceiving light and/or transmitting light signals in Arabidopsis (von Arnim and Deng, 1996; Fankhauser and Chory, 1997).

We reported previously that DNQX, an antagonist of AMPA/KA receptors in animals, also causes a “*hy*”-like phenotype when supplemented in the culture media of Arabidopsis seedlings (Lam et al., 1998a). The fact that two different iGluR interacting compounds (DNQX and BMAA) each induce hypocotyl elongation in light-grown seedlings provides support for the hypothesis that endogenous AtGLR genes in plants may be involved in photomorphogenic development in Arabidopsis. DNQX (an iGluR antagonist) could potentially antagonize Arabidopsis GLRs, which may be involved in light-mediated inhibition of hypocotyl growth. BMAA (an iGluR agonist) might inhibit AtGLR function but via a different mechanism. In animal systems, non-native agonists such as BMAA, can impair iGluR function because often iGluRs remain sensitized to these non-native

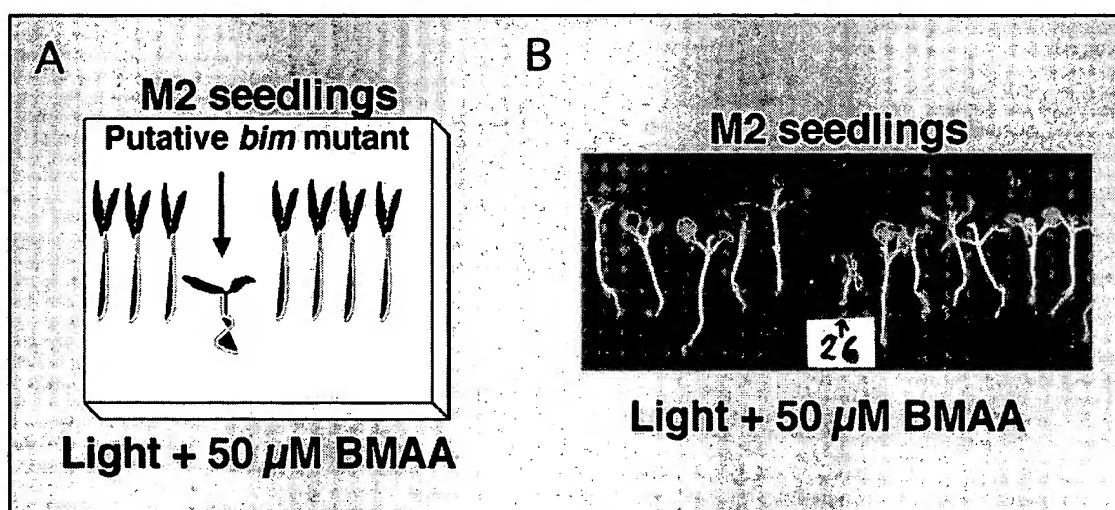


Figure 4. A genetic screen to isolate BMAA insensitive morphology (*bim*) mutants. A, Strategy to isolate Arabidopsis mutants resistant to the effects of BMAA is shown. Individual EMS mutagenized M2 seedlings are grown for up to 2 weeks on Murashige and Skoog media containing 50 μ M BMAA in the light. M2 individuals with short hypocotyls, compared with neighboring plants, are recovered from the BMAA-containing media and allowed to produce seed for analysis in the M3 generation. B, Representative M2 *bim* plant (*bim26*) is shown as detected in the primary screen.

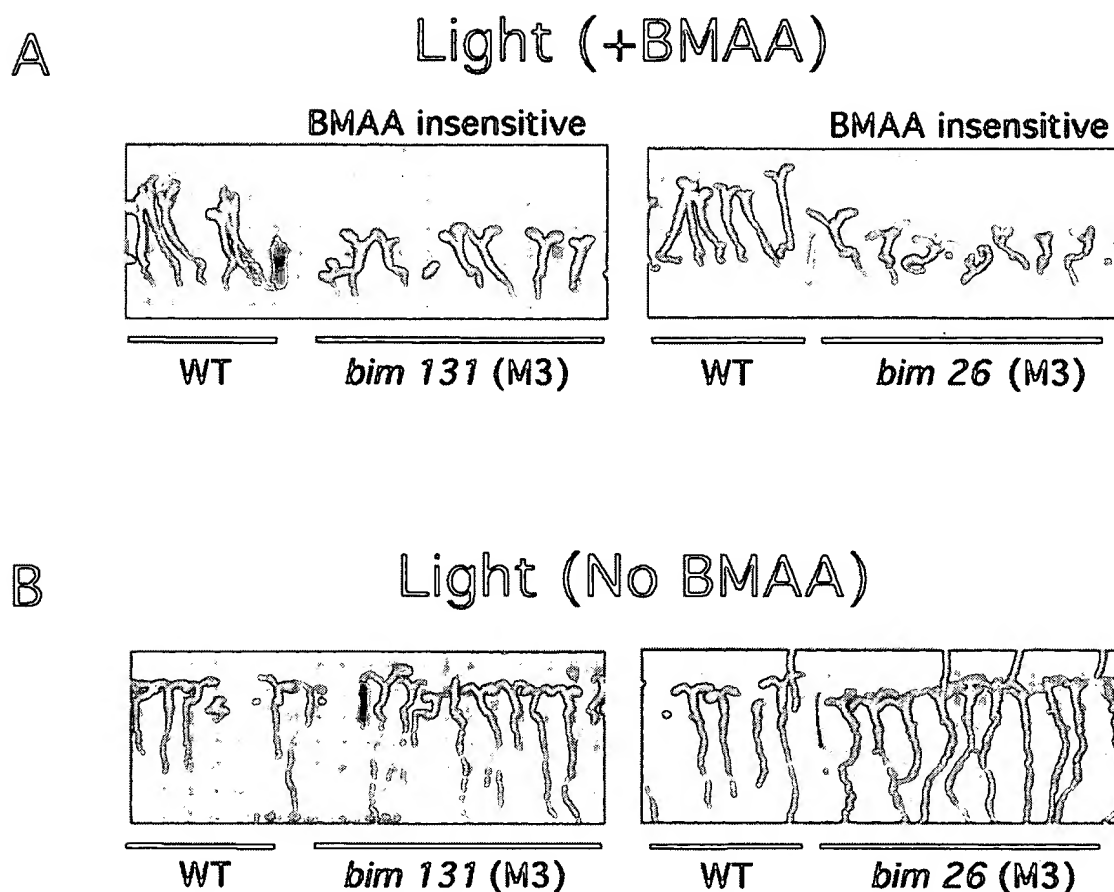


Figure 5. *bim* mutants are insensitive to BMAA-induced hypocotyl elongation. Two representative M3 *bim* mutants (*bim 131* and *bim 26*) were cultivated for 5 d in the light on Murashige and Skoog media in the presence of 50 μ M BMAA (A) or in the absence of BMAA (B). A, Both *bim 131* and *bim 26* have a short hypocotyl phenotype (right) when compared with wild type (left), which has an elongated hypocotyl in the presence of BMAA. B, Plants grown in the absence of BMAA where *bim 131* and *bim 26* appear similar to wild type at the early seedling stage.

ligands (Ross et al., 1989). In contrast, animal iGluRs become desensitized to the native agonist, Glu. Desensitization is necessary for ion channel closure and proper iGluR function (Geoffroy et al., 1991; Sprengel and Seeburg, 1995). The fact that the BMAA-induced effects on Arabidopsis morphogenesis are reversed by the addition of Glu (the native iGluR ligand), is consistent with the hypothesis that BMAA may act by blocking plant AtGLR signaling in Arabidopsis. In this scenario, increasing levels of Glu would compete with BMAA at the ligand-binding site and restore normal AtGLR desensitization and function. Alternatively, BMAA could act as an agonist to activate and open iGluR channels in plants, potentially regulating ion flow necessary for hypocotyl elongation. Hypocotyl expansion is largely due to increases in cell size, since most cells in the hypocotyl are formed during embryogenesis (Gendreau et al., 1997). Previous work has already detected the activation of chloride channels during hypocotyl elongation (Cho and Spalding, 1996). In this scenario, we hypothesize that BMAA-induced hypocotyl elongation may be caused by ac-

tivation of Arabidopsis GLRs important for cell expansion during hypocotyl elongation.

Among other amino acids tested, we have found that Gln could also reverse the effects of BMAA on Arabidopsis growth, whereas Asp could not. Thus, Gln may also act similar to Glu as a potential agonist at a BMAA responsive site. Gln and Glu both trigger ion transport of Glu receptors from the cyanobacteria, *Synechocystis* (Chen et al., 1999), when expressed in a heterologous system. Glu receptors from cyanobacteria show the strongest sequence similarity to Arabidopsis Glu receptors. Another possibility is that exogenously supplied Gln is assimilated and metabolized to Glu, which is then able to reverse the effects of BMAA on Arabidopsis. In fact, HPLC analysis has shown that exogenously added Gln leads to significantly higher levels of endogenous Glu in Arabidopsis (Oliveira and Coruzzi, 1999).

To test these different hypotheses and to determine the targets of BMAA action in plants, we have undertaken a mutant screen in Arabidopsis using BMAA as a pharmacological tool. This molecular-

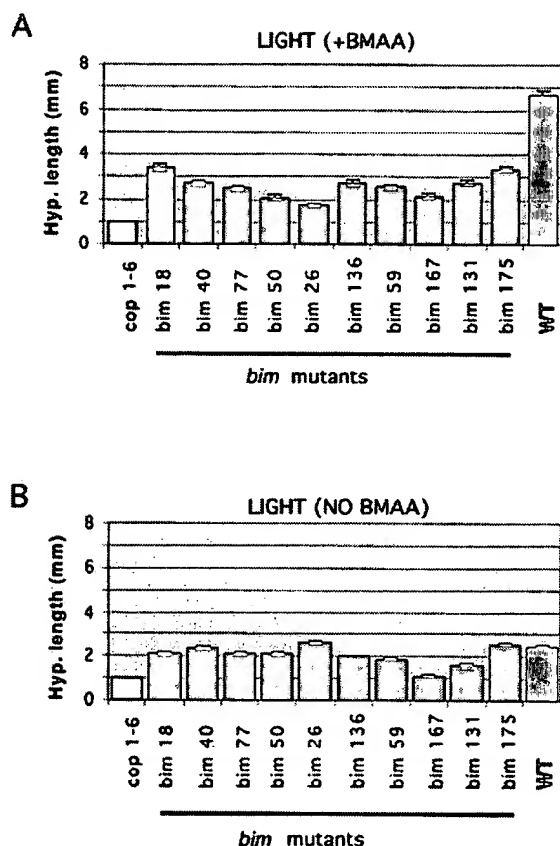


Figure 6. Quantification of hypocotyl lengths of *bim* mutants grown in the light in the presence or absence of BMAA. *bim* 18, 40, 77, 50, 26, 136, 59, 131, 167, and 175 were grown for 5 d in the light in the presence of 50 μ M BMAA (A) or with no BMAA (B). Hypocotyl lengths of *bim* seedlings and wild type were measured and quantified. Wild type is indicated with a black bar on the far right of each graph. *cop1-6* mutant is indicated with a white bar on the far left of each graph. The average hypocotyl length for each treatment is shown ($n = 30$). Error bars show the SE of the mean.

genetic approach should enable us to understand how BMAA might induce hypocotyl elongation and block cotyledon separation in light-grown Arabidopsis. We have isolated Arabidopsis mutants insensitive to the effects of BMAA on early morphogenesis in the light. BMAA insensitive morphology (*bim*) mutants have short hypocotyls when grown in the light in the presence of BMAA (Figs. 4–6). In contrast, wild-type plants display elongated hypocotyls under these conditions. The *bim* mutants were further separated into three classes based on their morphology in the dark (Fig. 7). The first class of *bim* mutants has a normal etiolated morphology in the dark. We have identified two *bim* mutants in this class (*bim* 131 and *bim* 175). The second class of *bim* mutant (*bim* 18, 40, 59, 77, 136, 167), has short hypocotyls in the dark and closed cotyledons. This phenotype is similar to the *proscute* (Desnos et al., 1996) and *korrigan* (Nicol et al., 1998) mutations, which affect cell wall formation

during development. This phenotype is also similar to a number of hormone mutants deficient in growth including *gai* (Gendreau et al., 1999) and *ctr1* (Kieber et al., 1993). The third class of *bim* mutants (*bim* 26 and 50) has short hypocotyls and open cotyledons. These two characteristics are analogous to the photomorphogenic mutants *cop* (Hou et al., 1993), *det* (Chory et al., 1989, 1991b), *fus* (Miséra et al., 1994; Kwok et al., 1996), and *shy* (Reed et al., 1994; Tian and Reed, 1999) mutants, which share these phenotypes. We tested the effects of BMAA on one constitutively

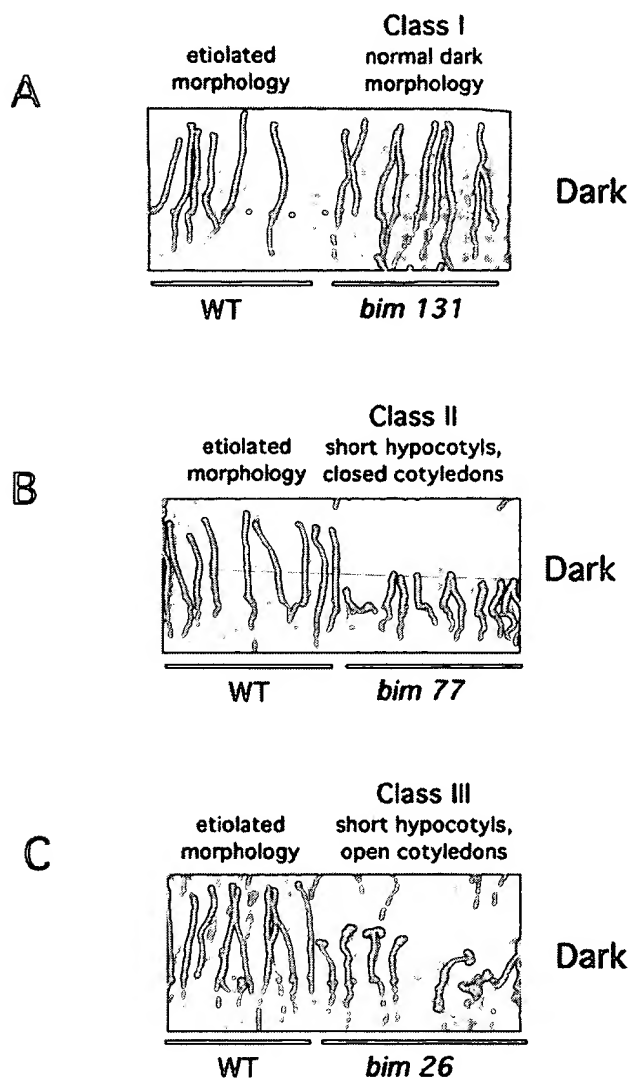


Figure 7. *bim* mutants are subgrouped into three separate classes based on their dark-grown morphology. *bim* mutants were cultivated on Murashige and Skoog media in the absence of BMAA and grown in the dark for 5 d. Class-I *bim* mutants exhibit a normal etiolated phenotype (Fig. 7A, right) when grown in the dark compared with wild type (Fig. 7A, left). Class-II *bim* mutants have a short hypocotyl and closed cotyledons (Fig. 7B, right) when compared with wild type (Fig. 7B, left). Class-III *bim* mutants have a short hypocotyl and open cotyledons (Fig. 7C, left) when compared with wild type (Fig. 7C, right).

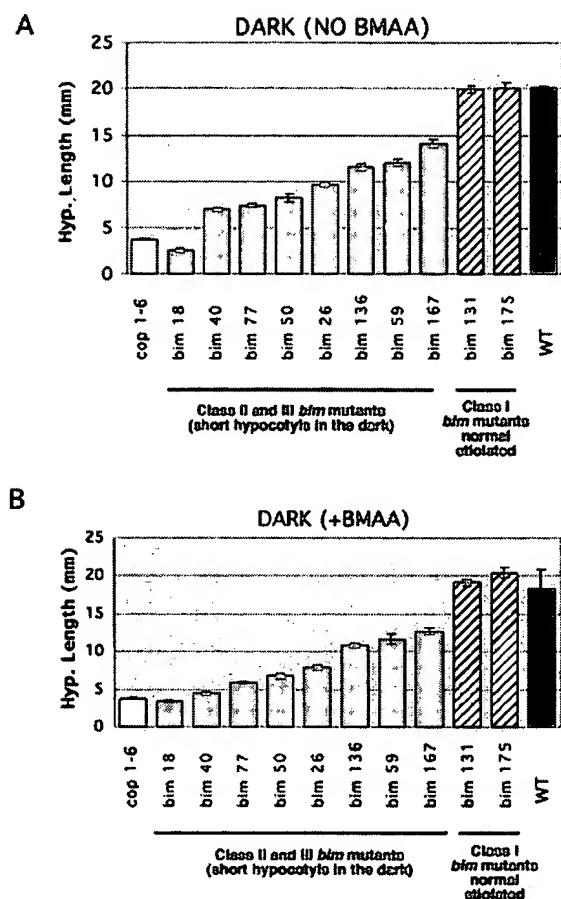


Figure 8. Quantification of hypocotyl lengths of *bim* mutants grown in the dark in the absence or presence of BMAA. *bim* 18, 40, 77, 50, 26, 136, 59, 131, 167, and 175 and wild type were grown for 5 d in the dark in the absence (Fig. 8A) or presence of 50 μ M BMAA (Fig. 8B). Hypocotyl lengths were quantified. Wild type is indicated with black bars. Class-I *bim* mutants (*bim* 131 and *bim* 175) have wild-type length hypocotyls and are indicated with hatched bars. Class-II and -III *bim* mutants, which have short hypocotyls in the dark, are marked with gray shaded bars. *cop1-6* is shown in the far left side of the graph (white bar). The average hypocotyl length for each treatment is shown ($n = 30$). Error bars show the SE of the mean.

photomorphogenic mutant, *cop1-6* (Kendrick and Nagatani, 1991; Deng and Quail, 1992) (Figs. 6 and 8). BMAA does not induce elongation of the *cop1-6* hypocotyl. However, interpretation of these results must await molecular analysis of lesions in the *bim* mutants. It is important to test whether class II and III *bim* mutants are allelic to these previously characterized *cop*, *det*, *fus*, and *shy* mutants or whether they represent new loci. It is also important to test for allelism between the different *bim* mutants and to map the *bim* mutants to determine whether they are genetically linked to any AtGLR genes in Arabidopsis.

An important aspect of development in seedlings involves the complicated interplay of light and various phytohormones. Auxin (Jensen et al., 1998; Kim

et al., 1998), gibberellin (Jacobsen and Olszewski, 1993; Steber et al., 1998), and brassinolide (Fujioka et al., 1997; Azpiroz et al., 1998) all act as positive regulators of hypocotyl elongation in Arabidopsis. Ethylene (Kieber et al., 1993) and cytokinins (Chory et al., 1991a), conversely, are believed to act as inhibitors of hypocotyl elongation. Thus, the BMAA-mediated effects on hypocotyl length in light-grown plants may also involve the interaction of one or more of these phytohormones. It is also possible that BMAA blocks transduction of light signals, which inhibit hypocotyl elongation. Blue light (Liscum and Hangarter, 1991; Ahmad and Cashmore, 1993; Lasceve, et al., 1999), red light (Somers et al., 1991; Nagatani et al., 1993), and far-red light (Dehesh et al., 1993) are the major, incident wavelengths perceived by plants that repress hypocotyl elongation in Arabidopsis. In future studies, it will be important to determine whether BMAA effects are specific to one or more of these wavelengths in Arabidopsis.

One interesting result from our studies is that BMAA induces hypocotyl elongation in Arabidopsis specifically in the light at low concentrations (20–50 μ M BMAA) (Fig. 2A). Because BMAA exerts its effects at low (μ M) concentrations, this suggests that BMAA could act as a signaling compound in plants. In species of the Cycadaceae, BMAA is detected at high levels (milligram BMAA/gram of tissue) (Vega and Bell, 1967; Duncan et al., 1989; Pan et al., 1997). The presence of high levels of BMAA in such tissues has led some researchers to suggest that BMAA may act as a toxin against predators (Ladd et al., 1993). This theory of herbivore deterrence may explain why neurotoxins, such as BMAA are synthesized at high levels in plants. Our phylogenetic studies on GLR genes in plants and animals suggests that iGluRs are derived from a primitive signaling mechanism that existed before plants and animals diverged (Chen et al., 1999; Chiu et al., 1999). Those studies, plus the ones described herein, suggest the intriguing possibility that iGluR agonists made by plants may serve not only as herbivore deterrents, but may also act as signaling molecules affecting developmental processes in plants. We postulate, for example that BMAA, which appears to affect photomorphogenesis in Arabidopsis, may also alter light signaling in cycads. Whether BMAA plays a signaling role in cycads, or is even present at low levels in other species of higher plants are open questions that remain to be answered. Using the Arabidopsis *bim* mutants to understand the mode of action of a cycad-derived iGluR agonist in plants may help to address these questions. Furthermore, using *bim* mutants to understand how BMAA mediates its effects in Arabidopsis could potentially lead to new therapeutic treatments of iGluR-related neurological disorders in humans.

MATERIALS AND METHODS

Culture of Arabidopsis Plants

Arabidopsis ecotype Columbia seeds were plated on Murashige and Skoog media (Murashige and Skoog, 1962), 0.1% (w/v) MES [2-(*N*-morpholino)ethanesulfonic acid] (Sigma M-2933) containing 0.5% (w/v) Suc and 0.7% (w/v) agar. Arabidopsis seeds were placed for 2 d at 4°C on the growth media. Plants were grown in square (100 × 15 mm) plates in a vertical position. Light grown plants were grown at 22°C during a cycle of 16-h light/8-h dark under cool-white fluorescent bulbs (General Electric, Fairfield, CT). Plants received a fluence level ranging from 40 to 60 μE. For dark grown seedlings, plants were incubated for an initial 4 h in the light to stimulate germination. After the light pretreatment, dark-grown plants were wrapped in two layers of foil and grown in the dark for 5 d at 22°C.

BMAA (L-BMAA hydrochloride) was purchased from RBI. L-Glu (Sigma G-1501), L-Asp (Sigma A-6558), and L-Gln (Sigma G-3126) stocks were dissolved in water and the pH was adjusted to 5.7.

cop 6-1 seeds used as a control were a gift from Dr. Kameda, Hokkaido University (Hokkaido, Japan).

Measurement of Hypocotyl Length and Cotyledon Opening

Plants were grown in the light for 5 to 8 d. Hypocotyl length was measured under the view of a dissecting scope. The top of the hypocotyl was defined as the point where the petioles of the cotyledons are attached to the axis. The bottom of the hypocotyl was determined as the root-shoot junction (with the root being defined as the point where root hairs are initially apparent). Cotyledon separation was measured by projecting the slide image of the seedlings onto a screen. Two lines were then drawn along the petioles over the image of the cotyledons and the angle was measured where these two lines intersected (at the shoot apex of the seedling).

Screen for *bim* Mutants in EMS Mutagenized M2 Lines

EMS mutagenized Columbia Co-3, glabrous seedlings (Lehle Seeds, Round Rock, TX) were cultivated as described above on Murashige and Skoog media (with 0.1% [w/v] MES, pH 5.7; 0.5% [w/v] Suc) plates containing 50 μM BMAA. Mutants with a *BMAA insensitive morphology* (*bim*) were screened after 8 to 12 d of growth, at which time they were transferred to Murashige and Skoog media lacking BMAA. After 1 to 2 weeks, the plants were transplanted to soil and allowed to set seed.

ACKNOWLEDGMENTS

The authors would like to thank Josh Layne, Yi Zhou (Joey), Brian Onken, and Josh Malamy for their helpful

contributions. We would also like to thank Philip Benfey, Joanna Chiu, Michael Shin, Andrew Kuronov, and Hidehiro Fukaki for useful discussion about this work. We would also like to thank Dr. Yoshibumi Komeda for the *cop1-6* mutant seeds.

Received August 11, 2000; modified August 27, 2000; accepted September 18, 2000.

LITERATURE CITED

- Ahmad M, Cashmore AR (1993) The HY4 gene of *Arabidopsis thaliana* encodes a protein with characteristics of a blue light photoreceptor. *Nature* 366: 162–166
- Azpiroz R, Wu Y, LoCascio JC, Feldmann KA (1998) An *Arabidopsis* brassinosteroid-dependent mutant is blocked in cell elongation. *Plant Cell* 10: 219–230
- Bettler B, Mulle C (1995) Review: neurotransmitter receptors II AMPA and kainate receptors. *Neuropharmacology* 34: 123–139
- Chamberlain CJ (1919) The living cycads. In EH Moore, JM Coulter, RA Millikan, eds, *The University of Chicago Science Series*. The University of Chicago Press, Chicago, p ix
- Chen G-Q, Cui C, Mayer ML, Gouaux E (1999) Functional characterization of a potassium-selective prokaryotic glutamate receptor. *Nature* 402: 817–821
- Chiu J, Desalle R, Lam H, Meisel L, Coruzzi G (1999) Molecular evolution of putative plant glutamate receptors and their relationship to animal ionotropic glutamate receptors. *Mol Biol Evol* 16: 826–838
- Cho MH, Spalding EP (1996) An anion channel in *Arabidopsis* hypocotyls activated by blue light. *Proc Natl Acad Sci USA* 93: 8134–8138
- Chory J, Aguilar N, Peto CA (1991a) The phenotype of *Arabidopsis thaliana det1* mutants suggests a role for cytokinins in greening. *Symp Soc Exp Biol* 41: 21–29
- Chory J, Nagpal P, Peto CA (1991b) Phenotypic and genetic analysis of *det2*, a new mutant that affects light-regulated seedling development in *Arabidopsis*. *Plant Cell* 3: 445–459
- Chory J, Peto C, Feinbaum R, Pratt L, Ausubel F (1989) *Arabidopsis thaliana* mutant that develops as a light grown plant in the absence of light. *Cell* 58: 991–999
- Copani A, Canonico PL, Catania MV, Aronica E, Bruno V, Ratti E, van Amsterdam FTM, Gaviraghi G, Nicoletti F (1991) Interaction between β-N-methylamino-L-alanine and excitatory amino acid receptors in brain slices and neuronal cultures. *Brain Res* 558: 79–86
- Dehesh K, Franci C, Parks BM, Seeley KA, Short TW (1993) *Arabidopsis* HY8 locus encodes phytochrome A. *Plant Cell* 5: 1081–1088
- Deng X-W, Quail PH (1992) Genetic and phenotypic characterization of *cop1* mutants of *Arabidopsis thaliana*. *Plant J* 2: 83–95
- Desnos T, Orbovic V, Bellini C, Kronenberger J, Caboche M, Traas J, Höfte H (1996) *Procuste1* mutants identify

- two distinct genetic pathways controlling hypocotyl cell elongation, respectively in dark- and light-grown *Arabidopsis* seedlings. *Development* 122: 683–693
- Duncan M, Kopin I, Crowley J, Jones S, Markey S (1989) Quantification of the putative neurotoxin 2-amino-3-(methylamino) propanoic acid (BMAA) in cycadales: analysis of the seeds of some members of the family Cycadaceae. *J Anal Toxicol* 13: 169–175
- Fankhauser C, Chory J (1997) Light control of plant development. *Annu Rev Cell Dev Biol* 13: 203–229
- Forsythe DI, Barnes-Davies M (1997) Synaptic transmission: well-placed modulators. *Curr Biol* 7: 362–365
- Fujioka S, Li J, Choi Y-H, Seto H, Takatsuto S, Noguchi T, Watanabe T, Kuriyama H, Yokota T, Chory J, Sakurai A (1997) The *Arabidopsis deetiolated2* mutant is blocked early in brassinosteroid biosynthesis. *Plant Cell* 9: 1951–1962
- Gendreau E, Orbovic V, Höfte H, Traas J (1999) Gibberellin and ethylene control endoreduplication levels in the *Arabidopsis thaliana* hypocotyl. *Planta* 209: 513–516
- Gendreau E, Traas J, Desnos T, Grandjean O, Caboche M, Höfte H (1997) Cellular basis of hypocotyl growth in *Arabidopsis*. *Plant Physiol* 114: 295–305
- Geoffroy M, Lambolez B, Audinat E, Hamon B, Crepel F, Rossier J, Kado RT (1991) Reduction of desensitization of a glutamate ionotropic receptor by antagonists. *Mol Pharmacol* 39: 587–591
- Hou Y, von Arnim A, Deng X-W (1993) A new class of *Arabidopsis* constitutive photomorphogenic genes involved in regulating cotyledon development. *Plant Cell* 5: 329–339
- Ikonomidou C, Turski L (1996) Neurodegenerative disorders: clues from glutamate and energy metabolism. *Crit Rev Neurobiol* 10: 239–263
- Isquierdo I, Medina JH (1995) Correlation between the pharmacology of long-term potentiation and the pharmacology of memory. *Neurobiol Learn Mem* 63: 19–32
- Jacobsen SE, Olszewski NE (1993) Mutations at the *spindly* locus of *Arabidopsis* alter gibberellin signal transduction. *Plant Cell* 5: 887–896
- Jensen P, Hangarter RP, Estelle M (1998) Auxin transport is required for hypocotyl elongation in light-grown but not dark-grown *Arabidopsis*. *Plant Physiol* 116: 455–462
- Kendrick RE, Nagatani A (1991) Phytochrome mutants. *Plant J* 1: 133–139
- Kieber JJ, Rothenberg M, Roman G, Feldmann KA, Ecker JR (1993) *CTR1*, a negative regulator of the ethylene response pathway in *Arabidopsis*, encodes a member of the Raf family of protein kinases. *Cell* 72: 427–441
- Kim BC, Soh MS, Hong SH, Furuya M, Nam HG (1998) Photomorphogenic development of the *Arabidopsis shy2-1D* mutation and its interaction with phytochromes in darkness. *Plant J* 15: 61–68
- Kwok SF, Piekos B, Miséra S, Deng X-W (1996) A complement of ten essential and pleiotropic *Arabidopsis* *COP/DET/FUS* genes is necessary for repression of photomorphogenesis in darkness. *Plant Physiol* 110: 731–742
- Ladd PG, Connell SW, Harrison B (1993) Seed toxicity in *Macrozamia riedlei*. In DW Stephenson, KJ Norstog, eds, *Proceedings of CYCAD 90 the second international conference on cycad biology*. Palm and Cycad Societies of Australia Ltd., Milton, Queensland, Australia, pp 37–41
- Lam H, Peng S, Coruzzi G (1994) Metabolic regulation of the gene encoding glutamine-dependent asparagine synthetase in *Arabidopsis*. *Plant Physiol* 106: 1347–1357
- Lam HM, Chiu J, Hsieh MH, Meisel L, Oliveira IC, Shin M, Coruzzi G (1998a) Glutamate-receptor genes in plants. *Nature* 396: 125–126
- Lam HM, Hsieh MH, Coruzzi G (1998b) Reciprocal regulation of distinct asparagine synthetase genes by light and metabolites in *Arabidopsis thaliana*. *Plant J* 16: 345–353
- Lasceve G, Leymarie LG, Olney MA, Liscum E, Christie JM, Vavasseur A, Briggs WR (1999) *Arabidopsis* contains at least four independent blue-light-activated signal transduction pathways. *Plant Physiol* 120: 605–614
- Liscum E, Hangarter RP (1991) *Arabidopsis* mutants lacking blue light dependent inhibition of hypocotyl elongation. *Plant Cell* 3: 685–694
- Miséra S, Müller AJ, Weiland-Heidecker U, Jürgens G (1994) The *FUSCA* genes of *Arabidopsis*: negative regulators of light responses. *Mol Gen Genet* 244: 242–252
- Monaghan DT, Bridges RJ, Cotman CW (1989) The excitatory amino acid receptors: their classes, pharmacology, and distinct properties in the function of the central nervous system. *Annu Rev Pharmacol Toxicol* 29: 365–402
- Muller D, Joly M, Lynch G (1989) Contributions of quisqualate and NMDA receptors to the induction and expression of LTP. *Science* 242: 1694–1697
- Murashige T, Skoog F (1962) A revised medium of rapid growth and bioassays with tobacco tissue culture. *Physiol Plant* 15: 473–479
- Nagatani A, Reed J, Chory J (1993) Isolation and initial characterization of *Arabidopsis* mutants deficient in phytochrome A. *Plant Physiol* 102: 269–277
- Nicol F, His I, Jauneau A, Vernhettes S, Canut H, Höfte H (1998) A plasma membrane-bound putative endo-1,4- β -D-glucanase is required for normal wall assembly and cell elongation in *Arabidopsis*. *EMBO J* 17: 5563–5576
- Nowak L, Bregestovski P, Ascher P, Herbert A, Prochiantz A (1984) Magnesium gates glutamate-activated channels in mouse central neurons. *Nature* 307: 462–465
- Oliveira IC, Coruzzi G (1999) Carbon and amino acids reciprocally modulate the expression of glutamine synthetase in *Arabidopsis*. *Plant Physiol* 221: 301–309
- Pan M, Mabry TJ, Cao P, Moini M (1997) Identification of nonprotein amino acids from cycad seeds as *N*-ethoxycarbonyl ethyl ester derivatives by positive chemical-ionization gas chromatography-mass spectrometry. *J Chromatogr A* 787: 288–294
- Reed J, Nagatani A, Elich T, Fagan M, Chory J (1994) Phytochrome A and phytochrome B have overlapping distinct functions in *Arabidopsis* development. *Plant Physiol* 104: 1139–1149
- Ross SM, Roy DN, Spencer PS (1989) β -*N*-Oxalylamino-L-alanine action on glutamate receptors. *J Neurochem* 53: 710–715

- Somers DE, Sharrock RA, Tepperman JM, Quail PH** (1991) The *hy3* long hypocotyl mutant of *Arabidopsis* is deficient in phytochrome B. *Plant Cell* 3: 1263–1274
- Spencer PS, Nunn PB, Hugon J, Ludolph AC, Ross SM, Roy DN, Robertson RC** (1987) Guam amyotrophic lateral sclerosis-parkinsonism-dementia linked to a plant excitant neurotoxin. *Science* 237: 517–522
- Sprengel R, Seeburg PH** (1995) Ionotropic glutamate receptors. In R North, ed, *Handbook of Receptors and Channels: Ligand- and Voltage-Gated Ion Channels*. CRC Press, Boca Raton, FL
- Steber CM, Cooney SE, McCourt P** (1998) Isolation of the GA-Response mutant *sly1* as a suppressor of *abi1-1* in *Arabidopsis thaliana*. *Genetics* 149: 509–521
- Tian Q, Reed JW** (1999) Control of auxin-regulated root development by the *Arabidopsis thaliana* *SHY2/IAA3* gene. *Development* 126: 711–721
- Tsien JZ, Huerta PT, Tonegawa S** (1996) The essential role of hippocampal CA1 NMDA receptor-dependent synaptic plasticity in spatial memory. *Cell* 87: 1327–1338
- Vega A, Bell EA** (1967) α -Amino- β -methylaminopropionic acid, a new amino acid from seeds of *Cycas circinalis*. *Phytochemistry* 6: 759–762
- von Arnim A, Deng X-W** (1996) Light control of seedling development. *Annu Rev Plant Physiol Plant Mol Biol* 47: 215–243
- Whiting MG** (1963) Toxicity of cycads. *Econ Bot* 17: 271–302

Overexpression of the *AtGluR2* Gene Encoding an Arabidopsis Homolog of Mammalian Glutamate Receptors Impairs Calcium Utilization and Sensitivity to Ionic Stress in Transgenic Plants

Sun A Kim¹, June Myoung Kwak^{1,2}, Seul-Ki Jae¹, Myeong-Hyeon Wang¹ and Hong Gil Nam^{1,3}

¹ Division of Molecular and Life Sciences, Pohang University of Science and Technology, Hyoja Dong, Pohang, Kyungbuk 790-784, Republic of Korea

² Division of Biology, Cell and Developmental Biology Section and Center for Molecular Genetics, University of California, San Diego, 9500 Gilman Drive, La Jolla, CA 92093-0116, U.S.A.

We have identified a homolog of the mammalian ionotropic glutamate receptor genes in *Arabidopsis thaliana* (*AtGluR2*). This gene was found to alter Ca^{2+} utilization when overexpressed in *A. thaliana*. These transgenic plants displayed symptoms of Ca^{2+} deficiency, including browning and death of the shoot apex, necrosis of leaf tips, and deformation of leaves. Supplementation with Ca^{2+} alleviated these phenotypes. Overall levels of Ca^{2+} in tissues of control plants were not significantly different from those of transgenic plants, suggesting that overexpression of the *AtGluR2* gene did not affect Ca^{2+} uptake. However, the relative growth yield as a function of Ca^{2+} levels revealed that the critical deficiency content of Ca^{2+} in transgenic plants was three times higher than that of control plants. The transgenic plants also exhibited hypersensitivity to Na^+ and K^+ ionic stresses. The ion hypersensitivity was ameliorated by supplementation with Ca^{2+} . The results showed that overexpression of the *AtGluR2* gene caused reduced efficiency of Ca^{2+} utilization in the transgenic plants. The promoter of the *AtGluR2* gene was active in vascular tissues, particularly in cells adjacent to the conducting vessels. This suggests that *AtGluR2* encodes a functional channel that unloads Ca^{2+} from the xylem vessels. The results together suggest that appropriate expression of the *AtGluR2* protein may play critical roles in Ca^{2+} nutrition by controlling the ion allocation among different Ca^{2+} sinks both during normal development and during adaptation to ionic stresses.

Key words: *Arabidopsis thaliana* — Calcium efficiency — Critical deficiency content — Glutamate receptor homolog — Ion hypersensitivity — Xylem unloading.

Abbreviations: *AtGluR2*, *Arabidopsis thaliana* glutamate receptor homolog 2; B5 medium, Gamborg B5 medium; CDC, critical deficiency content; EST, expressed sequence tag; GUS, β -glucuronidase; iGluR, ionotropic glutamate receptor; NCBI, National Center for Biotechnology Information.

The nucleotide sequences reported in this paper have been submitted to the GenBank under accession numbers AF159498 and AF159499.

Introduction

Calcium (Ca^{2+}) is the second most abundant metal ion in plants and is an essential element for survival in higher plants. Millimolar concentrations of Ca^{2+} are required at the outer surface of the plasma membrane to maintain its functional integrity and the structural stability of cell walls (Epstein 1972, Clarkson and Hanson 1980, Marschner 1995). Thus, when plants are subjected to Ca^{2+} starvation, the effects of Ca^{2+} deficiency are first noticed in the young and growing tissues, where cell division and cell enlargements are most active (Scaife and Turner 1984). In contrast, in the cytosol, free Ca^{2+} is present at levels of $\sim 10^{-7}$ M or less (Kretsinger 1977). The cytosolic free Ca^{2+} serves as an important second messenger that participates in signal transduction of the various environmental stresses. Numerous physiological stimuli, such as light, gravity, touch, cold or heat shock, oxidative stress, drought, osmotic shock, fungal elicitor, hormones, or salt stresses are known to induce transient elevations in cytoplasmic Ca^{2+} levels (Bush 1995, Sanders et al. 1999, Trewavas 1999). These transient increases in cytosolic Ca^{2+} concentration are believed to be critical in triggering specific adaptation responses and in maintaining cellular homeostasis.

Since the early 1960s, considerable research has been undertaken to understand the genetic mechanisms by which mineral nutrition is controlled in plants (Gerloff 1963, Epstein and Jefferies 1964). For example, the physiological basis underlying differences in Ca^{2+} nutrition has been assessed by screening cultivars of high Ca^{2+} efficiency from tomato, cowpea, and cauliflower under low Ca^{2+} stress (English and Maynard 1981, Behling et al. 1989, Horst et al. 1993, Hochmuth 1984). Comparisons between the inefficient and the efficient cultivars from these plants provided a physiological profile associated with Ca^{2+} efficiency (Clarkson 1984, Marschner 1995). Although the physiological basis for Ca^{2+} nutrition has been well described through these studies, the molecular mechanisms underlying the process of Ca^{2+} uptake, root-to-shoot translocation, allocation of Ca^{2+} among different tissues at the organismic level, or Ca^{2+} influx and its intracellular distribution still remains elusive.

At the organism level, Ca^{2+} movement is largely depend-

³ Corresponding author: E-mail, hgn@bric.postech.ac.kr; Fax, +82-54-279-2199.

ent on the apoplastic pathway (Kirkby and Pilbeam 1984). Ca^{2+} is taken up mainly via the apoplastic pathway in non-differentiated root-tip tissue and during side-root emergence. The process by which Ca^{2+} passes the Casparian band and enters the stele in the root zones is poorly defined. Once Ca^{2+} is loaded in the conducting tissues, the upward movement of Ca^{2+} is dependent on mass flow and cation exchange along the xylem walls. Transport of Ca^{2+} is controlled by the sink strength of adjacent tissues, which controls the unloading of Ca^{2+} from the xylem sap. When the Ca^{2+} supply from the roots is deficient, competition between Ca^{2+} sinks induces Ca^{2+} deficiency in the relatively weak sinks (Clarkson 1984). Therefore it is envisaged that the proper allocation among different Ca^{2+} sinks is necessary for plant growth. Such allocation may be regulated by a genetically defined mechanism, although this has not yet been established.

At the cellular level, Ca^{2+} is passively transported into the cytosol through the opening of various Ca^{2+} permeable channels located at either the endo-membranes or the plasma membrane (Knight et al. 1996, Sanders et al. 1999). Families of Ca^{2+} -channels have been reported through patch clamp studies, radioactive tracer fluxes studies, or reconstitution studies (White 1998, Reid and Tester 1992, Pineros and Tester 1997). Despite the wealth of electrophysiological information on Ca^{2+} -permeable channels, the molecular identities of Ca^{2+} -permeable channels in higher plants remain largely undefined. The wheat low-affinity cation transporter (LCT1) was shown to mediate Ca^{2+} as well as K^{+} uptake in yeasts (Schachtman et al. 1997, Clemens et al. 1998). The *Arabidopsis* cyclic nucleotide gated channels were recently identified and shown to be permeable to Ca^{2+} ions using human embryonic kidney (HEK) cells as a heterologous expression system (Kohler et al. 1999, Leng et al. 1999).

There is now a sufficiently large amount of sequence data available for the model plant, *Arabidopsis thaliana*. This now allows the homology screening of the database as a viable alternative strategy for cloning plant Ca^{2+} channels. Recent data from the *Arabidopsis* genome sequencing project led to the estimation that over 200 different plasma membrane transporters are encoded in the *Arabidopsis* genome (Frommer and Bohnert 1999). Recently, Lam et al. (1998) reported the existence of genes encoding putative glutamate receptors in *A. thaliana*. These genes display high sequence similarity to the ionotropic glutamate receptors (iGluRs), the neurotransmitter-gated ion channels found in the vertebrate central nervous system. The iGluRs assemble to form functional channels that are permeable to Ca^{2+} and monovalent cations when activated by L-glutamate (Gasic and Hollmann 1992, Wisden and Seeburg 1993, Hollmann et al. 1994). Influx of Ca^{2+} through iGluRs is thought to play a key role in numerous physiological responses.

In this study, we report the molecular identification and functional characterization of an iGluR gene homolog from *A. thaliana* in the context of its physiological role in Ca^{2+} nutrition.

Materials and Methods

Genomic cloning and generation of the full-length *AtGluR2* cDNA

Arabidopsis cDNA clone 162G7T7 (partial cDNA, accession number R29880) was obtained from the *Arabidopsis* Biological Resource Center. The identity of the clone was confirmed by sequencing. The DNA insert (1.3 kb) was used to screen an *Arabidopsis* genomic library prepared in λ Fix. From about 1×10^5 plaque-forming units, three independent clones were selected and purified. Bacteriophage genomic DNA was prepared by a standard purification procedure (1989). Two clones exhibited a 3.5 kb *SacI* fragment that hybridized with the cDNA probe. This fragment was cloned in pBlue-script KS(+) and sequenced. The full-length sequence of the cDNA was obtained by modified 5'-end rapid amplification of cDNA ends (5'-RACE) PCR. Poly(A)⁺ RNA was isolated from *A. thaliana* as described (Kwak et al. 1997a). The Marathon cDNA amplification kit (Clontech) was used to synthesize cDNA. The Marathon cDNA adapters (Clontech) were ligated to the cDNA and then the resulting cDNA product was subjected to PCR with LA *Taq* polymerase (Takara) using the gene-specific primers, 5'-gtttcaggatccgattaagccaaagctatg-3' (primer I-1), and 5'-ccttgagggtccgcggaactcatcg-3' (primer I-2). The amplified 1,890 bp product was inserted into the pGEM-Teasy vector (Promega) and three independent clones were sequenced. The nucleotide sequences were compared to the genomic clone to insure that no errors were introduced during PCR. The fragment was digested with *Bam*HI and *Sac*II, and the resulting 5'-fragment (1 to 1,853) was inserted into the EST clone, resulting in the full-length *AtGluR2* cDNA (1 to 2,975).

Plant transformation

Two sets of oligonucleotide primers, 5'-gtttcaggatccgattaagccaaagctatg-3' (primer II-1), 5'-cttccgggtcgtctatgtctagaagc-3' (primer II-2), 5'-catccatggaacgagccttaaacaccagc-3' (primer III-1), and 5'-taggatcccaactctctccatcccatg-3' (primer III-2) were designed from the sequence of the *AtGluR2* genomic clone. The primer set II was used to amplify 3.2 kb fragment corresponding to the *AtGluR2* coding region from the genomic DNA. The PCR fragment was inserted into the pGEM-Teasy vector (Promega) and three independent clones were subjected to DNA sequencing analysis. This construct was digested with *Bam*HI and *Sma*I, and the resulting fragment was subcloned into the plant expression vector (pBIN-JIT), which contains a tandem repeat of the cauliflower mosaic virus 35S promoter (kindly provided by Dr. Cathie Martin, John Innes Center, U.K.). The 1.5 kb promoter region was amplified using the primer set III and the PCR product was digested with *Nco*I and *Bam*HI. The insert was cloned into pCambia1303 (MRC Laboratory of Molecular Biology, U.K.). The resulting constructs, p35S-*AtGluR2* and p1.5-GUS, were introduced into the AGL1 strain of *Agrobacterium tumefaciens* and the resulting strains were used to transform *A. thaliana* ecotype Columbia (Col-0) by the vacuum infiltration method (Bechtold et al. 1993). Transformants were selected in 1 \times B5 medium (Gamborg et al. 1968) containing 50 $\mu\text{g ml}^{-1}$ kanamycin or 50 $\mu\text{g ml}^{-1}$ hygromycin, respectively.

RNA extraction and RNA gel blot analysis

Total cellular RNA was extracted from *Arabidopsis* seedlings using TRI reagent (Molecular Research Center, Inc.). Twenty micrograms of RNA was separated on a denaturing 1.2% agarose gel and then transferred to a Hybond-N⁺ nylon membrane (Amersham). The 0.3 kb fragment of the *AtGluR2* gene (nucleotide 2,424 to 2,730) was radiolabeled with [³²P]dCTP by using a random-priming labeling kit (Amersham). The blot was hybridized and washed as described (Kwak et al. 1997b). The blot was also probed with the 18S rRNA gene of *Brassica napus*, to assess the amount of RNA.

Table 1 Putative glutamate receptors in *Arabidopsis* genome

Chromosome	Clone source ^a	Genomic DNA ^b	cDNA ^c
I	AC000098	yUP8H12.19	AF183932(GLR4) AF167355(GLUR3) ^d
II	AC005700	T32F6.8	AF210701(Glr5)
		T32F6.9	AF170494(GLR6)
	AC005315	T9I4.18	hypothetical
		T9I4.19	hypothetical
		T9I4.20	hypothetical
	AC007266	F27A10.2	hypothetical
		F27A10.3	hypothetical
III	AL133452	F26O13.120	hypothetical
	AC009853	F21O3.23	hypothetical
	AC016829	T6K12.27	AC079998(GLR1)
IV	AL031004	F28M20.100	hypothetical
	AC002329	F5J6.2	AF038557(ACL1) AF079999 (GLR2) ^e
	AL022604	F23E12.150	AF159498(AtGluR2) ^f
	AF159499 ^g		
V	AF007271	T21B04.3	hypothetical
	AL360314	F2I11.70	hypothetical
		F2I11.100	hypothetical
	AB020745	BAA96960.1	hypothetical
		BAA96961.2	hypothetical

^a Accession number of the genomic clone.^b Annotation of the putative ORF in the YAC (Yeast artificial chromosome) or BAC (Bacterial artificial chromosome) clone.^c Identified cDNA corresponding to the ORF; Gene names are in parentheses.^d Putative splice variant of GLR4.^e Putative splice variant of ACL1.^f The cDNA identified in this study.^g The genomic clone identified in this study.

Plant growth

Plants were either grown in a composite soil in a greenhouse, or grown on sterile agar plates in petri dishes (22°C/19°C, 16 h light/8 h dark cycle, 100 $\mu\text{mol m}^{-2} \text{s}^{-1}$ photon flux density). For studies of Ca^{2+} supplementation, a soil-saturating volume of 4 mM CaCl_2 was added every 2 d. For ionic sensitivity analysis, surface-sterilized seeds were grown for 2 weeks in Ca^{2+} -depleted 1/4 \times B5 medium, supplemented with the appropriate ions.

Growth measurement and Ca^{2+} analysis

Seedlings were grown on sterile agar plates as described above. The aerial portions of the plants were harvested and the fresh weight was measured individually. The tissues were collected and dried at 70°C for 72 h. The dry weight was determined and then the dried tissues were digested with 65% nitric acid at 200°C. The resulting digestate was resuspended in 1 M nitric acid. The total Ca^{2+} content per gram of dry weight was determined by an atomic absorption spectrophotometer (Unicam Atomic Absorption, U.K.).

GUS assays

GUS histochemical staining was performed on whole seedlings. Tissues were vacuum infiltrated in a buffer containing 1 mg ml^{-1} X-

Gluc (5-bromo-4-chloro-3-indolyl- β -glucuronide), 100 mM sodium phosphate pH 7, 1% Triton X100, 5 mM potassium ferrocyanide, 5 mM potassium ferricyanide, and 1 mM EDTA. The enzymatic reaction was performed overnight at 37°C in the dark. After washing in a buffer containing 100 mM sodium phosphate (pH 7) and 1 mM EDTA, tissues were cleared through a graded ethanol series. Sections (7 μm thick) of GUS-stained material were prepared on paraffin embedded tissues and cut with an LKB microtome.

Results

Families of ionotropic glutamate receptor homologs from *A. thaliana*

In a previous study from our laboratory, a plant homolog of mammalian ionotropic glutamate receptors was isolated from *Brassica napus* (Kwak et al. 1997a). The *Brassica* expressed sequence tag (EST) was used as a query to search for related sequences from the GenBank database of *A. thaliana*. This search unveiled one EST (accession no R29880) and 19 genomic sequences for iGluR homologs (Table 1).

Molecular cloning of an Arabidopsis homolog of ionotropic glutamate receptors

The identified Arabidopsis EST corresponded to a 1.3 kb fragment of the C-terminal sequence. This DNA fragment was

used to screen both a genomic library and a cDNA library. A genomic clone (accession no AF159499) was obtained, but no hybridization was obtained in screening of the cDNA library. Thus, the full-length cDNA sequence was obtained by 5'-RACE-PCR. The full-length cDNA (accession no AF159498, nucleotide 1 to 2,975) was reconstituted from the cDNA and PCR clone. Sequence comparison of the genomic clone and the cDNA was performed to verify the accuracy of the PCR product. The sequence contained a deduced open reading frame encoding a polypeptide of 912 amino acid residues with a predicted molecular mass 102 kDa (Fig. 1A). Comparison of the predicted amino acid sequence of AtGluR2 against the NCBI non-redundant protein database revealed that the AtGluR2 sequence shares low (21% identity) but significant similarity to that of mammalian iGluRs throughout the transmembrane regions (62% identity in the TM III region) and pore-forming region of the peptide (Fig. 1B). The genomic organization of the AtGluR2 suggested that this gene also displays a distinctive exon-intron structure similar to that of the kainate subtypes in the pore-forming domain (Fig. 1C; Sommer et al. 1991, Herb et al. 1996). When hydropathy plots were constructed from the deduced amino acid sequence, AtGluR2 was predicted to display a three-plus-one transmembrane structure, as shown in Fig. 1D. This structure is consistent with the structure expected for ionotropic glutamate receptors (Hollmann et al. 1994, MacKinnon 1995).

A

```

1  MFVVLVLLSPFVILIGDMISEGAGLRPRYVDVGAIFSLGTLQGEVTNIAM
   V
51  KAAEEDVNSDPFLGGSKLRITTYDAKRNGFLTIMGALQFMETDAVAIIG
101  PQTSIMAHVLSHLANELSVPMLSFTALDPSLSALQFPFFVQTAPSDLFML
151  RAIAEMISYVGWSEVIALYNDNRSNGITALGDELEGRCKISYKAVLP
201  LDVVITSPREIINELVKIQMESRVIIIVNTFPKTKGKIFEEAQLGMMEX
251  GYVWIATTWLTSLLDVNPLPAKTAESLRGVLTLRIHTPNKKKDFVAR
301  WNKLSNGTVGLVYGLAYDTVWIIARAVKRLLDSRANISFSSDPKLTSM
351  KGGGSLNLGALSIFDQGSQFLDVIIVNTNMTGVTGQIQFLPDRSIQPSYD
401  IINVVDDGRQIGYVSNHSGLSIIPESLYKKLSNRSSNQHLNNVTWPG
451  GTSETPRGVFPNNGRRRLRGVPRASFKEFVSRLDGSNKVQGYAIDVFE
   V
501  AAVKLISYPVPHEFVLPGDGLKNPNFNEFVNNTIGVFDVAVGDIAIVTK
551  RTRIVDFTPQYIESGLVVAVPVKLNDFPWAFLRPFTPPMVAATAAFFLI
   V TM I
601  VGSVITWLEHRINDEFGRGPPRKQIVTILWFSFSTMFSSHRENTVSTLGRA
   Pore
651  VLLIWLFFVLIITSSYTSASLTSLITVQQLNSPIRGVDTLISSSGRVGFQV
   TM III
701  GSYAENYMIDELNIARSRLVPLGSPKEYAAALQNGTVAAIIVDERPPYVDF
   V
751  LSEFCGFAIRGQEFTRSGWGFAPFRDPSLAIDMSTAILGLSETGQLQKIH
801  DKWLSRNSCNLNGSVSDEDESQLKLRSEWGLFVCGISCFIALEIYFFX
   TM IV
851  IVRDFPRHGKYDEEATVSSPSSRSKSLQTFLAYFDEKEDESKRMKRKR
901  NDDLKPSRPI*
  
```

B

```

620      Pore      640 650      TM III      674
AtGluR2  PRKIVTILWFSFSTMFSSH...ALLLGLFVLLIITSSYTSASLTSLI
GLR2     PRQITITLWFSFSTMFSSH...MALLGLFVLLIITSSYTSASLTSLI
GLR6     PRQITITVWFSFSTMFSSH...FVLLGLFVLLIITSSYTSASLTSLI
GLUR3    PRQITITVWFSFSTMFSSH...FVLLGLFVLLIITSSYTSASLTSLI
BnGluR1  PRQITITLWFSFSTMFSSH...ALLLGLFVLLIITSSYTSASLTSLI
NtGluR1  SKQIVTILWFSFSTMFSSH...ALLLGLFVLLIITSSYTSASLTSLI

GluR1    EFGFNSLAFSLGAFMQGC...TGGGFWFPTLIITSSYTSANAAFE
GluR2    EFGFNSLAFSLGAFMQGC...TGGGFWFPTLIITSSYTSANAAFE
GluR5    NPTILNSFEGVGALMQGS...TGGGFWFPTLIITSSYTSANAAFE
  
```

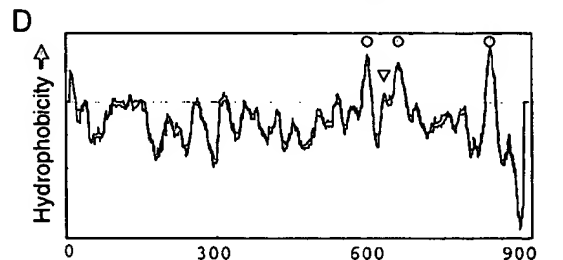
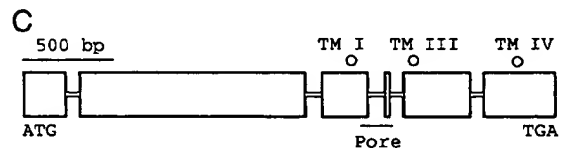


Fig. 1 Deduced amino acid sequence and the hydropathy analysis of AtGluR2, and the genomic structure of the *AtGluR2* gene. (A) The deduced amino acid sequence of AtGluR2 (GenBank accession no AF159498). The sequences corresponding to putative transmembrane domains (TM I, TM III, and TM IV) are underlined. The putative pore-forming domain (Pore) at residues 620–640 is double-underlined. The arrowheads indicate the positions of the exon-intron junctions identified in the genomic clone by comparison with the cDNA sequence. (B) Sequence alignment of the pore-forming region and the transmembrane domain III among plant glutamate receptor homologs and mammalian iGluRs. Numbers above the sequence correspond to amino acid residues of AtGluR2. Residues between the two domains are shown as dots. Identical and similar residues are indicated by dark and light shades, respectively. Arabidopsis glutamate receptor homologs used in the alignment are AtGluR2, GLR2, GLR6, and GLUR3 (GenBank accession nos AF159498, AF079999, AF170494, and AF167355). BnGluR1 and NtGluR1 sequences were derived from a *Brassica napus* cDNA (accession no AF109392) and a tobacco partial cDNA (unpublished data) clone. Mammalian iGluRs are AMPA/kainate subtypes, GluR1, GluR2, and GluR5 (GenBank accession nos X17184, M85035, and M83560). (C) Schematic diagram of the genomic clone (GenBank accession no AF159499). The boxes and the bold lines indicate the exons and the introns, respectively. The putative transmembrane domains are marked with dots. The pore-forming domain is underlined. (D) The hydropathy analysis of the AtGluR2 peptide sequence. The hydropathy plot is generated with TMPred (http://www.ch.embnet.org/software/TMPRED_form.html). The dots and the arrowhead indicate the putative transmembrane domains and the pore-forming domain, respectively.



Fig. 2 Expression of *AtGluR2* in transgenic *Arabidopsis* plants. Total RNA was extracted from 3-week-old seedlings of seven representative lines and 20 μ g of total RNA were analyzed for the *AtGluR2* gene expression. The RNA gel blot was hybridized with 0.4 kb fragment of the *AtGluR2* gene (nucleotide 2,424 to 2,730). Endogenous *AtGluR2* transcripts were not detected in wild-type Columbia plants and transgenic lines expressing the vector (control) alone.

AtGluR2 expression levels in transgenic *Arabidopsis*

To evaluate the physiological roles of the *AtGluR2* gene in plants, we generated transgenic *Arabidopsis* lines that stably express the sense-oriented *AtGluR2* cDNA under the control of the dual 35S promoter of the cauliflower mosaic virus. During the initial screening on selective media, 19 independent transgenic lines displayed distinctively abnormal development. Seven representative transgenic lines were tested for the *AtGluR2* expression by performing RNA gel blot analysis (Fig. 2, upper row). In wild-type *Arabidopsis* and the vector-transformed control plants, the *AtGluR2* mRNA expression could not be detected from total RNA extracted from whole seedlings. The homozygous transgenic lines showed increased expression of the *AtGluR2* transcript, although the level of expressions varied across the transgenic lines. Thus, the *AtGluR2* gene was successfully overexpressed in transgenic *Arabidopsis* lines.

AtGluR2 overexpression disrupts normal development

Figure 3 shows the growth characteristics of two representative transgenic lines. Transgenic plants exhibited symptoms that are highly consistent with Ca^{2+} deficiency. When plants are subjected to Ca^{2+} deficiency, the symptoms are easily noticed in the growing points of the upper parts of plants. Brown melanin compounds resulting from polyphenolic oxidation are also found in the Ca^{2+} deficient tissues (Kirkby and Pilbeam 1984). As shown in Fig. 3B, the G-5 line displayed browning and necrosis of the growing points, curling and deformation of leaves, and disintegration of petioles, when seedlings were grown on $1\times$ B5 medium for 2 weeks. When this line was grown in composite soil for 4 weeks, it produced necrotic and deformed leaves and many lateral buds. The whole growth was also severely retarded (Fig. 3C). The A-12

line developed milder symptoms than the G-5 lines, exhibiting bushy and dwarf stature with large numbers of short secondary inflorescences. Necrosis at the tips and margins of young leaves was also apparent (Fig. 3D). The fertility of transgenic lines was also reduced and this was positively correlated with the severity of other morphological defects (data not shown).

*Ca*²⁺ supplementation mitigates *AtGluR2*-induced symptoms

Since the morphological phenotypes of the transgenic lines was similar to the Ca^{2+} deficiency symptoms, we tested whether providing Ca^{2+} as a supplement could alleviate the morphological alterations caused by *AtGluR2* overexpression in the transgenic plants. After seed germination, plants were watered in the presence or absence of 4 mM CaCl_2 every 2 d. This concentration of Ca^{2+} is equivalent to that in Hoagland's nutrient solution (Hoagland and Arnon 1950). Transgenic A-12 and C-1 plants supplemented with Ca^{2+} displayed developmental patterns similar to that of plants carrying the empty vector, although the extent of amelioration provided by Ca^{2+} supplementation varied across the individual lines (Fig. 4). Addition of Ca^{2+} mitigated all abnormalities seen in the transgenic plants, including those in necrosis and deformity of leaves, repressed growth of stem elongation, reduced apical dominance and lowered fertility. The plants carrying the empty vector showed similar growth characteristics in the presence or absence of Ca^{2+} supplementation, although with extra supply of Ca^{2+} the plants grew more vigorously. The result confirmed that the symptoms exhibited by overexpression of the *AtGluR2* gene are due to Ca^{2+} deficiency.

*The Ca*²⁺ levels in shoots were similar in control and transgenic plants

To test whether the Ca^{2+} deficiency seen in the transgenic lines are due to disturbance Ca^{2+} accumulation, we measured Ca^{2+} contents as a function of Ca^{2+} concentration in the growth media. Plants were grown for two weeks in Ca^{2+} depleted $1/4\times$ B5 medium and then the medium was supplemented with 10 μ M, 100 μ M, 250 μ M, 1 mM and 6 mM of CaCl_2 , respectively. The control plants did not develop any signs of Ca^{2+} starvation at any of the Ca^{2+} concentrations tested. In contrast, the transgenic plants displayed Ca^{2+} deficiency symptoms when the external Ca^{2+} concentration was below 100 μ M. Since the symptoms of Ca^{2+} deficiency were primarily observed in aerial parts of the plants, the chemical analysis was performed with samples from the shoots. As shown in Fig. 5A, control and transgenic plants had little differences in Ca^{2+} levels in the shoots. Therefore, the differential responses to low Ca^{2+} nutrition between the control and transgenic plants could not be explained by differences in Ca^{2+} within the plant shoots. This indicates that the Ca^{2+} deficiency phenotype in the shoot of the transgenic plants was not attributable to reduced accumulation or uptake of Ca^{2+} .

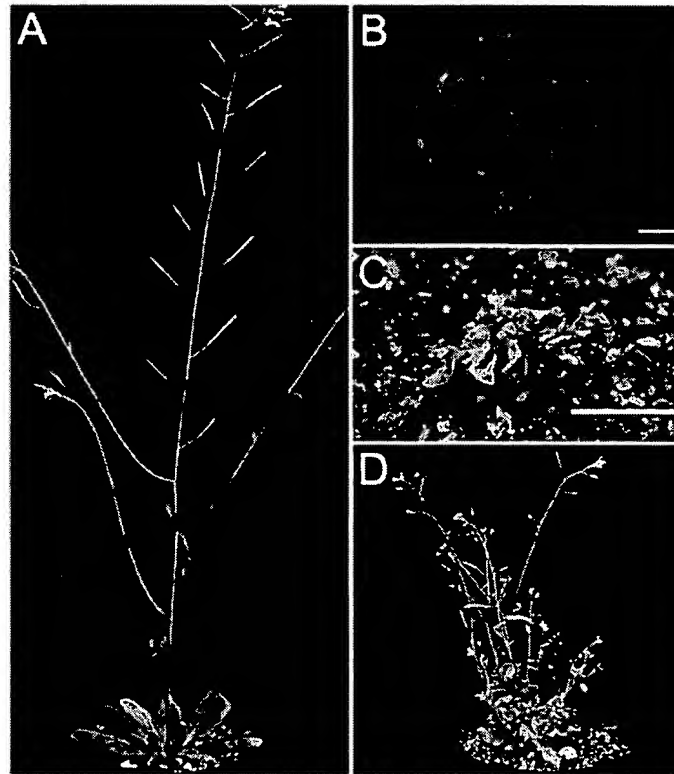


Fig. 3 Phenotypes of transgenic *Arabidopsis* overexpressing the *AtGluR2* gene. (A) The control plant transformed with the vector alone. (B) Seedling of the transgenic line G-5 grown on 1× B5 medium for 2 weeks. Necrosis and browning of the shoot apex and collapse of petioles were observed. Bar: 1 mm. (C) Close-up view of the soil-grown transgenic line G-5. Curled and deformed leaves and many undeveloped lateral buds were present. Bar: 1 cm. (D) The transgenic line A-12. Necrosis was evident at the tips and margins of young leaves. The plant exhibited a stunted and bushy stature with large numbers of short secondary inflorescences.

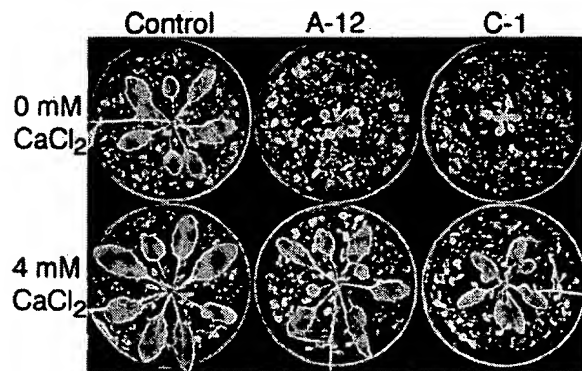


Fig. 4 Supplementary Ca^{2+} ameliorates the *AtGluR2*-induced symptoms. The vector control and the transgenic A-12 and C-1 plants overexpressing the *AtGluR2* gene were grown in a composite soil in a greenhouse for 3 weeks. Plants were watered every 2 d in the presence or absence of 4 mM Ca^{2+} .

The critical deficiency content (CDC) is higher in transgenic plants than that of control plants

To further reveal the physiological basis of the Ca^{2+} deficiency symptoms seen in the transgenic lines, we measured the degree of the efficiency of Ca^{2+} utilization in the plant shoots (Gerloff and Gabelman 1983, Marschner 1995). For this purpose, we characterized the relationship between Ca^{2+} content in shoots and relative shoot growth. When 90% of the maximal growth was taken as a reference point, the CDC of Ca^{2+} for the control plants and transgenic A-12 and C-1 plants were approximately 4 mg g⁻¹ dry weight, 13 mg g⁻¹ dry weight, and 12 mg g⁻¹ dry weight, respectively (Fig. 5B). Thus, the CDC is three-fold higher in the transgenic plants. This result together with the data in Fig. 5A demonstrates that overexpression of the *AtGluR2* gene induces Ca^{2+} deficiency symptoms by impairing the efficiency of Ca^{2+} utilization in the transgenic plant.

*Overexpression of *AtGluR2* renders transgenic plants hypersensitive to K^+ and Na^+ salt*

Ca^{2+} starvation in plants is rarely caused by a complete absence of Ca^{2+} in the soil. Rather, the deficiency is more often

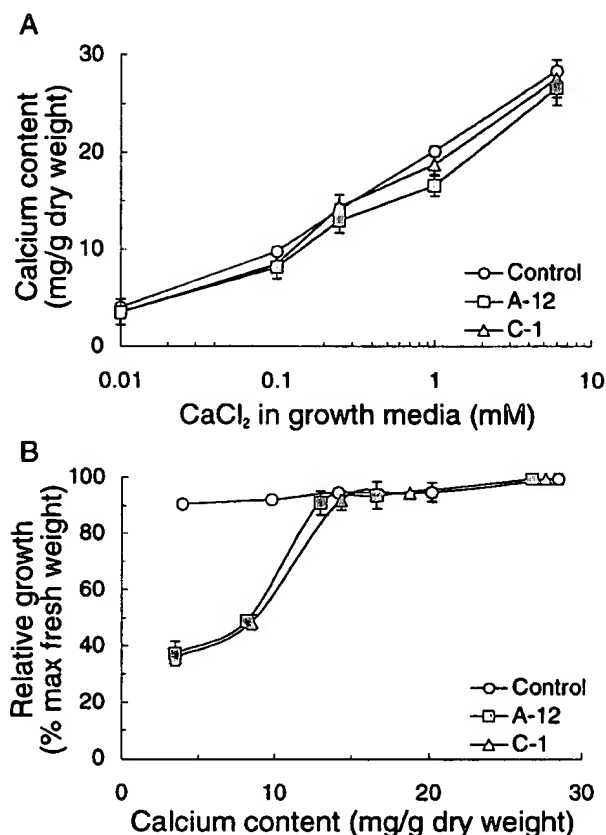


Fig. 5 The effect of Ca^{2+} concentration on plant growth. Plants were grown in the $1/4\times$ B5 medium supplemented with various concentrations of CaCl_2 . After 2 weeks of growth, the fresh weight was measured individually to analyze the relative growth. Seedlings were then pooled to yield the required dry weights for the chemical analysis. Ca^{2+} contents were determined with an atomic absorption spectrophotometer. (A) The effect of external Ca^{2+} on the concentration of Ca^{2+} in the aerial parts. Shoots were collected by excision below the rosette from whole seedling plants. Data represent the average \pm SD of three independent assays. (B) The relative growth as a function of Ca^{2+} concentration in the aerial parts. Data are expressed as the mean \pm SE of three independent experiments (25 seedlings were used for each measurement). Shown are values relative to the fresh weights of seedlings grown on $1/4\times$ B5 medium supplemented with 6 mM CaCl_2 .

induced by low concentrations of Ca^{2+} in relation to other cations, such as high K^+ , Na^+ , or Mg^{2+} (Adams and Ho 1990, Mass and Grieve 1987, Alcantara and De La Guardia 1987, Hirschi 1999). Increase of the external concentration of these elements often reduce the absorption of Ca^{2+} and thereby induce Ca^{2+} deficiency in salt-stressed plants (Robson and Pitman 1983). Furthermore, Ca^{2+} deficiency is often diagnosed by an increased sensitivity to other cations in crop plants (Scaife and Turner 1984). We, thus, tested sensitivity of the transgenic lines to other cations. The transgenic plants were grown in $1/4\times$ B5

medium with addition of K^+ , Na^+ , and Mg^{2+} for 2 weeks. The fresh weight of seedlings grown in $1/4\times$ B5 medium was similar in the control and transgenic plants. The relative growth was, then, analyzed as a function of concentration of these cations. The results showed that the transgenic plants showed notable hypersensitivity to K^+ and Na^+ (Fig. 6A, B). The sensitivity of the transgenic plants to Mg^{2+} was not significantly distinguishable from the control plants (Fig. 6C). The relatively different interaction of the Ca^{2+} with other cations has been observed in other plants, too (Hirschi 1999). The AtGluR2 transgenic plants were not notably hypersensitive to mannitol, suggesting that the hypersensitivity of the transgenic lines to K^+ and Na^+ ions are not due to general osmotic stress (Fig. 6D). The result, therefore, is consistent with the notion that overexpression of the AtGluR2 gene causes Ca^{2+} deficiency.

Ca²⁺ suppresses AtGluR2-induced hypersensitivity to ionic stresses

We, then, tested the effect of Ca^{2+} supplementation on the ionic stress response. Plants were grown in the salt stress media with supplementary Ca^{2+} for 2 weeks. As shown in Fig. 7, supplementing the media with 6 mM CaCl_2 dramatically attenuated the ion sensitivities of the AtGluR2-overexpressing plants. It was observed that supplementation of Ca^{2+} in the growth medium causes increase of the calcium contents in the plant shoots (Fig. 5A). Thus, supplementation of Ca^{2+} in the medium in the presence of other ions should have increased relative concentration of Ca^{2+} in the plant shoots. This, in turn, should have attenuated the effect of the cations in the transgenic lines. This interpretation is consistent with the notion that the transgenic lines have lowered efficiency in Ca^{2+} utilization, mediating the hypersensitivity to ionic stresses that can be rescued by increased Ca^{2+} concentration.

AtGluR2 expresses in vascular tissues

In initial experiments, we tried to determine the distribution of AtGluR2 mRNA among different organs by RNA gel blot analysis. However, we failed to detect any signal for AtGluR2 mRNA even when we used 25 μg of total RNA (data not shown). However, RT-PCR analysis showed that the AtGluR2 gene is expressed in leaves, stems, flowers, and roots (data not shown). A more detailed localization of the AtGluR2 gene expression was investigated using transgenic plants carrying the coding sequence of the *E. coli* β -glucuronidase (*GUS*) gene under the control of the AtGluR2 promoter. Activity of the *GUS* reporter gene was analyzed with the T2 progenies of three independent transgenic lines. The *GUS* activity was detected in the vascular tissues of both shoots and roots. Histochemical analysis in cross-sections revealed that the *GUS* activity was particularly strongly localized in cells adjacent to the conducting vessels (Fig. 8).

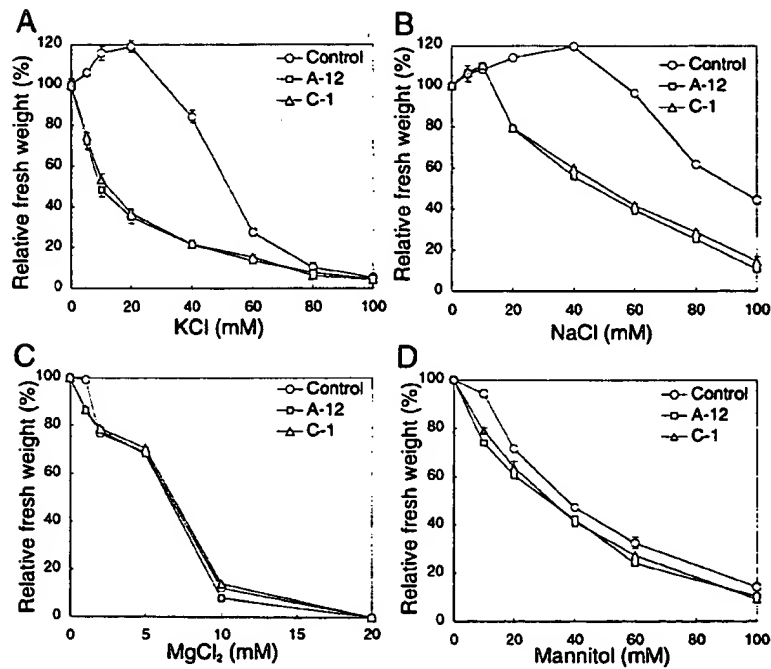


Fig. 6 Sensitivity of transgenic plants to ionic stresses and osmotic stress. Plants were grown in 1/4× B5 media supplemented with various concentrations of KCl, NaCl, MgCl₂, or mannitol. The fresh weight is presented as a percentage relative to the fresh weight in 1/4× B5 medium. Error bars represent the standard error of three independent experiments (25 seedlings were used for each measurement). (A) Sensitivity to KCl. (B) Sensitivity to NaCl. (C) Sensitivity to MgCl₂. (D) Sensitivity to mannitol.

Discussion

As an effort to understand the role of Ca²⁺ in nutrition and the mechanisms underlying Ca²⁺-mediated adaptation to stress in plants, we have focused on the Arabidopsis homologs of ionotropic glutamate receptors. We characterized one member of this gene family as a candidate for a Ca²⁺ permeable channel gene in higher plants. The family includes 19 genes that encode proteins with homology to mammalian ionotropic glutamate receptors (Table 1). Ionotropic glutamate receptors (iGluRs) are nonselective cation channels that are permeable to Ca²⁺, K⁺, and Na⁺ but not to Mg²⁺. However, the primary physiological function of these channels is thought to be regulation of Ca²⁺ influx into cells. The Arabidopsis homologs show relatively low overall sequence identities (21% or less) with the mammalian iGluRs. However, the transmembrane domains (62% identity in TM III region) and the pore-forming region display a substantially high similarity; thus it is reasonable to presume that these plant proteins also function primarily as ion channels. The hydropathy plot of AtGluR2 supports the three-plus-one transmembrane topology as has been suggested in iGluRs.

To investigate the physiological roles of the AtGluR2 gene in plants, we generated transgenic lines of Arabidopsis that

overexpress the AtGluR2 mRNA. The plants overexpressing AtGluR2 gene displayed symptoms that are characteristic indicators of Ca²⁺ deficiency in plant nutrition. The phenotype was exhibited in 19 independent transgenic lines and is therefore causally related to the introduced genes. The AtGluR2 gene overexpressing lines were also hypersensitive notably to K⁺ and Na⁺ ions. The ability to suppress the growth defects and ion sensitivity of the transgenic plants with exogenous Ca²⁺ strongly suggests that these plants are deficient in Ca²⁺.

Ca²⁺ deficiency can be caused by reduced uptake of Ca²⁺ in the root, reduced transportation of Ca²⁺ from root to shoot, or by reduced utilization of the transported Ca²⁺. Our data suggests that the major reason for Ca²⁺ deficiency in the transgenic lines is due to reduced utilization of the transported Ca²⁺.

Developing a hypothesis that explains how overexpression of an ion channel protein might cause the reduced utilization of Ca²⁺ in transgenic plants is challenging. It is possible that the ectopic expression of the AtGluR2 gene cause excess K⁺ or Na⁺ uptake if AtGluR2 is permeable to Ca²⁺ as well as monovalent cations as in the case of the mammalian iGluRs. Increased uptake of K⁺ or Na⁺ could compete with Ca²⁺, rendering reduced efficiency of Ca²⁺ utilization. An alternative possibility would be that the overexpression of the AtGluR2 gene might disturb the Ca²⁺ transport directly. If Arabidopsis gluta-

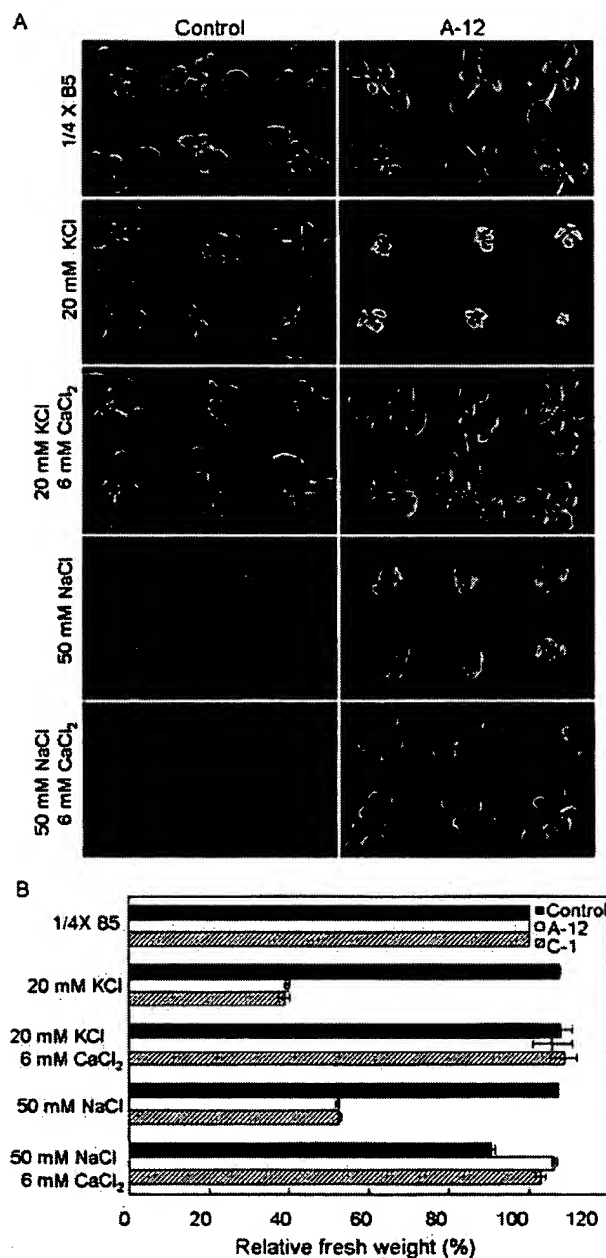


Fig. 7 The effects of supplemented Ca^{2+} on ion hypersensitivity. (A) Plants growth on ionic stress conditions in the presence or absence of 6 mM Ca^{2+} supplementation. Vector control plants are shown on left column and the transgenic A-12 plants on the right column. The plants were grown for 2 weeks. (B) Relative fresh weight of the vector control and the transgenic (A-12, C-1) seedlings. Data are given as the mean \pm SE of three independent experiments (25 seedlings were used for each measurement). Shown are values relative to the fresh weight of seedlings grown in 1/4 \times B5 medium.

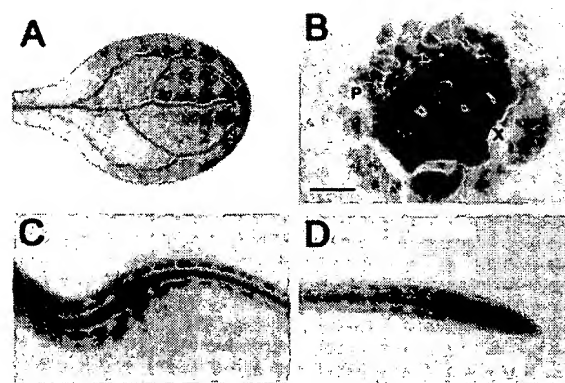


Fig. 8 Expression pattern of the *AtGluR2* gene in *Arabidopsis*. The GUS activity in transgenic *Arabidopsis* lines expressing the GUS reporter gene under the control of the *AtGluR2* gene promoter was examined. The GUS activity was detected in the vascular tissues of the shoots (A) and the roots (C, D). Cross-section analysis of the GUS expression (B). The cross section was 7 μm thick. P, phloem; X, xylem. Bar: 100 μm .

mate receptor homologs form heteromeric channels as in the case of the mammalian iGluRs, overexpression of a subunit could induce changes in overall channel activities. In the case that expression of the *AtGluR2* protein results in heteromeric channels that are less efficient in Ca^{2+} transport, then overexpression of *AtGluR2* might cause Ca^{2+} deficiency in low Ca^{2+} nutrition. In mammalian cells, Ca^{2+} influx evoked by glutamate treatments is reduced by co-expression of the GluR2 subunit (Hollmann et al. 1991).

The processes involved in unloading Ca^{2+} from xylem vessels to the apoplast and in uptake of Ca^{2+} by leaf cells are not fully understood. In fact, none of the mechanisms that regulate fluxes of Ca^{2+} between various tissues of higher plants are well characterized. However, it is reasonable to assume that Ca^{2+} channels should be involved at certain steps to mediate Ca^{2+} influx through plasma membranes. The promoter of the *AtGluR2* gene is expressed along the vascular tissues, particularly in cells adjacent to conducting vessels, where Ca^{2+} is removed from the xylem sap. The characteristics of the deduced peptide sequence and the preferential expression of the *AtGluR2* gene in vascular tissues suggests that it may play a functional role in Ca^{2+} unloading and allocation among different tissues.

In any event, the *AtGluR2* transgenic plants are of interest as a starting point for understanding the molecular components for regulating efficiency of Ca^{2+} utilization and for further functional characterization of the family of glutamate receptor channels in plants. In future studies, it will be of considerable interest to employ various heterologous expression systems to gain further insight into the biochemical and electrophysiological functions of these proteins.

Acknowledgement

We thank Julian Schroeder (University of California, San Diego, U.S.A.) for discussion, comments on the manuscript and support. This work was supported by a grant from the National Research Laboratory Program of the Ministry of Science and Technology to Hong Gil Nam and supported in part by DOE and NSF grants to Julian Schroeder. J.M.K. was supported by a fellowship from the Human Frontier Science Program organization.

References

- Adams, P. and Ho, L.C. (1990) Effect of salinity on calcium transport in tomato. In *Plant Nutrition — Physiology and Applications*. Edited by van Beusichem, M.L. pp. 469–472. Kluwer Academic Publishers, Netherlands.
- Alcantara, E. and De La Guardia, M.D. (1987) Inheritance of response of sunflower inbreds to a low calcium/magnesium ratio. In *Genetic Aspects of Plant Mineral Nutrition*. Edited by Gabelman, H.W. and Loughmanial, B.C. pp. 393–397. Martinus Nijhoff Publishers, Dordrecht.
- Bechtold, N., Ellis, J. and Pelletier, G. (1993) In planta *Agrobacterium* mediated gene transfer by infiltration of adult *Arabidopsis thaliana* plants. *C. R. Acad. Sci. Paris* 316: 1194–1199.
- Behling, J.P., Gabelman, W.H. and Gerloff, G.C. (1989) The distribution and utilization of calcium by two tomato (*Lycopersicon esculentum* Mill.) lines differing in calcium efficiency when grown under low-Ca stress. *Plant Soil* 113: 189–196.
- Bettler, B., Boulter, J., Hermans-Borgmeyer, I., O'Shea-Greenfield, A., Deneris, E.S., Moll, C., Borgmeyer, U., Hollmann, M. and Heinemann, S. (1990) Cloning of a novel glutamate receptor subunit, GluR5: expression in the nervous system during development. *Neuron* 5: 583–595.
- Boulter, J., Hollmann, M., O'Shea-Greenfield, A., Hartley, M., Deneris, E., Maron, C. and Heinemann, S. (1990) Molecular cloning and functional expression of glutamate receptor subunit genes. *Science* 249: 1033–1037.
- Bush, D.S. (1995) Calcium regulation in plant cells and its role in signaling. *Annu. Rev. Plant Physiol. Plant Mol. Biol.* 46: 95–122.
- Clarkson, D.T. (1984) Calcium transport between tissues and its distribution in the plant. *Plant Cell Environ.* 7: 449–456.
- Clarkson, D.T. and Hanson, J.B. (1980) The mineral nutrition of plants. *Annu. Rev. Plant Physiol.* 31: 239–298.
- Clemens, S., Antosiewicz, D.M., Ward, J.M., Schachtman, D.P. and Schroeder, J.I. (1998) The plant cDNA LCT1 mediates the uptake of calcium and cadmium in yeast. *Proc. Natl. Acad. Sci. USA* 95: 12043–12048.
- English, J.E. and Maynard, D.N. (1981) Calcium efficiency among tomato strains. *J. Amer. Soc. Hort. Sci.* 106: 552–557.
- Epstein, E. (1972) *Mineral Nutrition of Plants: Principles and Perspectives*. Wiley, New York.
- Epstein, E. and Jefferies, R.L. (1964) The genetic basis of selective ion transport in plants. *Annu. Rev. Plant Physiol.* 15: 169–184.
- Frommer, W.B. and Bohnert, H.J. (1999) Physiology and metabolism – talking through membranes. *Curr. Opin. Plant Biol.* 2: 173–177.
- Fox, T.C. and Gueriot, M.L. (1998) Molecular biology of cation transport in plants. *Annu. Rev. Plant Physiol. Plant Mol. Biol.* 49: 669–696.
- Gamborg, O.L., Miller, R.A. and Ojima, K. (1968) Nutrient requirement of suspensions cultures of soybean root cells. *Exp. Cell Res.* 50: 151.
- Gasic, G.P. and Hollmann, M. (1992) Molecular neurobiology of glutamate receptors. *Annu. Rev. Physiol.* 54: 507–536.
- Geiger, J.R., Melcher, T., Koh, D.S., Sakmann, B., Seeburg, P.H., Jonas, P. and Monyer, H. (1995) Relative abundance of subunit mRNAs determines gating and Ca^{2+} permeability of AMPA receptors in principal neurons and interneurons in rat CNS. *Neuron* 15: 193–204.
- Gerloff, G.C. (1963) Comparative mineral nutrition of plants. *Annu. Rev. Plant Physiol.* 14: 107–124.
- Gerloff, G.C. and Gabelman, W.H. (1983) Genetic basis of inorganic plant nutrition. In *Encyclopedia of Plant Physiology*. Edited by Lauchil, A. and Bielecki, R.L. pp. 453–480. Springer-Verlag, Berlin.
- Gilroy, S., Bethke, P.C. and Jones, R.L. (1993) Calcium homeostasis in plants. *J. Cell Sci.* 106: 453–461.
- Leonardo, E. B.G., Gabelman, W.H. and Gerloff, G.C. (1982) Inheritance of differences in calcium utilization by tomatoes under low-calcium stress. *J. Amer. Soc. Hort. Sci.* 107: 664–669.
- Herb, A., Higuchi, M., Sprengel, R. and Seeburg, P.H. (1996) Q/R site editing in kainate receptor GluR5 and GluR6 pre-mRNAs requires distant intronic sequences. *Proc. Natl. Acad. Sci. USA* 93: 1875–1880.
- Hirschi, K.D. (1999) Expression of *Arabidopsis* CAX1 in tobacco: altered calcium homeostasis and increased stress sensitivity. *Plant Cell* 11: 2113–2122.
- Hoagland, D.R. and Arnon, D.I. (1950) The water-culture method for growing plants without soil. In *Circular. Calif Agr Exp Station*, Berkeley.
- Hochmuth, G.J. (1984) Variation in calcium efficiency among strains of cauliflower. *J. Amer. Soc. Hort. Sci.* 109: 667–672.
- Hollmann, M., Hartley, M. and Heinemann, S. (1991) Ca^{2+} permeability of KA-AMPA-gated glutamate receptor channels depends on subunit composition. *Science* 252: 851–853.
- Hollmann, M. and Heinemann, S. (1994) Cloned glutamate receptors. *Annu. Rev. Neurosci.* 17: 31–108.
- Hollmann, M., Maron, C. and Heinemann, S. (1994) N-glycosylation site tagging suggests a three transmembrane domain topology for the glutamate receptor GluR1. *Neuron* 13: 1331–1343.
- Hollmann, M., O'Shea-Greenfield, A., Rogers, S.W. and Heinemann, S. (1989) Cloning by functional expression of a member of the glutamate receptor family. *Nature* 342: 643–648.
- Horst, W.J., Currie, C. and Wissemeier, A.H. (1993) Differences in calcium efficiency between cowpea (*Vigna unguiculara* (L.) Walp.) cultivars. In *Genetic Aspects of Plant Mineral Nutrition*. Edited by Randal, P.J. et al. pp. 59–68. Kluwer Academic Publishers, Netherlands.
- Hume, R.I., Dingle, R. and Heinemann, S.F. (1991) Identification of a site in glutamate receptor subunits that controls calcium permeability. *Science* 253: 1028–1031.
- Kirkby, E.A. and Pilbeam, D.J. (1984) Calcium as a plant nutrient. *Plant Cell Environ.* 7: 397–405.
- Knight, H., Trewavas, A.J. and Knight, M.R. (1996) Cold calcium signaling in *Arabidopsis* involves two cellular pools and a change in calcium signature after acclimation. *Plant Cell* 8: 489–503.
- Kohler, C., Merkle, T. and Neuhaus, G. (1999) Characterisation of a novel gene family of putative cyclic nucleotide- and calmodulin-regulated ion channels in *Arabidopsis thaliana*. *Plant J.* 18: 97–104.
- Kretsinger, R.H. (1977) Evolution of the informational role of calcium in eukaryotes. In *Calcium-Binding Proteins and Calcium Function*. Edited by Wasserman, R.H., Corradino, R.A., Carafoli, E., Kretsinger, R.H., MacLennan, D.H. and Siegel, F.L. pp. 63–72. North Holland, New York.
- Kwak, J.M., Kim, S.A., Hong, S.W. and Nam, H.G. (1997a) Evaluation of 515 expressed sequence tags obtained from guard cells of *Brassica campestris*. *Planta* 202: 9–17.
- Kwak, J.M., Kim, S.A., Lee, S.K., Oh, S.A., Byoun, C.H., Han, J.K. and Nam, H.G. (1997b) Insulin-induced maturation of *Xenopus* oocytes is inhibited by microinjection of a *Brassica napus* cDNA clone with high similarity to a mammalian receptor for activated protein kinase C. *Planta* 201: 245–251.
- Lam, H.M., Chiu, J., Hsieh, M.H., Meisel, L., Oliveira, I.C., Shin, M. and Coruzzi, G. (1998) Glutamate-receptor genes in plants. *Nature* 396: 125–126.
- Lauchil, A. (1990) Calcium, salinity and the plasma membrane. In *Calcium in Plant Growth and Development*. Edited by Leonard, R.T. and Helper, P.K. pp. 26–35. American Society of Plant Physiologists, Rockville, MD.
- Leng, Q., Mercier, R.W., Yao, W. and Berkowitz, G.A. (1999) Cloning and first functional characterization of a plant cyclic nucleotide-gated cation channel. *Plant Physiol.* 121: 753–761.
- MacKinnon, R. (1995) Pore loops: an emerging theme in ion channel structure. *Neuron* 14: 889–892.
- Marschner, H. (1983) General introduction to the mineral nutrition of plants. In *Encyclopedia of Plant Physiology*. Edited by Lauchil, A. and Bielecki, R.L. pp. 5–60. Springer-Verlag, Berlin.
- Marschner, H. (1995) *Mineral Nutrition of Higher Plants*. Academic Press, San Diego.
- Mass, E.V. and Grieve, C.M. (1987) Sodium-induced calcium deficiency in salt-stressed corn. *Plant Cell Environ.* 10: 559–564.
- Newman, T., de Bruijn, F.J., Green, P., Keegstra, K., Kende, H., McIntosh, L., Ohlrogge, J., Raikhel, N., Somerville, S., Thomashow, M. et al. (1994) Genes galore: a summary of methods for accessing results from large-scale partial sequencing of anonymous *Arabidopsis* cDNA clones. *Plant Physiol.* 106: 1241–1255.

- Pineros, M. and Tester, M. (1997) Calcium channels in higher plant cells: selectivity, regulation and pharmacology. *J. Exp. Bot.* 48: 551–577.
- Reid, R.J. and Tester, M. (1992) Measurements of Ca^{2+} fluxes in intact plant cells. *Philos. Trans. R. Soc. Lond B Biol. Sci.* 338: 73–82.
- Robson, A.D. and Pitman, M.G. (1983) Interactions between nutrients in higher plants. In *Encyclopedia of Plant Physiology*. Edited by Lauchli, A. and Bielecki, R.L. pp. 147–180. Springer-Verlag, Berlin.
- Sanders, D., Brownlee, C. and Harper, J.F. (1999) Communicating with calcium. *Plant Cell* 11: 691–706.
- Scaife, A. and Turner, M. (1984) *Diagnosis of Mineral Disorders in Plants*. Edited by Robinson, J.B.D. Chemical Publishing, New York.
- Schachtman, D.P., Kumar, R., Schroeder, J.I. and Marsh, E.L. (1997) Molecular and functional characterization of a novel low-affinity cation transporter (LCT1) in higher plants. *Proc. Natl. Acad. Sci. USA* 94: 11079–11084.
- Sommer, B., Kohler, M., Sprengel, R. and Seeburg, P.H. (1991) RNA editing in brain controls a determinant of ion flow in glutamate-gated channels. *Cell* 67: 11–19.
- Trewavas, A. (1999) Le calcium, C'est la vie: calcium makes waves. *Plant Physiol.* 120: 1–6.
- Verdoorn, T.A., Burnashev, N., Monyer, H., Seeburg, P.H. and Sakmann, B. (1991) Structural determinants of ion flow through recombinant glutamate receptor channels. *Science* 252: 1715–1718.
- White, P.J. (1998) Calcium channels in the plasma membrane of root cells. *Ann. Bot.* 81: 173–183.
- Wisden, W. and Seeburg, P.H. (1993) Mammalian ionotropic glutamate receptors. *Curr. Opin. Neurobiol.* 3: 291–298.

(Received September 12, 2000; Accepted October 25, 2000)

Glutamate-Gated Calcium Fluxes in Arabidopsis¹

Kirsten L. Dennison and Edgar P. Spalding*

Department of Botany, University of Wisconsin, 430 Lincoln Drive, Madison, Wisconsin 53706

It is well accepted that endogenous and environmental signals can influence cellular activities by changing $[Ca^{2+}]_{cyt}$ (Malhó et al., 1998; Sanders et al., 1999). Despite the importance of this mechanism for coupling stimuli to responses (Malhó et al., 1998), the molecules responsible for generating increases in $[Ca^{2+}]_{cyt}$ during cell signaling in plants are not known at the genetic level. The results presented here raise the possibility that ligand-gated ion channels in plants such as those predicted by the discovery of ionotropic glutamate receptor (iGluR)-like genes in Arabidopsis (Lam et al., 1998) are key components of a Ca^{2+} influx mechanism important to signal transduction.

In animal brains iGluR channels mediate fast chemical transmission across synapses by increasing the permeability of the post-synaptic cell membrane to K^+ , Na^+ , and Ca^{2+} after binding Glu released by the presynaptic cell (Hille, 1992; Hollmann and Heinemann, 1994; Dingledine et al., 1999). The resulting Ca^{2+} entry in particular has been associated with long-term potentiation of the synapse, a physiological adaptation important to the learning process (Baudry and Lynch, 1993; Bliss and Collinridge, 1993). The Glu receptor homologs recently identified in plants (Lam et al., 1998) are too divergent from animal iGluRs to know with any certainty what ligand(s) gate them, what ions are conducted in the open state, and in which membrane(s) of the cell they function (Chiu et al., 1999). Thus the identification of iGluR sequences in the Arabidopsis genome raises intriguing questions about the physiological functions of neurotransmitter-gated channels in plant cells.

The possibility that Glu gates Ca^{2+} -permeable channels at the plasma membrane of plant cells was explored by measuring $[Ca^{2+}]_{cyt}$ in transgenic seedlings expressing aequorin, a Ca^{2+} -sensitive luminescent protein (Knight et al., 1991). As shown in Figure 1A, Glu application immediately triggered a very large, transient spike in $[Ca^{2+}]_{cyt}$. In separate experiments the effect of Glu on membrane potential (V_m) was measured with intracellular microelectrodes inserted into root apices of intact seedlings. Figure 1A also shows that switching the bathing medium from 1 mM KCl to 1 mM K-Glu induced a

large and rapid depolarization of the membrane, as would be expected if the abrupt increase in $[Ca^{2+}]_{cyt}$ was due to Glu opening Ca^{2+} -permeable channels at the plasma membrane. The average peak change in V_m induced by 1 mM Glu was 55 ± 7 mV ($n = 6$ seedlings). This positive shift in V_m , though consistent with Glu gating an inward electrogenic Ca^{2+} current across the plasma membrane, may also be due to secondary effects of the increased $[Ca^{2+}]_{cyt}$ on other ion transporters. Another scenario to consider is that Glu directly gates channels permeable to ions such as Cl^- (Cully et al., 1994) in addition to Ca^{2+} -permeable channels to cause the depolarization. And last, an electrogenic Glu-uptake mechanism (Boorer et al., 1996) may also contribute to the electrical response. Because these and perhaps other scenarios are not mutually exclusive, more electrophysiological studies of the connection between the large Glu-gated changes in $[Ca^{2+}]_{cyt}$ and the effect on V_m are warranted.

Figure 1B shows that the magnitude and time course of the rapid increase in $[Ca^{2+}]_{cyt}$ was similar to the well-studied response to cold shock, i.e. in the micromolar concentration range and completed within several seconds (Knight et al., 1991, 1996; Lewis et al., 1997). Treatment with 1 mM Glu induced a response that was typically hundreds of fold higher than the control injection of equimolar KCl, which produced a touch response that may reflect Ca^{2+} entering the cytoplasm from internal stores (Haley et al., 1995; Legué et al., 1997). The post-peak shoulder apparent in the selected response to Glu was often, but not always observed. Activation of iGluRs by Glu causes very similar Ca^{2+} changes in cells of the mammalian nervous system (Kirischuk et al., 1999; Obrietan and van den Pol, 1999).

If the increase in $[Ca^{2+}]_{cyt}$ triggered by Glu resulted at least in part from flux across the plasma membrane from the apoplast, impermeant channel blockers and external chelators of Ca^{2+} should reduce the response. The results in Figure 2A demonstrate that pretreatment with La^{3+} , a frequently used blocker of plasma membrane Ca^{2+} channels, inhibited the Ca^{2+} spike to the low level induced by the control treatment. Chelating extracellular Ca^{2+} by pre-treating seedlings with EGTA was similarly inhibitory (Fig. 2B). The combined evidence support our suggestion that Glu triggers an influx of Ca^{2+} across the plasma membrane and this leads to a dramatic change in $[Ca^{2+}]_{cyt}$. Calcium-induced Ca^{2+} -release from inter-

¹ This work was supported by the National Science Foundation (career award no. IBN-9734478 to E.P.S.).

* Corresponding author; e-mail spalding@facstaff.wisc.edu; fax 608-262-7509.

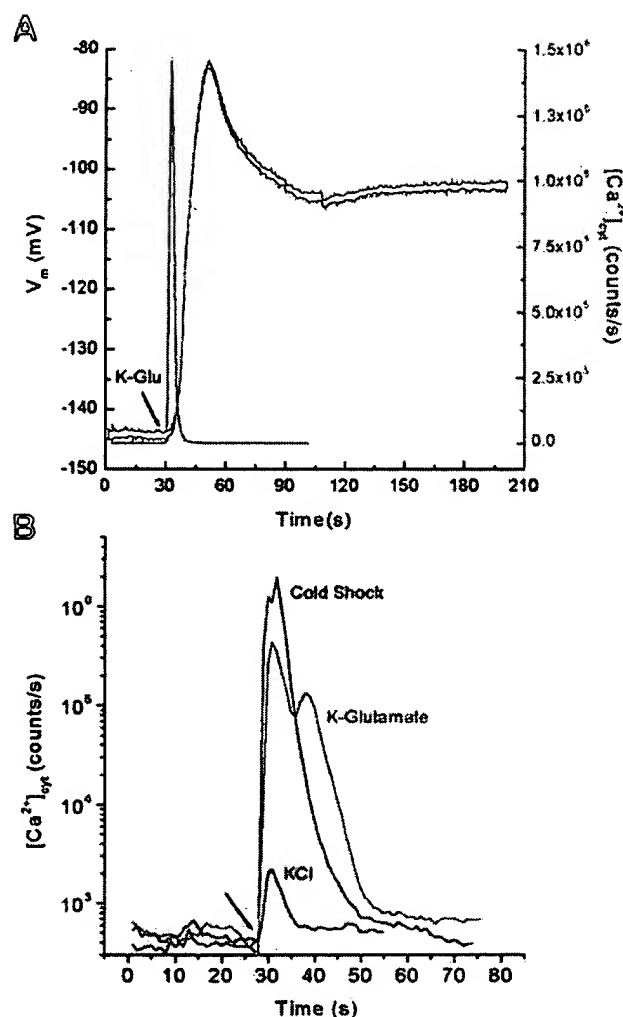


Figure 1. Glu triggers a large transient increase in $[Ca^{2+}]_{cyt}$ and an accompanying membrane depolarization. A, The red trace shows Ca^{2+} -dependent luminescence from whole aequorin-expressing *Arabidopsis* seedlings (5- to 8-d-old) measured with a luminometer as described previously (Lewis et al., 1997). The black trace shows the response of V_m measured by impaling a cell near the root apex with an intracellular microelectrode as previously described (Spalding et al., 1999). Intact seedlings between 7- and 14-d-old were used for the V_m measurements. Glu at a final concentration of 1 mM was delivered as the K^+ salt. The pH was buffered at 5.7 with 2.3 mM MES [2-(*N*-morpholino)-ethanesulfonic acid]. B, The kinetics and magnitude of the change in $[Ca^{2+}]_{cyt}$ induced by Glu resembles the response to cold shock, but is much larger than the touch response induced by the control treatment. Cold shock was achieved by injecting 0°C 1 mM KCl into the luminometer cuvette, whereas the control treatment was room temperature 1 mM KCl. Glu was delivered as 1 mM K-Glu and all solutions were buffered at pH 5.7. Arrow indicates the time of treatment.

nal stores such as the vacuole may also contribute (Allen et al., 1995).

La^{3+} also blocked the depolarization triggered by Glu without affecting the resting V_m (Fig. 2C), indicating that the depolarization is a consequence of the inward Ca^{2+} movement. However, La^{3+} is not a spe-

cific Ca^{2+} -channel blocker (Lewis and Spalding, 1998) and it may prevent the depolarization by blocking a separate Glu-gated conductance in addition to the Ca^{2+} pathway. Thus despite the fact that La^{3+} blocks the Ca^{2+} flux and the membrane depolarization, the exact relationship between the two Glu-

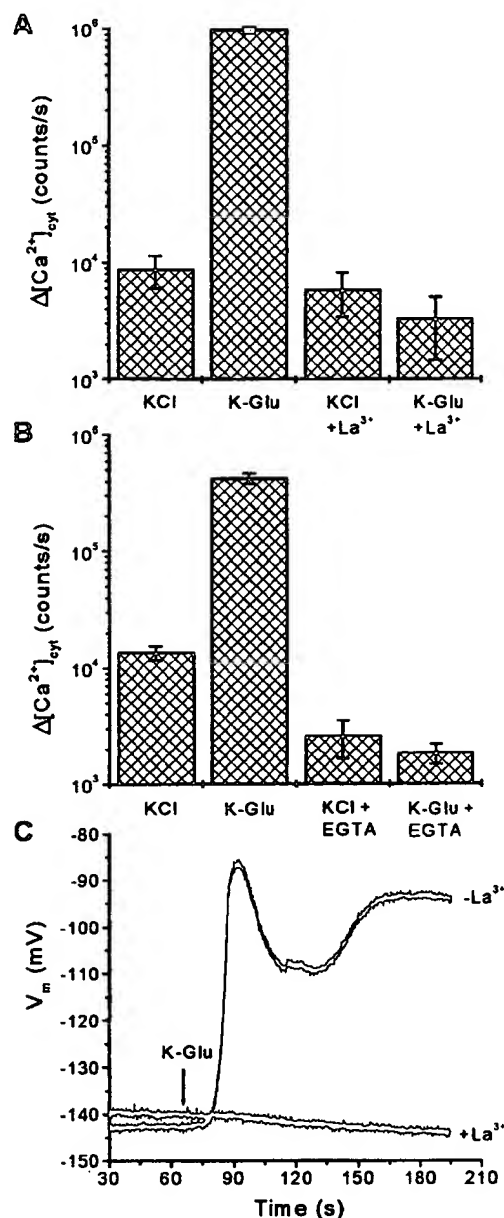


Figure 2. Inhibitory effects of La^{3+} and EGTA. A, Pretreatment of seedlings with 5 mM La^{3+} , an extracellular Ca^{2+} -channel blocker, inhibited the change in $[Ca^{2+}]_{cyt}$ induced by Glu, but had a much lesser effect on the 100-fold smaller response to the control treatment. B, Chelating extracellular Ca^{2+} by pretreatment with EGTA inhibited the Glu-induced Ca^{2+} response. The data plotted are means (\pm SEM) from three or four independent trials. C, Treatment of roots with La^{3+} blocked the Glu-induced depolarization without affecting the resting V_m . Roots were treated with 5 mM $LaCl_3$ before and during exposure to 1 mM K-Glu.

gated phenomena should be considered an open question. An alternative test would be to determine if EGTA treatment also inhibits the depolarization triggered by Glu, but stable recordings of V_m are difficult to obtain when extracellular Ca^{2+} is depleted to an extent that significantly affects its availability for inward fluxes. Patch-clamp studies of the ionic currents activated by Glu would be the preferred means of obtaining a biophysical description of the depolarization mechanism.

Glu is the primary natural ligand of iGluRs in the central nervous system although other non-native ligands are effective and have been used to classify receptor subtypes. The effectiveness of different ligands was tested using the aequorin reporter plants. Figure 3 demonstrates that Glu was clearly the most effective agonist tested (note the logarithmic y-scale). α -amino-3-hydroxy-5-methylisoxazole-4-propionate and N-methyl-D-aspartate, potent agonists of animal iGluRs, did not induce a response above the control treatment (approximately 2% of the L-Glu response). These non-native agonists of animal iGluRs also did not activate the *Synechocystis* GLU0 (Chen et al., 1999). It may be that affinity for α -amino-3-hydroxy-5-methylisoxazole-4-propionate and N-methyl-D-aspartate evolved in Glu receptors after the divergence of plants and animals. An alternative possibility is that Glu-gated Ca^{2+} entry in *Arabidopsis* does not involve iGluR-like molecules, but instead some unrelated Ca^{2+} -permeable pathway lacking affinity for typical iGluR agonists is responsible for the phenomenon.

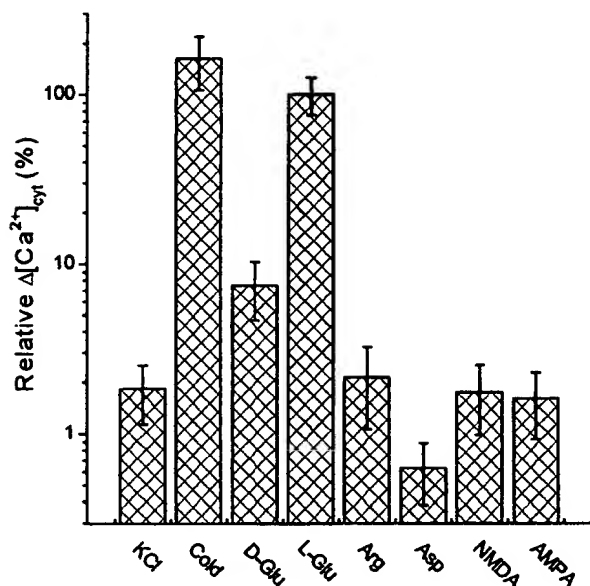


Figure 3. Relative effectiveness of related compounds. L-Glu was much more effective than other potential agonists, including D-Glu and the animal iGluR agonists, NMDA and AMPA. Note the logarithmic scale of the y axis, and that the response magnitudes are shown relative to the response induced by L-Glu. All compounds were administered at a final concentration of 1 mM. The plotted values are the means (\pm SE) of six independent trials.

The fact that the response to D-Glu was less than 10% of the L-Glu response indicates high stereochemical specificity of the binding site(s) on whatever molecules are responsible. Although Glu is clearly an effective ligand in a plausible concentration range, other ligands may be more physiologically important. The *Arabidopsis* genome contains several iGluR-like genes (Chiu et al., 1999) and that diversity may be matched by a similar diversity of agonists.

Information on the effective concentration range of Glu would help to establish a physiological context for this ligand-gated response in plants. The change in $[\text{Ca}^{2+}]_{\text{cyt}}$ induced by Glu increased between 0.3 and 3 mM, with the concentration for half-maximal response (EC_{50}) being approximately 1 mM (data not shown). This value is approximately 10-fold greater than the typical value for prokaryotic and animal iGluRs, but very similar to the EC_{50} of Cl^- -permeable iGluRs from nematodes (Cully et al., 1994).

If Glu or some other related small organic acid is the primary endogenous ligand, then it is important to consider how and when the external ligand-binding site would experience 0.3 to 3 mM concentrations. Anion channels at the plasma membrane of plant cells are known to function in the transduction of several signals important to plant growth and development (Ward et al., 1995). These channels are relatively non-selective among anions and may conduct significant efflux of dicarboxylic anions such as malate (Hedrich, 1994; Schmidt and Schroeder, 1994), and therefore perhaps Glu, as well. When environmental or endogenous signals activate such anion channels, apoplastic Glu concentration may rise into the effective range, causing a transient change in $[\text{Ca}^{2+}]_{\text{cyt}}$ that serves to couple a stimulus to downstream responses. This hypothetical scenario may be most plausible in roots, where anion-channel mediated release of dicarboxylic acids has been proposed as a mechanism for combating Al^{3+} stress (Delhaize and Ryan, 1995; Ryan et al., 1997). Perhaps it is no coincidence that dissection experiments revealed most of the Ca^{2+} signal recorded from intact *Arabidopsis* seedlings was contributed by the root; leaves and cotyledons of young plants displayed smaller Glu responses (data not shown).

The results presented here form the basis of our proposition that a key element of a mechanism for altering $[\text{Ca}^{2+}]_{\text{cyt}}$ in plant cells during signaling is similar to that responsible for neurotransmitter action in the central nervous system of animals. The evidence would be bolstered considerably if mutational studies revealed a link between specific iGluR-like genes and Glu-gated Ca^{2+} fluxes. Plant biologists interested in Ca^{2+} signaling are presently particularly well equipped to test this connection because there is a wealth of published details about iGluR-mediated Ca^{2+} signaling in neurons, the *Arabidopsis* genome is essentially sequenced and searchable, so-

phisticated reverse-genetic strategies are very practical, and electrophysiological techniques can measure function with high resolution. The stage for exciting developments in Ca^{2+} signaling is set.

ACKNOWLEDGMENT

We thank Jamie Verheyden for technical assistance.

Received September 11, 2000; accepted September 25, 2000.

LITERATURE CITED

- Allen GJ, Muir SR, Sanders D (1995) *Science* 268: 735–737
- Baudry M, Lynch G (1993) In Baudry M, Thompson RF, Davis JL, eds, *Synaptic Plasticity*. MIT Press, Cambridge, MA, pp 87–115
- Bliss TVP, Collinridge GL (1993) *Nature* 361: 31–39
- Boorer KJ, Frommer WB, Bush DR, Kreman M, Loo DDF, Wright EM (1996) *J Biol Chem* 271: 2213–2220
- Chen G-Q, Cui C, Mayer ML, Gouaux E (1999) *Nature* 402: 817–821
- Chiu J, DeSalle R, Lam H-M, Meisel L, Coruzzi G (1999) *Mol Biol Evol* 16: 826–838
- Cully DF, Vassilatis DK, Liu KK, Paress PS, Van der Ploeg LHT, Schaeffer JM, Arena JP (1994) *Nature* 371: 707–711
- Delhaize E, Ryan PR (1995) *Plant Physiol* 107: 315–321
- Dingledine R, Borges K, Bowie D, Traynelis SF (1999) *Pharmacol Rev* 51: 7–61
- Haley A, Russell AJ, Wood N, Allan AC, Knight M, Campbell AK, Trewavas AJ (1995) *Proc Natl Acad Sci USA* 92: 4124–4128
- Hedrich R (1994) *Curr Top Membr* 42: 1–33
- Hille B (1992) *Ionic Channels of Excitable Membranes*. Sinauer, Sunderland, MA, pp 140–169
- Hollmann M, Heinemann S (1994) *Ann Rev Neurosci* 17: 31–108
- Kirischuk S, Kirchoff F, Matyash V, Kettenmann H, Verkhratsky A (1999) *Neuroscience* 92: 1051–1059
- Knight H, Trewavas AJ, Knight MR (1996) *Plant Cell* 8: 489–503
- Knight MR, Campbell AK, Smith SM, Trewavas AJ (1991) *Nature* 352: 524–526
- Lam H-M, Chiu J, Hsieh M-H, Meisel L, Oliveira IC, Shin M, Coruzzi G (1998) *Nature* 396: 125–126
- Legué V, Blancaflour E, Wymer C, Perbal G, Fantin D, Gilroy S (1997) *Plant Physiol* 114: 789–800
- Lewis BD, Karlin-Neumann G, Davis RW, Spalding EP (1997) *Plant Physiol* 114: 1327–1334
- Lewis BD, Spalding EP (1998) *J Membr Biol* 162: 81–90
- Malhó R, Moutinho A, van der Luit A, Trewavas AJ (1998) *Phil Trans R Soc Lond B* 353: 1463–1473
- Obrietan K, van den Pol A (1999) *J Neurophysiol* 82: 94–102
- Ryan PR, Skerrett M, Findlay GP, Delhaize E, Tyerman SD (1997) *Proc Natl Acad Sci USA* 94: 6547–6552
- Sanders D, Brownlee C, Harper JF (1999) *Plant Cell* 11: 691–706
- Schmidt C, Schroeder JI (1994) *Plant Physiol* 106: 383–391
- Spalding EP, Hirsch RE, Lewis DR, Qi Z, Sussman MR, Lewis BD (1999) *J Gen Physiol* 113: 909–918
- Ward JM, Pei Z-M, Schroeder JI (1995) *Plant Cell* 7: 833–844